Spring 5-2020

Influence of Extracellular Cues of Hydrogel Biomaterials on Stem Cell Fate

Haley Barnett

INFLUENCE OF EXTRACELLULAR CUES

OF HYDROGEL BIOMATERIALS ON STEM CELL FATE

by

Haley Barnett, B.S.

A Dissertation Presented in Partial Fulfillment
of the Requirements of the Degree
Doctor of Philosophy

May 2020

COLLEGE OF APPLIED AND NATURAL SCIENCES
LOUISIANA TECH UNIVERSITY

LOUISIANA TECH UNIVERSITY

GRADUATE SCHOOL

April 7, 2020
Date of dissertation defense

We hereby recommend that the dissertation prepared by

Haley Barnett

entitled **Influence of Extracellular Cues of Hydrogel Biomaterials**

on Stem Cell Fate

be accepted in partial fulfillment of the requirements for the degree of

Doctor of Philosophy in Molecular Sciences and Nanotechnology

M. Caldorera-Moore
Mary Caldorera-Moore
Supervisor of Dissertation Research

William Campbell
Head of Molecular Sciences and Nanotechnology

Doctoral Committee Members:
Mary Caldorera-Moore
Jamie Newman
Yuri Voziyanov
Gergana Nestorova
Bruce Bunnell

Approved:
Gary A. Kennedy
Dean of Applied & Natural Sciences

Approved:
Ramu Ramachandran
Dean of the Graduate School

GS Form 13a
(01/20)

ABSTRACT

The field of tissue engineering has developed to try and find an alternative approach to treat lost or damaged tissue. The field of tissue regeneration aims to develop tissue scaffolds composed of biomaterials, a cell source, and appropriate biochemical/phsysiochemical stimuli to replace current therapies. Stem cells offer great promise due to their self-renewal capabilities and their numerous differentiation possibilities. However, stem cells are extremely sensitive to their external environment which presents a challenge when culturing them on biomaterials. Surface elasticity, topography, surface chemistry, and exposure to biomolecules all represent environmental stimuli that could affect stem cell behavior. This research aims to help bridge the gap currently associated with tissue engineering by gaining a better understanding of how these biomaterial properties influence stem cell fate. A tailorable poly(ethylene glycol) dimethacrylate (PEGDMA) hydrogel will be utilized along with adult stem cells. It is hypothesized that PEGDMA hydrogels that have an elasticity, architecture, and surface chemistry more closely mimicking the extracellular matrix of the natural tissue environment, will enhance stem cell differentiation towards a desired cell lineage (i.e. bone, muscle, etc.). The project will look at different extracellular cues of a PEGDMA hydrogel biomaterial and analyze how they affect stem cell differentiation. Through a better understanding of cell-environment interactions the research from this project will

help lead to the development of a tailorable tissue scaffold for tissue regeneration purposes that can be manufactured on a large scale.

APPROVAL FOR SCHOLARLY DISSEMINATION

The author grants to the Prescott Memorial Library of Louisiana Tech University the right to reproduce, by appropriate methods, upon request, any or all portions of this Dissertation. It is understood that "proper request" consists of the agreement, on the part of the requesting party, that said reproduction is for his personal use and that subsequent reproduction will not occur without written approval of the author of this Dissertation. Further, any portions of the Dissertation used in books, papers, and other works must be appropriately referenced to this Dissertation.

Finally, the author of this Dissertation reserves the right to publish freely, in the literature, at any time, any or all portions of this Dissertation.

Author _____

Date _____

DEDICATION

This dissertation is dedicated to my daughter, Harper Barnett. She is my motivation to continuously better myself and the light of my life.

TABLE OF CONTENTS

LIST OF FIGURES

LIST OF TABLES

ACKNOWLEDGMENTS

First and foremast I would like to thank my husband, Heath Barnett. Without his constant support and encouragement, I would not be finishing this work. He never failed to believe in me, even when I didn't believe in myself. Thank you, Heath, for providing the emotional support when I needed it and for reminding me to work harder when I needed that extra push. To my daughter, Harper Barnett, you have taught me more in the last year of my PhD than I have learned in all my years prior. You taught me time management, prioritization, and that it's okay to have a work-life balance. Harper, you are my motivation to wake up every day and strive to be better.

To my parents, Jackie and Chelette Harris, I can't thank you enough for all of the support when I decided to pursue a graduate degree. Thank you for listening to me call and cry when things were tough and reassuring me that I could handle it. Thank you for helping me to remain focused on what my goal was and not letting me quit when I wanted to. To my brother Nick Harris, his wife Tiffany Harris, and my niece Emma Harris, thank you all for opening your home when I needed a break from school and wanted to enjoy time with family. To my best friend April Stelly, thank you for listening to me whine constantly and reminding me that I would eventually graduate. My family and friends have been the greatest source of motivation and encouragement that I could ask for.

A huge thank you to both Caldorera-Moore Lab and Newman Lab and the lab mates that I have met during my time at Tech. Notably I want to thank Anna Whitehead for all of the time she spent training me. Anna taught me how to lead a project and helped me to drastically improve my presentation skills. Without her knowledge and patience, I would not have been as successful as I have. To India Pursell, the best lab mate I have had the honor to work with, I can't thank you enough. You worked harder than I have ever seen anyone work and did it all while balancing classes and a job. I learned more from you than I could have hoped to teach you. You quickly turned into one of my best friends and allies. I will always cherish the times we had in lab, from the absolute worst failures to all of the success we had.

Finally, thank you to my incredible advisor, Dr. Mary Caldorera-Moore and co-advisor, Dr. Jamie Newman. I really can't express how grateful I am to have had the honor to work on a collaborative project under you both. Your guidance the last four years has not only made me a better scientist, but a better person. Thank you for your patience, encouragement, and constructive criticism through the years. I fully believe that I have the best mentors possible.

CHAPTER 1

INTRODUCTION AND SPECIFIC AIMS

1.1 Introduction

Regenerative medicine is a rapidly growing interdisciplinary field that aims to repair, replace, or enhance cell, tissue, or organ function through clinically applicable procedures.[1,2] In most cases, successful regeneration of tissue requires the use of a biomaterial scaffold to serve as the framework for cells to develop into functional tissue. The development of scaffolds composed of materials with optimal chemical and physical properties, adequate cell sources, and appropriate biochemical or biophysical cues – i.e. biomimetic, is a vital aspect of the research in the field.[3] Professionals in this field utilize biomaterials, biochemical factors, biophysical stimulation, cell sources, or a combination of many of these factors, to create therapies for a wide variety of applications.[4,5] Repairing or replacing damaged tissues and organs, wound healing, degenerative diseases such as muscular dystrophy, congenital conditions like diabetes, and stem cell based therapies are all areas of research that are encompassed under the theme of regenerative medicine.[6–10] The potential cures and treatments that could emerge from regenerative medicine research continues to drive the field forward.

1.1.1 Tissue Engineering and Regenerative Medicine

Tissue engineering is a relatively new area of research, as the term "tissue engineering" was coined in 1987 at a National Science Foundation meeting.[1] Tissue engineering developed from the field of biomaterials and according to the NIH can be defined as "the practice of combining scaffolds, cells, and biologically active molecules into functional tissues".[11] Tissue engineering has grown and is now considered its own field of research and is in and of itself a multidisciplinary field that is often used interchangeably with regenerative medicine.[11] The basis for tissue engineering (**Figure 1-1**) is a scaffold with biomimetic properties including the proper biocompatibility, degradation properties, mechanical properties similar to the innate tissue, and architecture similar to that found in the body.[12,7]

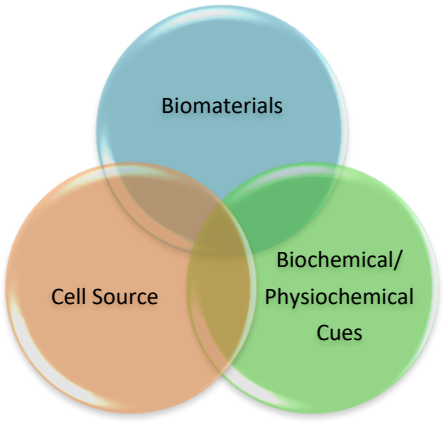

Figure 1-1: Diagram depicting the relationship of materials, cells, and extracellular cues in tissue engineering. Tissue engineering in a multidisciplinary field that requires biomaterials with appropriate mechanical properties, clinically relevant cell sources, and adequate chemical or physical stimuli.

Skin replacement therapy research gained popularity in the 1990's and became the first engineered tissues.[1,9] This research led to commercially available skin replacements that aided in severe burn cases, reconstructive surgeries, and diseases that led to skin necrosis.[13,14] Advances in engineered skin therapies led to utilizing tissue engineering scaffolds for potential therapies in chronic wound healing.[7]

Many have hope that tissue engineering will eventually lead to bioengineered organs or at the very least, scaffolds that could stimulate tissue repair and restore function in the damaged areas.[6,15] Optimistically, advances in tissue engineering could eliminate the need for organ transplants, which is currently the treatment option for end-stage organ failure.[6] There is a critical shortage of organ donors, which leads to thousands of individuals without any course of treatment and reduces their life expectancy. According to the United Network for Organ Sharing (UNOS), as of December 2019, 113,288 patients are currently waiting for a lifesaving organ transplant (**Figure 1-2**).[16] In contrast, there have only been 11, 876 donors from January-November 2019.[16]

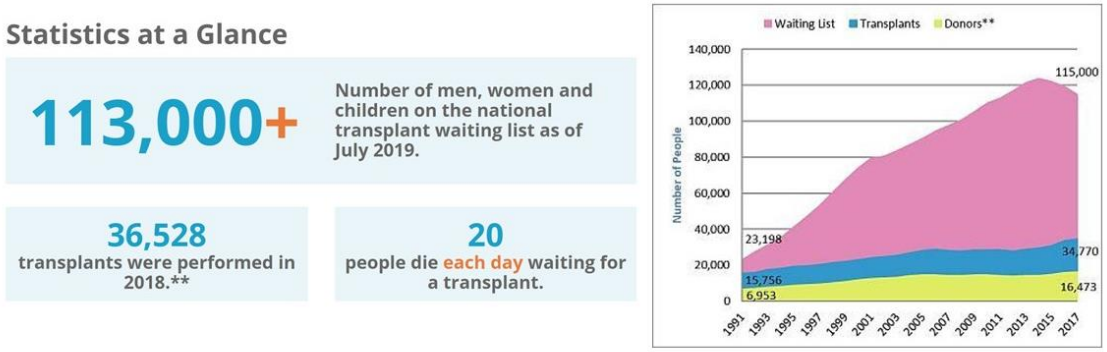

Figure 1-2: Infographic on the need for alternative tissue replacement therapies. Statistics showing the growing need for the creation of organs and tissue to address the organ donor shortage.[17]

Despite the drastic need for engineered organs, the process of creating fully functional organs in a laboratory setting is extremely complex. Beyond just creating a scaffold in the shape of an organ it must provide vascularization, signaling molecules, and be able to interact with surrounding tissue to be physiologically relevant.[18] There are hundreds of researchers working around the world[19] on the creation of fully functional engineered organs such as bladders,[20] lungs,[21] and hearts.[22]

While this field still faces quite a few challenges, materials scientists, engineers, and cell biologists continue working diligently to advance the field. A wide variety of materials and cell sources have been utilized to create scaffolds for tissue regeneration. There are three main classes of biomaterials used for creating tissue scaffolds: ceramics, synthetic polymers, and natural polymers because of their mechanical stability, tailorability, and biodegradability respectively.[12,23] Ceramics and ceramic composites are most commonly used in engineering of bone deformations, repair, or replacement due to their high mechanical strength, ability to fuse with bone, and degradation properties.[12,24] Hydroxyapatite (HA), calcium phosphate, argonite, bioactive glass, and tetracalcium phosphate are a few of the ceramic materials that have been explored for tissue repair/replacement.[25–30] Numerous synthetic polymers have been and continue to be investigated for a wide variety of therapeutic applications in tissue engineering. A few, but certainly not all of those used, include polymers such as polylactic acid (PLA), polyglycolic acid (PGA), polycaprolactones, polycarbonates, poly(ethylene) glycol (PEG), and poly(2-hydroxyethyl methacrylate-co-methacrylic) (pHEMA).[12,29,31–35] Tissue engineering also relies heavily on natural polymeric scaffolds including collagen, elastin, silk, fibronectin, alginate, hyaluronan, chitosan, gelatin, and chondroitin sulfate for

scaffold development.[12,31,32,35–38] More on synthetic polymers will be discussed in **Chapter 2**.

Advances in the field of tissue engineering have occurred in parallel with innovations in stem cell research as stem cells provide a source of self-renewing, multipotent cells for autologous treatments. The cellular component of tissue constructs is arguably one of the most challenging aspects. The cell source is one consideration that must be evaluated. Cells can be autologous, meaning from the patient themselves, allogenic, which are donor cells from another individual, or xenogeneic, which come from another species altogether.[39] The type of cell, mainly primary or stem cells, used will also influence the function of the scaffold. Primary cells are fully differentiated cells that are harvested from tissue-specific locations.[40] Stem cells retain self-renewal capabilities and have the ability to differentiate into multiple different cell types.[41] The determination of which cell type is better suited will vary from application to application. Primary cells will be the most compatible immunologically and will be fully differentiated so the environment will not influence the type of tissue being formed although typically yields are low.[40] Stem cell are found abundantly in the body, however, they are sensitive to their chemical and physical environment which can lead to changes in predicted cell behavior and alter cell fate.[42] Multipotent stem cells, such as human adipose stem cells (hASCs) offer the most promise in cell-based regenerative therapies due to their self-renewal capabilities, and ability to differentiate into cells found in mesoderm tissues such as myoblasts, adipocytes, osteoblasts, and chondrocytes, and can easily be harvested from patients. More specifics on stem cells used for regenerative medicine applications will be presented in **Chapter 2**.

1.1.2 Challenges Facing Tissue Engineering

Even with the need and ever-growing popularity of tissue engineering andall the advances made thus far, there is still a long way to go to reach reliable clinical application. Every case where tissue engineering and regenerative medicine offers hope, there will be unique and diverse challenges.[5] Each case will be unique in terms of injury, severity of condition, inflammation, natural tissue remodeling, age, and degeneration, complicating treatment. Some cases will require materials with high mechanical stability, such as bone tissue engineering, while other injuries will need softer, more elastic materials to mimic the extracellular matrix.[43] Constructs can either be degradable, which means the scaffold dissipates over a period of time, or they can be non-degradable so the scaffold is permanent. One example of where a degradable scaffold would be advantageous is for wound healing applications. The scaffold could be utilized to promote healing and recruit cells to repair the tissue and degrade over time leaving only healthy tissue in its place.[44] Permanent scaffolds would be advantageous in whole organ replacement to provide a stable platform for new tissue, cells and vascularization to incorporate into. With the complexity of these issues, no one approach will be the answer. Instead, it will likely be an approach of different materials, cell sources, and techniques that offer solutions.[9]

For these constructs to be successful they should be analogous to the natural environment of the extracellular matrix (ECM) niche in which they will be implanted.[45] For this reason, hydrogel-based materials are of particular interest in creating tissue scaffolds due to their biocompatibility, capability to retain large amounts of water, innate biomimetic properties, and the minimal tendency to adsorb proteins from body fluids.[46]

The challenge with using scaffolds for regenerative medicine lies in reproducibly differentiating stem cells on these materials to desired lineages. Cell-microenvironment interactions control vital cell processes such as proliferation, differentiation, and cell migration.[47] Despite the volume of research being conducted in this area, these interactions between stem cells and the external environment created using biomaterial substrates are not well understood.

1.2 Specific Aims

Previous work in our lab has synthesized poly(ethylene glycol) dimethacrylate (PEGDMA) hydrogels on which mouse embryonic stem cells (mESCs), human bone marrow-derived stem cells (hMSCs), and human adipose stem cells (hASCs) were successfully seeded.[48] Cell viability assays confirmed that each cell type was able to remain viable on the PEGDMA hydrogel platform. In addition, quantitative reverse transcriptase polymerase chain reaction (qRT-PCR) of multipotent and pluripotent markers demonstrated that the cells retain their multipotent and pluripotent state. It was also shown that the PEGDMA hydrogels could be synthesized to have different elastic moduli by varying the percentage and molecular weight of the polymer.[48] My Ph.D. project has focused on expanding this research by investigating how extracellular cues specifically, cell culture material elasticity and surface chemistry influence stem cell fate. The specific aims for this project were:

1) Evaluate the Influence of Hydrogel Elasticity on Stem Cell Fate
2) Evaluate the Effects of Post-processing Drying Methods on PEG Based Hydrogels
3) Evaluate the Influence of Biochemical Cues on Myogenic Differentiation of hASCs

Upon completion of this project a better understanding of environmental influence on stem cell fate as well as procedures for more efficiently directing myogenic differentiation of hASCs will be gained.

1.2.1 Specific Aim 1: Evaluate the Influence of Hydrogel Elasticity on Stem Cell Fate

The goal of Aim 1 was to investigate the interactions between an elastically tailorable polyethylene glycol (PEG)-based hydrogel platform and human bone marrow-derived mesenchymal stem cells (hMSCs). For these studies, poly (ethylene glycol) dimethacrylate (PEGDMA) hydrogels of two varying elasticities were utilized; “soft hydrogels” (8-10 kPa) and “stiff hydrogels” (50-60 kPa). These two PEGDMA hydrogel blends were then surface functionalized with the ECM protein fibronectin. Human MSCs were then seeded on each hydrogel blend as well as tissue culture plate controls. The effect of varying hydrogel elasticity on hMSC attachment, multipotency, proliferation, and differentiation towards osteogenic and adipogenic lineages was then examined. By evaluating the attachment, proliferation, multipotency, and differentiation potential of hMSCs cultured on soft hydrogels, stiff hydrogels, and tissue culture plates we are able to determine if PEGDMA hydrogel elasticity influences stem cell fate.

1.2.2 Specific Aim 2: Evaluate the Effects of Post-processing Drying Methods on PEG Based Hydrogels

The goal of Aim 2 was to create a PEGDMA hydrogels with multiscale porosity with suitable properties for stem cell culture that could be used to further investigate the influence spatial configuration has on stem cell fate. Varying blends and thicknesses of PEGDMA hydrogels were synthesized, flash frozen, and dried by lyophilization to create scaffolds with multiscale porosity. Air-dried hydrogels of varying thickness were used as a control for comparison. Environmental scanning electron microscopy (ESEM) was utilized to visualize changes in hydrogel morphology in a dry state as well as in their hydrated state. Equilibrium swelling studies were conducted to evaluate changes in swelling behavior as well as used to calculate the average pore size diameter of hydrogels of varying blend, thickness, and drying method.

Rheology data was also obtained to find the shear elastic modulus of each PEGDMA blend of varying thickness and drying method. The shear elastic modulus will help to determine which hydrogel blend may be most appropriate for tissue engineering applications. In addition, all combinations of hydrogel blend, thickness, and drying method were subjected to a series of solutions they would be exposed to if used for stem cell culture as to analyze degradation properties. Cell viability and morphology was also evaluated to confirm the potential use of these scaffolds for stem cells and tissue engineering applications.

1.2.3 Specific Aim 3: Evaluate the Influence of Biochemical Cues on Myogenic Differentiation of hASCs

The goal of Aim 3 was to expand on previous differentiation work by inducing myogenic differentiation of hASCs using myogenic differentiation media recipes that contain different biochemical factors that have been reported in the literature.[49,50] While several groups have shown that hASCs have the potential to differentiate towards a myogenic lineage,[49–51] there is no universal myogenic differentiation media.[52] Therefore, there is a need to determine the optimal myogenic media for hASC differentiation.

Optimization of differentiation involved the culturing of hASCs on standard polystyrene tissue culture plates for different time points. The hASCs were cultured in 3 different medias for up to 6 weeks. RNA was then collected and reverse transcriptase-polymerase chain reaction (RT-PCR) was performed to evaluate gene expression of common myogenic genes. Immunofluorescence to examine MYOD and myosin protein expression and localization was also utilized to further validate myogenic differentiation. All assays were completed in triplicate to allow for analysis of statistical significance. Human skeletal myoblasts (HSkMs) were used as a positive control for RT-PCR and immunofluorescence.

Optimizing myogenic differentiation of hASCs by controlling the exposure to biochemical factors in tissue culture will allow for the progression of the project in determining how extracellular cues of PEGDMA hydrogel biomaterials influence stem cell fate. At the completion of this aim we will have not only a reliable media recipe for differentiation of hASCs, we will also have a set of assay protocols in place to allow for efficient characterization of myogenesis in future experiments.

1.3 Overview

In the subsequent chapters the background and significance of this research which focuses on creating a better understanding of how the extracellular cues provided by PEGDMA hydrogel biomaterials influences stem cell fate, will be presented. Understanding the dynamic interactions between cells and materials is the first step in producing innovative and adaptable hydrogel biomaterials to advance the clinical potential of cell-based regenerative therapies. This will allow for the creation of more reproducible, efficient, and tailorable scaffolds to be used in clinically repairing and replacing lost and damaged tissue. The background and more in-depth discussion of stem cells, hydrogels, and significance of work such as this is presented in **Chapter 2**. Following the presentation of background information, **Chapter 3** will focus on investigating the influence that PEGDMA hydrogel elasticity has on hMSC fate and compared to tissue culture controls. This work was published in the Oxford Academic journal *Regenerative Biomaterials* in April of 2018. **Chapter 4** will focus on the development of PEGDMA hydrogels with multiscale porosity for tissue engineering applications through the use of freeze-dry lyophilization. The work presented in **Chapter 4** was published by Taylor and Francis in the *Journal of Biomaterials Science, Polymer Edition* in July of 2019. In **Chapter 5** data collected while optimizing myogenic differentiation of hASCS through a combination of cell culture medias, ECM proteins, and a DNA methylation inhibitor will be presented and demonstrate the most efficient method to promote myogenic differentiation in hASCs. This work is being prepared for

submission to *Journal of Experimental Biology*. Finally, **Chapter 6** will focus on project conclusions, future directions, and the significance of the results from this research.

CHAPTER 2

BACKGROUND

2.1 Overview of the Extracellular Matrix

Cells are highly sensitive to their surroundings with hundreds of different proteins having a role in stimulating cell receptors, which in turn determines numerous responses. This highly defined and specialized cell microenvironment, which is essential for tissue development and function, is the extracellular matrix (ECM).[53,54] The extracellular microenvironment surrounds cells and is a highly hydrated network that contains molecular signals.[55] The ECM is composed of a variety of molecules (**Figure 2-1)**[56] including members of the collagen family, elastic fibers, glycosaminoglycans (GAGs), proteoglycans, and adhesive glycoproteins.[53]

The ECM can effect cell behavior by directly regulating cell functions through receptor-mediated signaling, and this network can control the mobilization of growth factors or differentiation factors.[53] This means that the ultimate decision for a cell to differentiate, proliferate, migrate, apoptose, or perform other functions, is a coordinated response to the molecular interactions with these ECM effectors.[55]

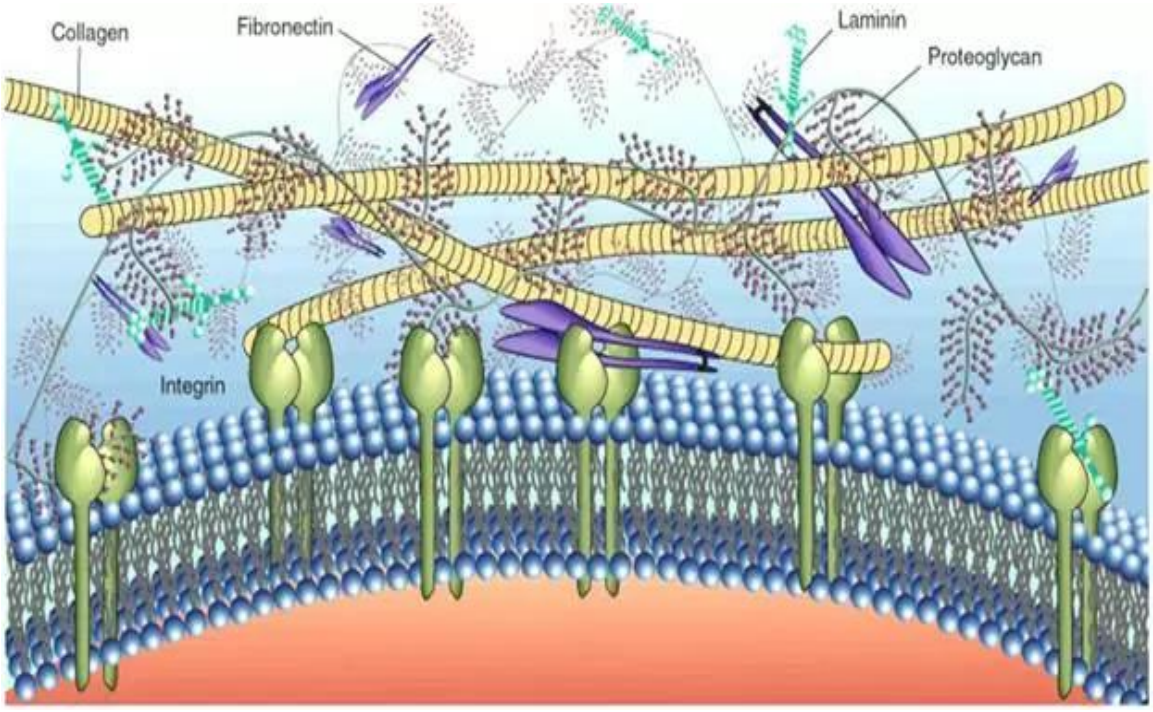

Figure 2-1: An illustration of the extracellular matrix. Visual representation of the extracellular matrix depicting some of the major protein components.[56]

2.1.1 Challenges for Tissue Engineering

For a tissue scaffold to be successful it must support the formation of tissue-relevant mimics, as well as promote cell adherence, cell migration, foster transport of nutrients and waste, and form new extracellular matrix.[57] Since the ECM is critical in cell proliferation and differentiation, tissue engineering approaches usually utilize exogenous three-dimensional ECM's to engineer new tissues from isolated cells.[58] Synthetic ECMs should facilitate the localization and delivery of cells to specific sites in the body, maintain a 3D space for the formation of new tissues, and guide the development of new tissues with appropriate functions.[53,58,59] Synthetic ECMs need a large surface-to-volume ratio to allow for a high density of cells. Since the ECM varies in different tissues and at different stages of development, choosing the appropriate mechanical and degradative

properties is important.[54] The cells that compose the engineered tissue need to express appropriate genes so that the cells maintain tissue-specific function. The function of seeded cells is dependent upon the specific cell-surface receptors used by cells to interact with the material, interaction with surrounding cells, and on the presence of growth factors.[53] This can be controlled by incorporating cell-adhesion peptides or growth factors into the synthetic ECM or by subjecting the synthetic ECM to mechanical stimuli.[53,58] Therefore, the biomaterial used in tissue engineering plays an important role as it can serve as a substrate for attachment, be used as a cell delivery vehicle, and activate specific cellular functions in localized regions.[60]

The chemical and spatial configuration of surfaces on which cells grow also plays a key role in controlling cell behavior. Properties like those of surface topography or spatial conformation, hydrophobicity, and specific interactions of a material with a cell surface can affect the cells activity.[61] The surface properties of a biomaterial also determine which biomolecules will adsorb.[62] In the ECM cells interact with nanoscale topographical features that vary in size and composition. The topography can affect cells in terms of adhesion, morphology, migration, proliferation, cytoskeletal arrangement, and gene expression.[63–65] Different surface treatments can be used to modify the topography and surface chemistry of the biomaterials to improve adhesive interactions with cells.[62,66] The energy at the surface with a net positive or negative charge is more likely to be hydrophilic, whereas a surface with a neutral charge is likely to be more hydrophobic. The surface energy of the material can influence which proteins adhere to the biomaterial. Therefore, the changes in hydration can change the behavior of adsorbed proteins.[62] To achieve more biomimetic biomaterials, the surfaces of materials have been modified to

include bioactive molecules. Biomaterials can be coated with ECM proteins to promote cell adhesion, proliferation, and differentiation.[60] These modifications make the material mimic the ECM more closely, which in turn makes it a more viable tissue scaffolding option.

The ECM structure also provides spatial control that can promote cell-to-cell communication. Contact-dependent, cell-cell signaling (juxtacrine signaling) provides constant morphogenic cues, while the diffusion of soluble signals from neighboring cells (paracrine signaling) transiently affects proximal populations of cells. These interactions between cell populations influence a range of stem cell behavior including the induction of programs of differentiation[67] and self-renewal properties.[68–71] Positioning within the stem cell microenvironment, achieved by the spatial distribution of the ECM and cell-cell contacts, physically confines stem cell self-renewal and differentiation behavior by guiding the position of the mitotic axis in asymmetric division.[72,73]

Superimposed on all of these mechanisms, is the mechanical environment (**Figure 2-2**) that governs ECM interactions, changes sensitivities to soluble cues and physically alters cell populations within tissues. The mechanical environment influences all aspects of tissue behavior, since the majority of all cells require interaction with the ECM to maintain viability. Adherence allows cell to exert contractile forces on their environment and sense compliancy to induce appropriate cellular behavior.[74] Research in the area has demonstrated that 2D substrates with mechanical properties that match native tissue (neuronal, muscle, and bone) more efficiently promote mesenchymal stem cell differentiation down specific lineages.[75]

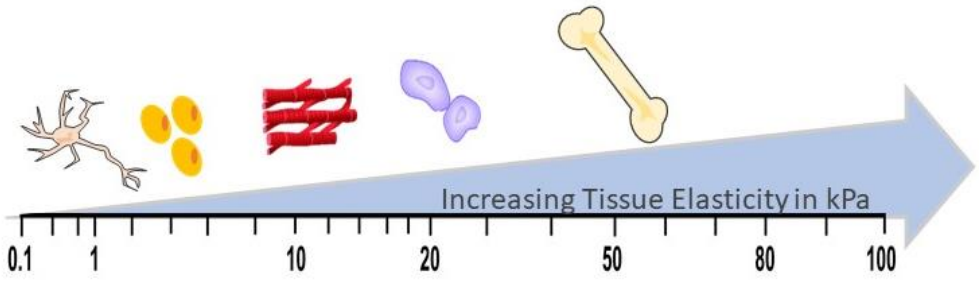

Figure 2-2: Elastic moduli of natural tissue. One important component of the mechanical environment is the elasticity of tissue. Elasticity has been shown to affect cell behavior, therefore material elasticity is an important component of tissue engineering scaffolds. *Image credit: Rachel Eddy. Adapted from Butcher et al. 2009*[76]

2.2 Brief Overview of Stem Cells

The knowledge gained from stem cell biology is paving the way for the generation of unlimited cells of specific phenotypes to be incorporated into tissue engineering constructs.[40,77] Stem cells are undifferentiated and unspecialized cells that retain the ability to differentiate into multiple cell lineages.[40,77,78] (**Figure 2-3**) Stem cells can be categorized based on their potency (totipotent, pluripotent, multipotent, oligopotent, or unipotent).[79]

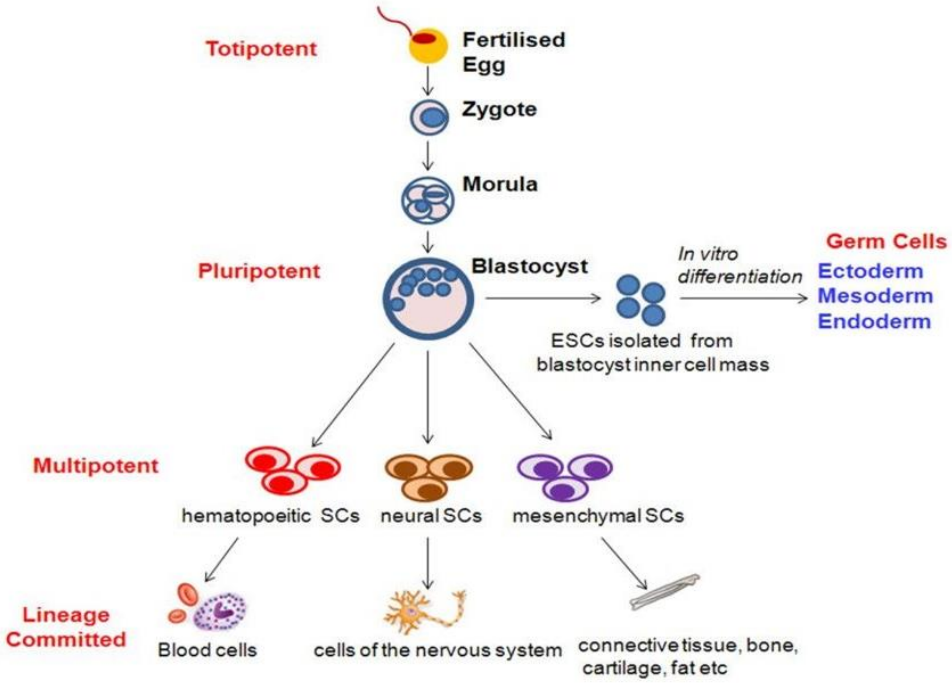

Figure 2-3: A hierarchal structure showing the differentiation potential of stem cells based on their potency. Totipotent stem cells have the most differentiation potential while unipotent cells have limited differentiation potential into tissues they are found in, and are fully committed to becoming that tissue.[80]

2.2.1 Totipotent Stem Cells

Totipotency is the ability to differentiate into embryonic and extra-embryonic tissues.[79] Totipotent cells represent the ability to form a whole functioning organism from that one single cell.[81] In humans, the zygote, which is produced from the fusion of an egg and sperm cell, represents a totipotent cell.[81] Only the zygote and their direct descendants (referred to as morula stem cells) undergo symmetrical cell division and are the only totipotent stem cells.[79,81,82] Cells are classified as totipotent until at least the 4-cell embryo stage and potentially until the 16-cell stage where they begin to further commit to a more specified lineage.[79,81]

2.2.2 Pluripotent Stem Cells

Pluripotency refers to the ability of cells to differentiate into the three germ layers.[79,81–83] However they do not contribute to extra-embryonic tissues such as the placenta.[79,84] These cells also retain an ability to proliferate indefinitely under the right conditions.[83–85] Pluripotent stem cells are descendants of totipotent cells and are naturally found in the inner cell mass of embryos.[81,83,85] There are two classes of pluripotent stem cells: embryonic stem cells (ESCs) and induced pluripotent stem cells (iPSCs).

Embryonic stem cells are those cells found in the inner cell mass during embryogenesis.[86] These cells fit the criteria of a pluripotent cell as they maintain their self-renewal capability and can differentiate into all three germ layers.[85] Mouse embryonic stem cells were the first pluripotent cells to be isolated and cultured *in vitro* in 1981.[87,88] and set the requirements for pluripotent stem cell classification. These critera mandate that the cells

(1) originate from a pluripotent cell population

(2) have and maintain a normal karyotype

(3) be immortal

(4) be able to be propagated indefinitely in the embryonic state

(5) be capable of spontaneous differentiation into somatic cells of all three germ layers[79,86]

Embryonic stem cells are also characterized by the expression of hallmark transcription factors: Oct4, Sox2 and Nanog.[84,85,89] These cells have increased plasticity in that they can be more easily manipulated since they lack specific epigenetic modifications.[78,90] Their indefinite undifferentiated proliferation *in* vitro with the potential to differentiate

into any of the tissues found in a body gives them great promise for regenerative medicine applications. However, the use of human embryonic stem cells for research has been an ethical debate since their discovery.[90] One such concern comes from the origin of these stem cells. Human embryonic stem cells come from "pre-implantation" embryos, with the majority coming from leftover IVF embryos that were donated.[91] While embryonic stem cell pluripotency is commonly seen as their biggest advantage, this property can lead to the formation of teratomas. Teratomas are tumors that contain tissues from all three germ layers,[92] which poses a potential complication for translation into human subjects. Human embryonic stem cells used for therapies would be of an allogenic source, which increases the chances of eliciting an immune response since the donor cells would not be immunologically identical to the recipient.[93]

Fortunately, an alternate pluripotent cell population for research was discovered that in many ways could address the ethical concerns associated with embryonic stem cells. In 2006 Kazutoshi Takahashi completely changed the stem cell field with the first publication on induced pluripotent stem cells (iPSCs).[94] For the first time, adult mouse fibroblasts were reprogrammed using a retrovirus and the result was a cell line that expressed the characteristics of mouse embryonic stem cells. It wasn't long before the research extended into human cells as well.[95] These iPSCs meet all of the requirements outlined for ESCs. [96] Now cells such as keratinocytes, T cells, fibroblasts, and cord blood cells among others are being reprogrammed to produce iPSCs.[2,79] Introduction of the required transcription factors for reprogramming can be delivered though viruses, proteins, plasmids, mRNAs, and other small molecules.[2,79] Even more than 10 years after the discovery of iPSC cells, they remain a complex and difficult cell type to expand and

differentiate in culture.[97,98] Even when using the same differentiation method to reprogram cells there are varying levels of efficiency making it difficult to reproduce results.[99] The main concern with utilizing iPSCs is their epigenetic memory of the DNA from the starting cell.[90,100] The hope is that iPSCs could be engineered to be patient and even disease specific torevolutionize regenerative medicine. [90]

2.2.3 Multipotent Stem Cells

Multipotent stem cells are capable of self-renewal and differentiation into multiple tissue types.[101,102] However, their differentiation is limited in comparison to totipotent and pluripotent stem cells. Often times they have finite self-renewal capabilities as well.[79] There are a variety of stem cells with multipotent properties including bone marrow-derived mesenchymal stem cells, adipose-derived stem cells, neural stem cells, mesenchymal cardiac-specific stem cells, fetal stem cells, amniotic stem cells, placental stem cells, hematopoietic stem cells, endothelial stem cells, and muscle-derived stem cells among others.[79,101,103–106] While there are numerous types of multipotent stem cells, this work will only focus on two populations of adult stem cells: bone marrow-derived mesenchymal stem cells (MSCs) and adipose-derived stem cells (ASCs).

Human bone marrow-derived MSCs and ASCs are adult, mesenchymal stem cells. Mesenchymal stem cells are uncommitted, nonhematopoietic progenitor cells that originate from mesoderm tissue and that can differentiate into multiple cell types under the appropriate stimulus.[107,108] These stem cells are found in the bone marrow, adipose tissue, periosteum, synovial cartilage, and deciduous teeth.[49,79,101,109] Mesenchymal stem cells are attractive for tissue engineering due to their ability to differentiate into

chondrocytes, osteocytes, adipocytes, fibroblasts, neural cells, or myoblasts based on culture conditions and growth factors.[107,110–112] Mesenchymal stem cells are also characterized by their fibroblast-like morphology, expression of the surface markers CD 44, CD73, CD90, and CD105 and lack the expression of CD14, CD34, and CD45.[79,107,113] In addition, adult mesenchymal stem cells have been found to have immunomodulatory properties, making them excellent options for tissue engineering applications.[79,114] Bone marrow-derived MSCs and ASCs have the same basic properties that are characteristic of all mesenchymal stem cells. However, there are a few key differences between these two stem cell populations. As their names would suggest, bone marrow-derived MSCs are harvested from bone marrow, while ASCs are harvested from adipose tissue.[79,101,107,113,115,116] Mesenchymal stem cells have finite life spans when cultured *in vitro*.[110] Studies have suggested that bone-marrow derived MSCs have a shorter culture life compared to ASCs.[8] In addition, while they are present throughout life, the concentration of the population of bone marrow-derived MSCs is inversely related to the age of the person.[110,114] Meanwhile, with the rate of obesity in the world today adipose-derived stem cells are readily available.[101] Adipose-derived stem cells can be harvested in greater quantities when compared to bone marrow-derived MSCs.[8] Finally, the harvesting of bone marrow-derived MSCs is also an invasive and painful procedure, whereas lipoaspiration is minimally invasive.[101,113] While both cell populations are viable candidates for regenerative medicine applications, ASCs appear to hold more promise due to their abundance and ease of collection.

2.2.4 Oligopotent and Unipotent Stem Cells

Oligopotent stem cells retain the ability to self-renew and differentiate into a limited number of lineages, typically two lineages.[79,117] These cell are found in adults and they differentiate into tissue specific lineages.[117] Oligopotent stem cells have been found on the ocular surface of mammals as well as in vascular tissue.[79,118] Unipotent cells are also referred to as precursor cells.[79] Unipotent cells can only differentiate into one cell type.[117] A population of stem cells found in the epithelium give rise to new skin cells and allows for skin to be grown *in vitro* for tissue grafts.[79] While oligopotent and unipotent stem cells play important roles in adults, they are not often utilized in tissue engineering and regenerative medicine due to their limited differentiation potential.

While stem cells have the potential to be powerful tools in tissue repair and regeneration, they are extremely complex cells. Not only do we have to understand the background of the stem cell type of interest, but we also need understand how the environment and growth factors affect differentiation. Combining these dynamic cells with a hydrogel scaffold that could provide the optimal environment for specific differentiation, is an attractive method to combat the need for tissues for repair and regeneration.

2.3 A Brief Overview on Hydrogels

Hydrogels are an advantageous approach to tissue engineering due to their chemical similarity to that of the extracellular matrix, their flexibility, rapid diffusion of hydrophilic nutrients and metabolites, as well as their low content of dry mass, which causes reduced irritation and much lower level of degradation products.[119] These

properties allow hydrogels to provide an environment that is similar to the ECM as well as provide additional structural support. Synthetic, natural, and synthetic/natural hybrid hydrogels are viable options for tissue engineering and appealing in their own ways.

2.3.1 Common Hydrogel Properties

Hydrogels were first introduced in 1960 by Wichterle and Lim when soft contact lenses were created from a hydrophilic network of poly(2-hydroxyethyl methacrylate) (pHEMA).[46,120] Hydrogels are three-dimensional, cross-linked polymer networks that tend to be very hydrophilic in nature.[46,120–122] Their innate properties and tailorability make them an attractive option for tissue engineering. Hydrogels tend to have viscoelastic and diffusion properties similar to those found naturally in the extracellular matrix (ECM).[123] Advances in biomaterials has led to the development of hydrogels made from numerous materials yielding a wide range of properties making it easier to tailor hydrogels to mimic the target tissue (**Figure 2-4**).[123] Depending on their chemical composition, hydrogels have the potential to absorb up to thousands of times their dry weight in water.[46,120] The hydrophilicity of a hydrogel determines the absorption and diffusion of solutes through the hydrogel, which can be crucial depending on their application.[120,122] The polymer networks of a hydrogel can be held together by hydrogen bonds, ionic forces, primary covalent cross-links, bio-recognition interactions, hydrophobic interactions, physical entanglements of polymer chains, polymer crystallites, or a combination of these.[46,120,124,125] There are different types of hydrogels that are classified based on their preparation and synthesis, charge, mechanical, and structural properties.[46]

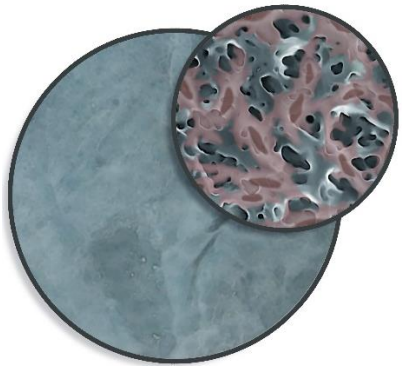

Figure 2-4: Graphical illustration of a hydrogel biomaterial. This figure illustrates the crosslinked hydrogel network (middle insert) along with an illustration of cells seeded onto the hydrogel surface (smallest callout). *Image credit: Rachel Eddy.*

Hydrogels can be composed of a number of different materials, all falling within three categories: natural polymers, synthetic polymers, or a combination of the two (semisynthetic) can be used in the formation of hydrogels.[120,122] Based on the material used and synthesis process hydrogels can be neutral in charge, cationic, anionic, or ampholytic.[124,126,127] Hydrogels may also be chemically stable and therefore permanent, or they can eventually degrade depending on how they are designed.[46] In addition, these polymer networks can be designed to be responsive networks. Most commonly hydrogels can be thermally-responsive, pH-responsive, and light-responsive.[128,129] They can also be sensitive to other environmental stimuli such as glucose, pressure, specific ions, enzymes and specific antibodies.[128] The highly tailorable nature of hydrogels is the drive behind the widespread use as a biomaterial in areas of research such as drug delivery, wound healing, agriculture, hygienic products, and tissue engineering.[120,121,125,127,130,131]

There are some limitations associated with hydrogels biomaterials. It is difficult to sterilize the materials if it is from a natural polymer and this is an important step if a material is to be implemented into the human body.[120] In addition, while hydrogels tend

to be biocompatible and many even bioinert, certain materials such as poly(ethylene glycol) (PEG) do not promote cell adherence,an issue in tissue engineering and wound healing.[132] However, PEG is bio-stealth and does not elicit an immune response.[130] Each polymer interacts differently with cells and it is important to keep that in mind when choosing a hydrogel composition. Hydrogel permeability can also be an issue dependent on application. For migration of cells it is advantageous, but could cause issues with controlled release of drugs or biomolecules.[133] What is likely the biggest disadvantage to hydrogels is their low mechanical strength.[134] This makes the materials harder to handle and limits how effective they will be in different environments in the body. Low mechanical strength limits hydrogel efficiency for bone regeneration but is advantageous for engineering soft tissues. Hydrogels can be composed of synthetic polymers, natural polymers, or a hybrid of the two. A brief overview of synthetic polymers is in the following sections. Overviews of natural and hybrid polymers is located in **Appendix A**.

2.3.2 Synthetic Hydrogels

Hydrogels composed of synthetic polymers are easier to reproduce and their chemical make-up and properties can be controlled through the synthesis process.[132] This information is summarized in **Table 2-1**. Hydrogels composed of poly(N-isopropylacrylamide (PNIPAAm), poly(ethylene oxide) (PEO), polyvinyl alcohol (PVA), poly(propylene fumarate-co-ethylene glycol) P(PF-co-EG) and polyphosphazenes are commonly studied synthetic hydrogels for tissue engineering.[119,132] PEO/PEG is currently FDA approved for numerous medical applications, and is one of the most commonly used synthetic hydrogels for tissue engineering.[132,135] The main disadvantage of PEG is that when it is formed into a triblock polymer, there is a lack of degradation.

Table 2-1. An overview of synthetic polymers used in making hydrogel biomaterials.

Polymer	Uses	Disadvantages	Advantages
PEO/PEG	Many	Lack of biodegradation	FDA approved; currently used in numerous medical applications; bio-inert
PVA	Space filling and drug delivery	Some formulations are not dissolvable in aqueous solutions	Bio-inert; higher mechanical strength and flexibility; hydroxyl groups to attach proteins/biological molecules
P(PF-co-EG)	Injectable carrier for bone and blood vessel engineering	Homopolymer (PPF) is hydrophobic polyester that undergoes degradation by hydrolysis of the ester linkage	Swelling ratios characteristic of highly crosslinked polymers with flexural moduli similar to the aorta suggesting promise in blood vessel engineering
PNIPAAm	Injectable delivery mechanism for cartilage and pancreas engineering	Nondegradable cross-links; vinyl monomers and crosslinking molecules are toxic, carcinogenic, and teratogenic	Inverse solubility upon heating
Polyphosphazenes	Controlled delivery of protein drug; possibility of use in skeletal tissue regeneration or encapsulation of hyridoma cells	Lack of rigorous reviews of material	Nontoxic, neutral degradation products

This lack of degradation can be altered if it is linked with a biocompatible material that degrades well in the body.[130,132] PVA has been used as a space filling agent in tissue engineering as well as drug delivery. PVA is bio-inert and has ample hydroxyl groups that allow for easy attachment of growth factors, proteins, or other biological molecules.[136] However, some formulations of PVA is not dissolvable in aqueous solutions. Poly(PF-co-EG) has been shown to have a swelling ratio characteristic of highly crosslinked polymers with flexural moduli similar to the aorta, suggesting promise in blood vessel engineering.[137] It has also been studied as an injectable carrier for bone and blood vessel engineering.[138] The homopolymer it is composed of, (PPF), is a hydrophobic, linear polyester that undergoes degradation by hydrolysis of the ester linkage.[137] PNIPAAm has been studied as a delivery mechanism for cartilage and pancreas tissue regeneration.[132,139,140] PNIPAAm has also been used as a molecular switch in thermoresponsive substrates due to its inverse solubility upon heating.[140,141] Unfortunately, the vinyl monomers and cross-linking molecules are potentially toxic, carcinogenic, and teratogenic.[128] Polyphosphazenes have the potential to be beneficial in skeletal tissue regeneration or for the encapsulation of hybridoma cells.[132,139] With all synthetic polymer hydrogels, there is always a slight chance of an immunogenic response since a foreign substance has been implemented into the body. This is why it is crucial to undergo *in vitro* and *in vivo* studies before implanting a scaffold of a substance with unknown biocompatibility into humans for clinical use.

2.3.3 PEG Based Hydrogels

Poly(ethylene glycol) or PEG is one of the most commonly utilized polymers for tissue engineering applications.[132] As previously mentioned, PEG is synonymous with

poly(ethylene oxide) (PEO), the only difference is the molecular weight being used.[130] One attraction for using PEG and PEG-based materials is that PEG is FDA approved and used in several medical applications.[130,135,139] PEG is a non-toxic polymer that is soluble in water as well as many organic solvents.[130,135] This polymer has minimal protein and cell adsorption so it is not recognized by the immune system and is therefore classified as bioinert.[31,121,130] It can also be rapidly cleared from the body.[130] PEG hydrogels are easily tailorable and can have a broad range in elasticity.[121] Taken together, these properties makes PEG-based hydrogels desirable when investigating the influence of material elasticity, spatial configuration, and surface chemistry treatments because the PEG hydrogels themselves are bioinert to cells. One notable feature of PEG is that when it is crosslinked with another molecules, it can transfer its properties to that molecule (i.e. make them non-toxic).[130] The biocompatibility and physiochemical properties of PEG is what makes this polymer and its derivates appealing for tissue engineering.[130,132,135]

2.3.4 Hydrogels in Tissue Engineering

Scaffolds for tissue engineering in many cases are used to initially fill a space that would normally be occupied by natural tissue. The scaffold's job is to provide the framework so the tissue can be regenerated. The physical properties of the scaffold are imperative for success. For hydrogels, the physical properties inherent to its success includes the gel formation dynamics, mechanical properties and its degradation behavior.[132] The hydrogel formation dynamics can alter the hydrogel morphology, structure, mechanical properties, and what cells, drugs, or biomolecules can be incorporated.[132,142] Hydrogels offer an exciting approach in that cells and molecules can be mixed with the hydrogel precursor solution to be injected *in vivo*.[143,144] The

mechanical properties of the hydrogel can be controlled by the polymer composition, the crosslinker type and density, swelling characteristics, and gelling conditions.[43,48,125,145,146] The kinetics behind the hydrogel scaffold degradation will be dependent upon the tissue engineering application. In an ideal scaffold, the hydrogel will degrade at a rate that matches that of new tissue formation.[132]

The mass transport properties and biological properties of the hydrogel scaffold are also important considerations in designing a tissue engineering scaffold.[147,148] The scaffolds need to allow for the appropriate transport of gases, nutrients, proteins, and waste into and out of the cell.[132,149] Diffusion properties are determined by the interaction of the cells, molecules, waste, etc. compared to the pore size in the hydrogel.[149] Knowing the pore size in the hydrogel scaffold becomes important when determining what substances can be transported. The hydrogel scaffold also needs to be able to promote desirable cellular functions for its specific applications while not causing an inflammatory response.[142] Thus, the biological properties of the hydrogel play a key role in success. Different polymers used to engineer hydrogel scaffolds have different biological properties, all with their own strengths and weaknesses.[132]

The unique and tailorable features of hydrogels make them an attractive candidate to minimize or eliminate the need for tissue and organ donors. These promising hydrogel scaffolds can provide molecularly tailored biofunctions, adjustable mechanical properties, and an environment that closely resembles the extracellular matrix to stimulate cell growth and tissue formation.[125] Hydrogel scaffolds in tissue engineering show promise in creating a renewable source of transplantable tissue with desirable tissue regeneration properties.[150]

CHAPTER 3

POLY (ETHYLENE GLYCOL) HYDROGEL ELASTICITY INFLUENCES HUMAN MESENCHYMAL STEM CELL BEHAVIOR

3.1 Permission for Publication

This chapter has been reproduced from *Regenerative Biomaterials* with permission from their publisher, Oxford Academic.

3.2 Introduction

Parallel advances in biologically mimicking (biomimetic) material constructs and in stem cell technologies enable the restoration and direct replacement of diseased cells and tissues. To achieve these outcomes clinically, fully functional cells and tissues must be produced on a large scale.[151] Despite advances in the design and synthesis of biomaterial scaffolds, one of the biggest obstacles facing tissue engineering is a lack of understanding regarding the influence of extracellular cues on cell proliferation and differentiation. The extracellular matrix (ECM) is a highly defined and specialized microenvironment, which is essential for tissue development and function. The ultimate decision of a cell to differentiate, proliferate, migrate, apoptose, or perform other

functions, is a coordinated response to the physical and chemical interactions with these ECM effectors.[55]

Matrix elasticity is one mechanical property of the ECM that differs between tissues and can be manipulated in synthesized scaffolds to enhance tissue engineering success and applications.[152] Several studies have demonstrated that matrix elasticity can influence stem cell behavior and differentiation toward certain lineages, indicating the power of physical environment on cell state.[75,153–158] Notably, Engler et al. initially demonstrated that lineage specification in stem cells can be directed by altering the elastic modulus of polyacrylamide (PA) gels, showing that elasticities of 0.1-1, 8-17, and 25-40 kPa influence mesenchymal stem cell (MSC) differentiation toward neurogenic, myogenic, and osteogenic lineages, respectively.[75] Later, Wen et al. systematically modulated the porosity, ligand density, and stiffness of PA hydrogels demonstrating that varying substrate porosity did not significantly change the osteogenic and adipogenic differentiation of human adipose-derived stromal cells and marrow-derived mesenchymal stromal cells. These findings imply that the stiffness of planar matrices regulates stem cell differentiation independently of protein tethering and porosity.[159] However, the influence of the many dynamic extracellular cues of scaffolds on stem cell proliferation and differentiation remains unclear. Understanding these interactions are paramount for the field of tissue engineering and regenerative medicine.

The importance of elasticity in influencing and directing cell behavior generates a need for tailorable biomaterial scaffolds. Hydrogel based biomaterials have rapidly become an attractive medium because their innate network closely resembles the structure of the extracellular matrix, their elasticity can be tailored, they allow for rapid

diffusion of hydrophilic nutrients, and they have a low content of dry mass, which reduces irritation and degradation.[160] These features allow the hydrogels to provide an environment that is like that of the *in vivo* environment, as well as provide additional control of the physical and mechanical properties affecting cellular proliferation and differentiation. To be effective, the hydrogel scaffold must be capable of promoting desirable cellular functions for its specific applications without causing an inflammatory response. Different polymers used to engineer hydrogel scaffolds have different biological properties, all with their own strengths and weaknesses. For example, polyethylene glycol (PEG) polymers are biocompatible and bio-inert in nature. While PEG has been studied for multiple applications the usefulness of PEG polymers for the formation of tailorable biomimetic scaffolds in tissue engineering and regenerative medicine has not been fully investigated.[161–163] However, PEG acrylates are popular polymers utilized as hydrogel biomaterials for tissue engineering applications.[164] Previously, we demonstrated the generation of biomaterial scaffolds of varying elasticity by implementing tailorable PEG hydrogels. Results showed that our hydrogel platform are compatible with multiple stem cell types, specifically mouse embryonic stem cells (mESC), human adipose stem cells (hASCs), and human bone marrow-derived mesenchymal stem cells (hMSCs).[48] Here, we further characterize the interactions of our hydrogel platform with hMSCs. Mesenchymal stem cells (MSCs) are adult, multipotent stem cells harvested from bone marrow, adipose tissue, umbilical cords, and muscle [49,165–167]. MSCs are known for their ability to differentiate into cell types of the mesoderm lineage, with their differentiation into adipogenic, osteogenic, and chondrogenic lineages being well described.[102,168] These cells have the potential to be patient specific and, with

several regenerative and immunosuppressive properties, clinically relevant, having been used in approximately 700 clinical trials. [169] MSCs are currently being investigated as potential cell sources to regenerate bone tissue, cartilage, ligament tissue, muscle, and adipose tissue.[170–174]

To analyze the interactions between bone marrow-derived hMSCs and a hydrogel platform, we selected two hydrogel compositions: 10% wt. PEG dimetharcylate (PEGDMA) Mw 1000 and 10% wt. PEGDMA Mw 20,000 and the 3% wt. PEGDMA Mw 1000 and 17% wt. PEGDMA Mw 20,000, which yield elastic moduli in the ranges of 50-60 kPa and 8-10 kPa, respectively. These two hydrogel compositions were chosen because they are at the upper and lower ends of the physiologically relevant elasticities. For conciseness, the hydrogels with an elastic modulus of 50-60 kPa are referred to as "stiff hydrogels" and the hydrogels with an elastic modulus of 8-10 kPa are referred to as "soft hydrogels". Expanding on our previous work, here we demonstrate the utilization of our PEG-based hydrogel blends to study the effect of elasticity on the characteristics and differentiation potential of bone marrow-derived MSCs.[48] We show that the hydrogels of different elasticities produce changes in hMSC morphology and proliferation, which provides support that the platform has the potential to produce changes in hMSC behavior and cell state. Furthermore, we find that the different elasticities can subtly influence stem cell differentiation potential, primarily in cell types of stiffer elasticity. Our findings enhance the fundamental understanding of stem-cell biomaterial interactions and open the door for the continued exploration of PEG-based hydrogel scaffold in tissue engineering and regenerative medicine.

3.3 Materials and Methods

3.3.1 Materials

Poly(ethylene glycol) dimethacrylate (PEGDMA) MW 1000 and MW 20,000 were purchased from Polysciences and were used as received. The ultraviolet (UV) photoinitiator, 2-hydroxy-1-[4-(hydroxyethoxy) phenyl]-2-methyl-1 propanone (I2959) and fibronectin were purchased from Sigma Aldrich. Methacrylate acid (MAA) was purchased from Fisher Scientific and was passed through a basic alumina column prior to use to remove inhibitor. Heptane was purchased from Fisher Scientific. 1-Ethyl-3-(3-dimethylaminopropyl) carbodiimide (EDC), sulfo- N-hydroxysulfosuccinimide (sulfo-NHS), 2-(N-morpholino) ethanesulfonic acid (MES) Buffer, and 1X Phosphate Buffer Saline (PBS) were purchased from Thermo Fisher Scientific.

Human MSCs were provided by Dr. Bruce Bunnell from Tulane University. Adipogenic differentiation media and osteogenic differentiation media were purchased from LaCell. MEM α, L-Glutamine, Penicillin Streptomycin, ReadyProbes® Cell Viability Imaging Kit (Blue/Red), Alexa Fluor 555 Phalloidin, and TRIzol reagent were purchased from ThermoFisher Scientific. Fetal Bovine Serum (FBS) was purchased from Atlanta Biologicals. Formalin was purchased from Azer Scientific. Triton X-100 was purchased from Alfa Aesar. Methanol was purchased from VWR. BSA was purchased from Amresco. qScript cDNA SuperMix was purchased from Quanta Biosciences. Powerup SYBR green master mix was purchased from Applied Biosystems. AlamarBlue® reagent, and 4',6-Diamidino-2-Phenylindole, Dihydrochloride (DAPI) was purchased from ThermoFisher Scientific.

3.3.2 Hydrogel Preparation

Hydrogel solutions for the "stiff" hydrogels (10% wt. PEGDMA Mw 1000 and 10% wt. PEGDMA Mw 20,000) and the "soft" hydrogels (3% wt. PEGDMA Mw 1000 and 17% wt. PEGDMA Mw 20,000) were prepared in deionized water (DH_2O) as previously reported[7]. 0.1% wt. UV photoinitiator, 2-hydroxyl-1-[4-(hydroxyl) phenyl]-2-methyl-1 propanone (I2959), which is below concentrations previously determined to be cyto-compatible[175] and 2% wt. MAA was added to the hydrogel solution. Solution was sonicated for 20 minutes and then pipetted in between two photomasks separated by 0.55mm stripes of teflon and UV polymerized at a wavelength of 365 nm and an intensity of ~ 34 mW/cm^2. Stiff and soft hydrogels were UV polymerized for 10 minutes and 20 minutes, respectively. The hydrogels were then rinsed for 10 days in DH_2O (periodically changed) to remove any un-reacted polymer or monomer. Prior to cell culture, hydrogels were functionalized with fibronectin via EDC/Sulfo-NHS chemistry as previously described.[48]

3.3.3 Characterization of Hydrogel Swelling

Hydrogel swelling studies were performed as previously reported.[176,177] After UV polymerization, hydrogel films were cut into ~19.5 mm discs and were weighed in air as well as in heptane (a solvent the PEG hydrogels will not swell in) to obtain the volume of the hydrogels immediately after UV-polymerization. The hydrogels were then rinsed for 10 days in DH_2O (periodically changed) to remove any un-reacted polymer. Hydrogel discs were then dried for 5 days under vacuum and subsequently weighed to obtain dry (or polymer) mass. The dried hydrogels were then swollen for 48 hours in DH_2O to

reach swollen equilibrium. The polymer volume fraction in the swollen state, $\nu_{2,s}$ and relaxed state $\nu_{2,r}$ was calculated from the measured hydrogel mass in air and in heptane:

$$v_{2,s} = \frac{W_{a,d} - W_{n,d}}{W_{a,s} - W_{n,s}} \quad \textbf{Eq. 3-1}$$

$$v_{2,r} = \frac{W_{a,d} - W_{n.d}}{W_{a,r} - W_{n.r}} \quad \textbf{Eq. 3-2}$$

where $W_{a.d}$ is the hydrogel weight in dry state in air, $W_{n.d}$ is the hydrogel weight in dry state in heptane, $W_{a.s}$ is the hydrogel weight in swollen state in air, $W_{n.s}$ is the hydrogel weight in swollen state in heptane, $W_{a.r}$ is the hydrogel weight in the relaxed state in air, and $W_{n.r}$ is the hydrogel weight in the relaxed state in heptane. The equilibrium volume swelling ratio (Q) was calculated by comparing the ratio of the equilibrium swollen volume with the polymer volume at the dry state.[175] Pore sizes were determined using the equation:

$$\xi = v_{2,s}^{-1/3} \left(\frac{2C_n M_c}{M_r}\right)^{1/2} l \quad \textbf{Eq. 3-3}$$

Where ξ is the pore size, $v_{2,s}$ is the polymer volume fraction in the swollen state, C_n is Flory characteristic ratio, M_c is the average molecular weight between crosslinks, M_r is the molecular weight of the monomer, and l is the bond-length along the backbone chain. The M_c is found by using the Merrill and Peppas equation:

$$\frac{1}{M_c} = \frac{2}{M_n} - \frac{\left(\frac{\bar{v}}{V_1}\right)\left(\ln(1-v_{2,s}) + v_{2,s} + \chi_1 v_{2,s}^2\right)}{v_{2,r}\left(\left(\frac{v_{2,s}}{v_{2,r}}\right)^{\frac{1}{3}} - \left(\frac{v_{2,s}}{2v_{2,r}}\right)\right)} \quad \textbf{Eq. 3-4}$$

Where M_n is the number average molecular weight of the uncrosslinked polymer, v is the specific volume of the polymer, $V_1$is the molar volume of the water, $v_{2,r}$ is the polymer volume fraction in the relaxed state, and χ_1 is the polymer-solvent interaction parameter.

3.3.4 Maintenance of hMSCs

Human MSCs were cultured on 10 cm polystyrene tissue culture dishes in maintenance medium containing MEM α, L-Glutamine, penicillin streptomycin and 16.5% FBS. The cells were incubated at 37°C with 5% CO_2.

3.3.5 Osteogenic and Adipogenic Differentiation

Human MSCs were seeded on tissue culture plates and soft hydrogels at a density of 2.0x103 cells/cm2 and grown until 80% confluence. Due to decreased proliferation of hMSCs on stiff hydrogels, hMSCs were seeded on these specific gels at 4.0x103 cells/cm2 and attached at 80% confluence. The appropriate differentiation media (adipogenic differentiation media or osteogenic differentiation media) was added to the cells in all cases when cells demonstrated 80% confluence. Differentiation media was changed every 72 hours until time point for analysis.

3.3.6 Cell Viability Assay

Cell viability was determined using the ReadyProbes® Cell Viability Imaging Kit (Blue/Red) and imaged on the EVOS FL imaging system. Assay was done following manufacturer's protocol.

3.3.7 F-actin Staining

Alexa Fluor 555 Phalloidin was dissolved in methanol to create a stock solution with a final concentration of 200 units/mL. The final staining solution contained a 1:40 ratio of Methanolic stock to PBS, with 1% BSA. Cells were protected from direct light and incubated in staining solution for 15 minutes. DAPI was added to each well at a final concentration of 1:2000 and incubated for an additional 5 minutes. Cells were washed with PBS three times and imaged.

3.3.8 Cell Attachment Studies

Human MSCs were seeded at a density of $2.0x10^3$ cells/cm^2 per sample and allowed to attach for 18 hours. Cells were fixed with formalin and permeabilized with 0.2% Triton X-100. Cells were incubated in a 1:1000 solution of DAPI and blocking buffer (0.2% Triton X-100 and 1% wt. BSA in 1X PBS) for 10 minutes. Cells were washed with PBS three times, and 500µL of PBS was added to each well for imaging. The fluorescence was visualized and imaged using the EVOS FL cell imaging system. Three images were taken per well (top, middle, and bottom). ImageJ was used to count the nuclei per image. The average of the three images was taken for each sample.

3.3.9 Quantitative RT-PCR

RNA was collected and extracted from each cell type using TRIzol reagent following the manufacturer's protocol. The RNA was quantified using a Take3 plate on a BioTek plate reader. RNA concentrations used for cDNA synthesis are shown in Table S1. Due to low RNA concentrations in undifferentiated MSCs, each sample for that experiment was a pool of three wells from a 24-well plate. cDNA was synthesized following the protocol provided by Quanta Biosciences for their cDNA SuperMix kit.

The expression levels for each marker were quantified by qRT-PCR according to the manufacturer's protocol on an Applied Biosystems StepOne Plus instrument. Each reaction was performed in triplicate for every sample and the relative expression levels were determined by normalizing to *gapdh.*

3.3.10 AlamarBlue™ Assay

$4.0x10^3$ hMSCs were seeded on all three surface types and grown under standard conditions for 72 hours. At 72 hours, alamarBlue® reagent was added to culture media at 10% of the sample volume. Blanks for each sample were prepared by adding equivalent amounts of culture media and alamarBlue® reagent to wells containing corresponding elasticity conditions, without hMSCs. Samples were incubated at 37ºC and protected from direct light. Readings were taken at 1, 2, 3, 4, and 24 hours post alamarBlue® reagent introduction. Fluorescence was measured at excitation 560/emission 590 using a BioTek plate reader.

3.3.11 Statistical Analysis

All data are expressed as mean with error bars representing standard error (SE) for all quantitative comparison experiments. Statistical analysis was carried out via one-way analysis of variance (ANOVA) tests, using SPSS software v 24. $p < 0.05$ was considered statistically significant. Significant results were further analyzed via Tukey HSD post-hoc test and a p-value < 0.05 was considered significant.

3.4 Results

3.4.1 Characterization of Hydrogel Swelling

Swelling behavior of the synthesized stiff (50-60 kPa) and soft (8-10 kPa) hydrogels was measured to determine the average molecular weight between crosslinks,

network pore size, and swelling ratio using standard swelling protocols reported previously. The results are summarized in **Table 3-1**.

While the total percent polymer was held constant at 20% wt. the amount of Mw 1000 and Mw 20000 was varied to create more elastic hydrogels. As expected, the molecular weight between crosslinks and the pore sizes was larger in the soft hydrogels compared to the stiff hydrogels. The equilibrium swelling ratio (Q) of the soft hydrogel formulations is twice that of the stiff hydrogels.

Table 3-1. Pore sizes of Stiff and Soft Hydrogels. *Reprinted with permission from Oxford Academic.*

	Composition	**Elastic Modulus (kPa)**	**$V_{2,r}$**	**$V_{2,s}$**	**Mc (g/mol)**	**Q**	**ζ (Å)**
Stiff Hydrogels	10% MwPEGDMA 20,000 / 10% PEGDMA Mw 1000	50-60	0.18 ± 5.11E-3	0.094 ± 2.31E-3	1379.11 ± 50.98	10.58 ± 0.26	52.58 ± 1.34
Soft Hydrogels	17% MwPEGDMA 20,000 / 3% PEGDMA Mw 1000	8-10	0.19 ± 7.71E-3	0.043 ± 1.72E-3	4691.12 ± 130.88	23.45 ± 0.91	127.82 ± 3.21
Patel et al. reference hydrogels	20% Mw PEGDMA 1000	388-390	0..24 ± 0.01	0.18 ± 1.30E-3	256.13 ± 8.32	5.56 ± 0.04	17.77 ± 0.32

3.4.2 hMSC Attachment to Hydrogels

Bone marrow-derived hMSCs were seeded on the hydrogel scaffolds and after 72 hours a viability assay was performed to determine if the cells survived on each of the

three elasticity conditions: tissue culture plates, soft hydrogels, and stiff hydrogels. Based on propidium iodide staining (dead cells stained red), we observe few, if any, dead cells on each of the elasticity conditions (**Figure 3-1A).** The difference in image brightness observed from the stiff hydrogels is attributed to the decreased porosity, which further obstructs visualization. The difference in brightness does not alter the number of live/dead cells.

Cell morphology can be an indicator of cellular state, and changes to this morphology could indicate changes in cell behavior. Therefore, F-actin filaments of cells cultured on all three elasticity conditions were stained and visualized (**Figure 3-1B**). Cells on the soft hydrogels maintained similar morphology to the tissue culture plate controls. In contrast, hMSCs cultured on stiff hydrogels displayed a more elongated morphology than mesenchymal stem cells cultured on tissue culture plates or soft hydrogels.

ImageJ software was used to analyze the images from the F-actin staining experiment to further confirm differences in cell number observed between the three elasticity conditions. The number of DAPI stained nuclei in each image was counted and the average of three samples per condition type was determined. Importantly, all hMSCs shown in Figure 1B were seeded at the same density, cultured for 72 hours, and analyzed at the same exposure. As mentioned above, the differences in image brightness observed from the stiff hydrogels is attributed to the decreased porosity, which further obstructs visualization when viewed through an inverted microscope. The difference in brightness does not affect the cell count, as ImageJ was still able to differentiate individual nuclei (**Figure 3-1C**). The cell count analysis revealed a significant difference in the number of

nuclei on stiff hydrogels compared to the tissue culture plate control, but no significant difference between the soft gels and that same control was observed (**Figure 3-1D**).

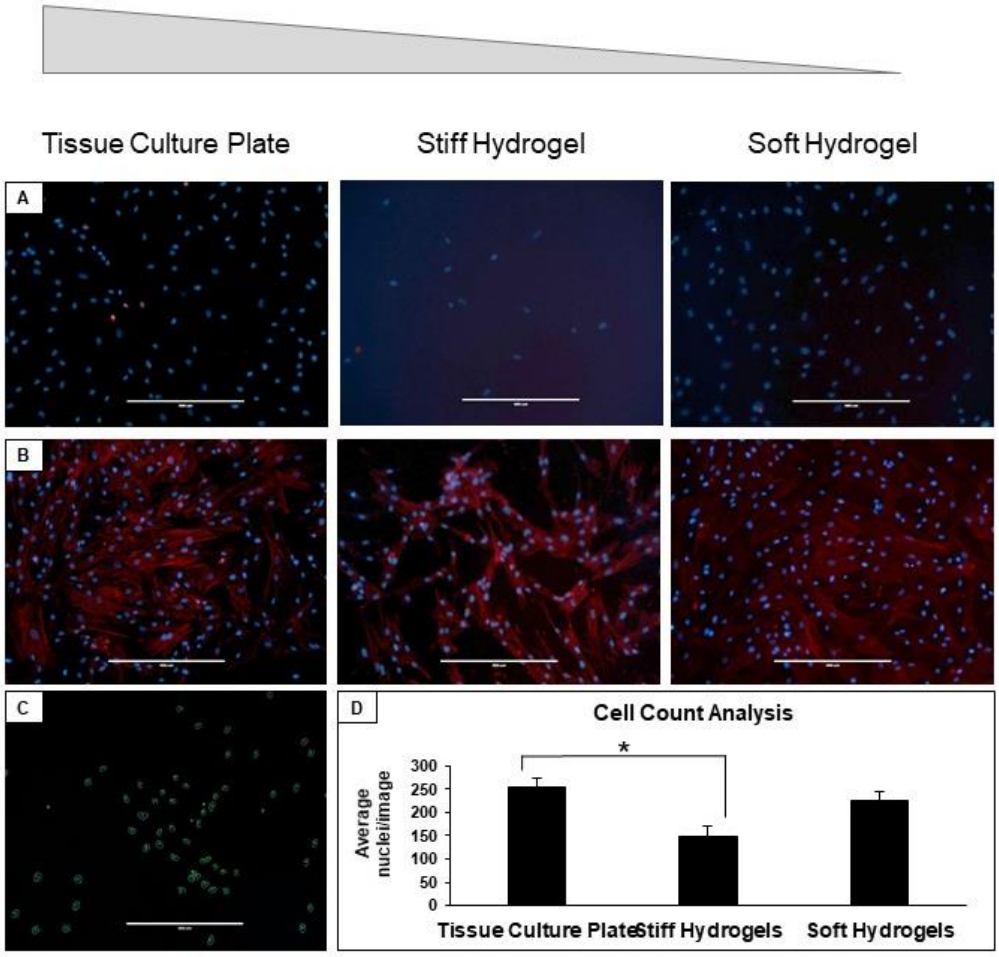

Figure 3-1: hMSCs attach to and survive on the different hydrogel compositions. A) Viability assay of hMSCs cultured on tissue culture plates, stiff hydrogels, and soft hydrogels for 72 hours. Live cell nuclei are shown in blue, while dead cell nuclei are shown in red. B) Morphology of hMSCs cultured on the three surfaces for 72 hours. The cell nuclei are shown in blue, while the F-Actin filaments are shown in red. C) Visual depiction of ImageJ analysis highlighting nuclei for count. D) Cell count results from ImageJ quantification of cells seeded for 72 hours. *= Tukey HSD resulting $P < 0.05$. n=3. Scalebars: 400µm. *Reprinted with permission from Oxford Academic.*

To determine if this difference in cell number was the result of a difference in initial cell attachment, the number of adherent cells was counted 18 hours after seeding. ImageJ analysis of DAPI stained cells on each surface revealed a significant increase in the number of cells attached to both soft and stiff hydrogels compared to the tissue culture plate control. This indicates that attachment is not responsible for the decrease in the number of cells present on the hydrogels after 72 hours. Alternatively, differences in rate of proliferation could explain a difference in cell number. An alamarBlue assay was utilized as an indicator of cellular proliferation, and the results show significantly less metabolic activity in cells cultured on stiff hydrogels compared to soft hydrogels and tissue culture plates at 3, 4, and 24 hours. At 24 hours, metabolic activity was significantly higher in cells cultured on tissue culture plates compared to both stiff and soft hydrogels. Given that proliferation is slower on the stiff hydrogels, the expression of the multipotency marker *sox2* was analyzed to see if there were significant changes in multipotency. Cells were seeded at the same density on each surface and cultured for 72 hours before collecting RNA. Results of qRT-PCR of *sox2* (**Figure 3-2E**) indicates that there is no statistically significant difference in expression levels between each surface, demonstrating that the elasticity conditions do not immediately influence the levels of certain multipotency transcription factors.

3.4.3 Effect of Elasticity on hMSC Osteogenic Differentiation

To be useful in tissue engineering and regenerative medicine, biomaterial scaffolds must be able to support and potentially direct stem cell differentiation toward desired lineages. Elasticity can play a role in directing stem cell state, thus the effects of the hydrogel elasticities on hMSC differentiation towards an osteogenic lineage were

investigated. Osteogenic differentiation was chemically induced in hMSCs seeded on all three elasticity conditions, and morphology was analyzed using phase contrast microscopy (**Figure 3A**). Due to the limited visibility in phase contrast images with hydrogels, phalloidin staining was also used to visualize F-actin filaments (**Figure 3B**). There was noticeable differentiation and calcium deposition on all three elasticity conditions. qRT-PCR of osteogenic markers *runx2* and *alp* (**Figure 3C**) was performed on samples collected at Day 7 of differentiation.

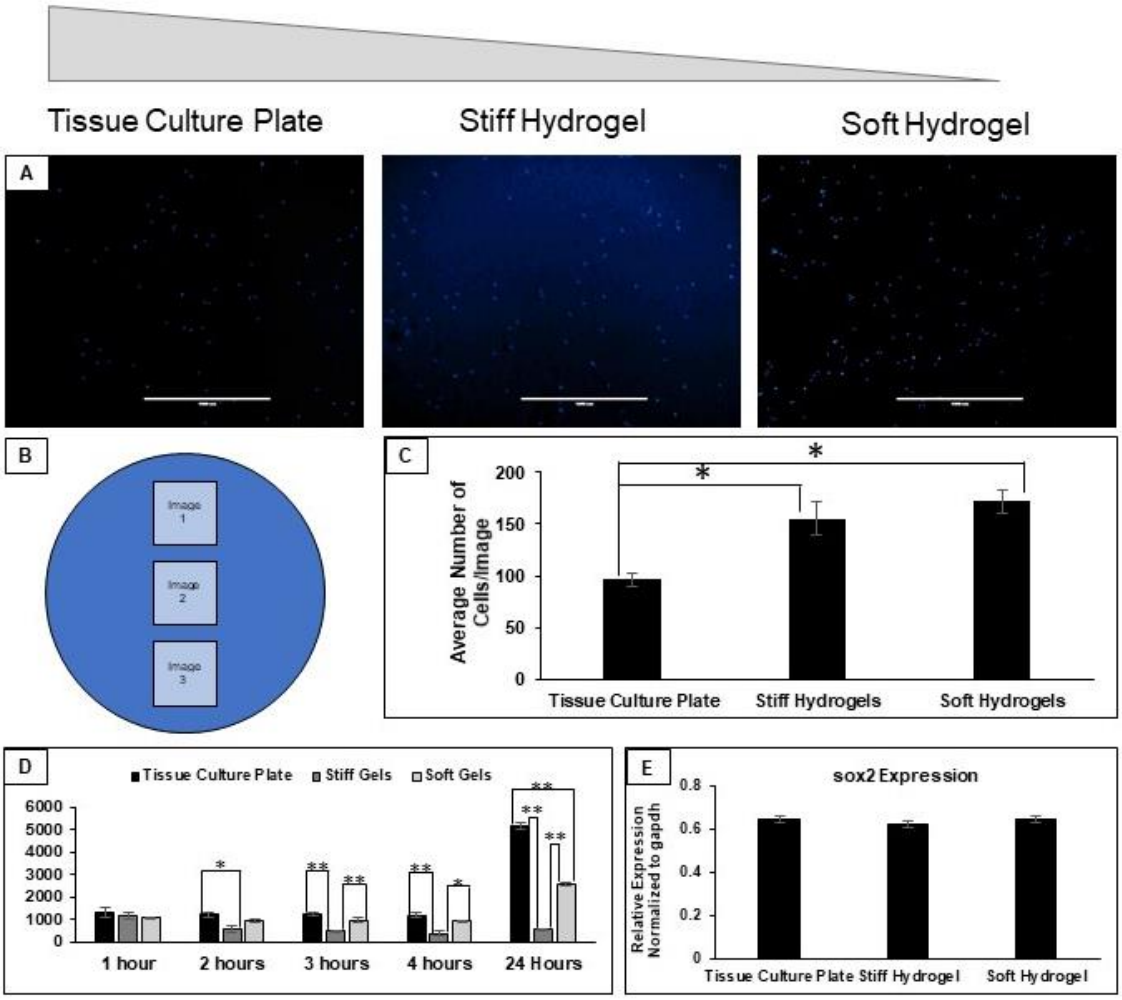

Figure 3-2: hMSCs attach more readily to hydrogels, but display decreased proliferation, despite equal expression of sox2. A) Example images of DAPI stain hMSCs 18 hours post-seeding on the different surfaces. B) Schematic representation of imaging method used for attachment studies. Three images were taken (as shown in panel A) of each sample, with three samples per surface. C) Results of ImageJ quantification of nuclei per image. D) Results of AlamarBlue analysis of hMSCs cultured on each surface. AlamarBlue was added after cells were cultured for 72 hours, and timepoints shown in graph represent hours after AlamarBlue introduction. E) Quantitative Reverse-Transcriptase PCR analysis of *sox2* expression in hMSCs cultured on surfaces for 72 hours. *= Tukey HSD resulting $P < 0.05$. **= Tukey HSD resulting $P < 0.01$. n=3 for C, D, and E. Scalebars: 1000µm. *Reprinted with permission from Oxford Academic.*

Analysis indicated no significant differences in the early osteogenic differentiation marker *runx2* expression in hMSCs cultured on each surface. However, there were significant differences in *alp* expression, an early marker of osteogenesis, between soft hydrogels and stiff hydrogels ($P<0.05$), between soft hydrogels and tissue culture plates ($P<0.05$), and between stiff hydrogels and tissue culture plates ($P<0.01$).

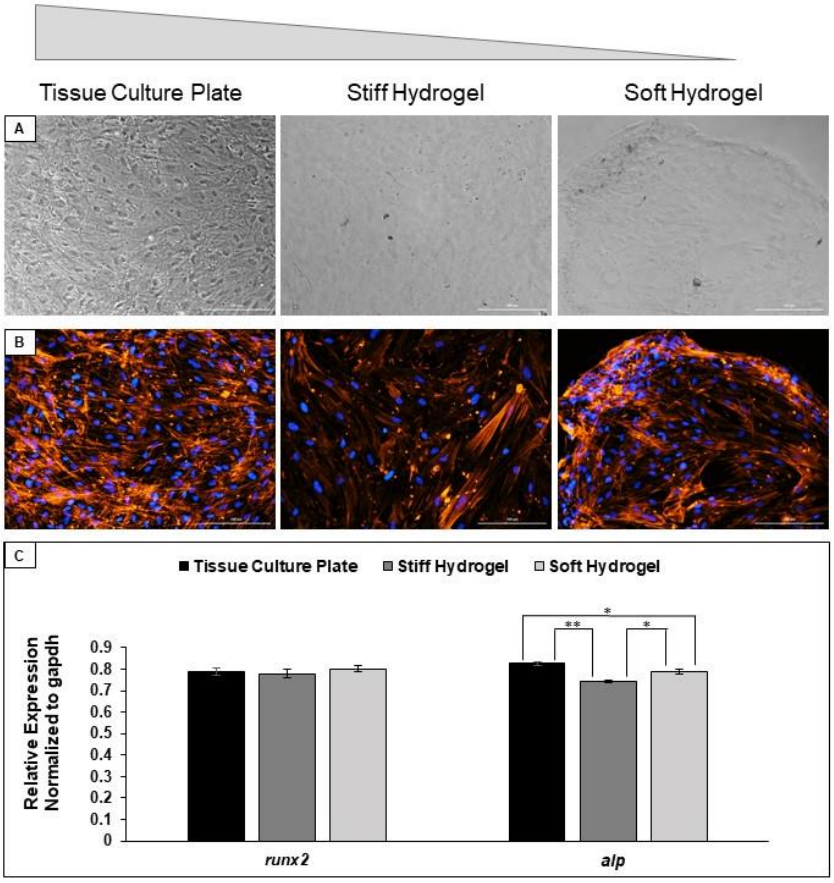

Figure 3-3: hMSCs retain the ability to differentiate toward osteogenic lineages on all surfaces**.** A) Phase contrast images of hMSCs at Day 7 of osteogenic differentiation. B) Morphology of hMSCs at Day 7 of osteogenic differentiation, corresponding to the phase contrast images in Panel A. The cell nuclei are shown in blue, while the F-Actin filaments are shown in orange. C) Quantitative Reverse-Transcriptase PCR analysis of the osteogenic differentiation markers *runx2* and *alp* in hMSCs at Day 7 of osteogenic differentiation. *= Tukey HSD resulting $P < 0.05$. **= Tukey HSD resulting $P < 0.01$. n=3 for C, D, and E. Scalebars: 200µm. *Reprinted with permission from Oxford Academic.*

3.4.4 Effect of Elasticity on hMSC Adipogenic Differentiation

Since hMSCs also have the potential to be used for adipogenic tissue regeneration, we further assessed adipogenesis of these cells on each of the selected surfaces. Adipogenic differentiation was chemically induced in cells seeded on all three elasticity conditions, and morphology was analyzed using phase contrast microscopy (**Figure 3-4A**). As in the previous set of experiments, phalloidin staining was used to visualize F-actin filaments and provide higher resolution images of cell morphology (**Figure 3-4B**).

Noticeable differentiation had taken place on each surface, with round globules, some of which are indicated by green arrows in Figures 4A and 4B, indicating vacuoles and adipogenic differentiation. Phalloidin staining of the cells shows that in areas where lipid vacuoles formed there is a decrease in F-actin filaments. This trend is seen on tissue culture plates, soft hydrogels, and stiff hydrogels. qRT-PCR of early adipogenic markers *ppar-y* and *srebp1c* was performed on samples collected at Day 7 of differentiation. Analysis indicates no significant differences in expression of these early adipogenic markers between each surface.

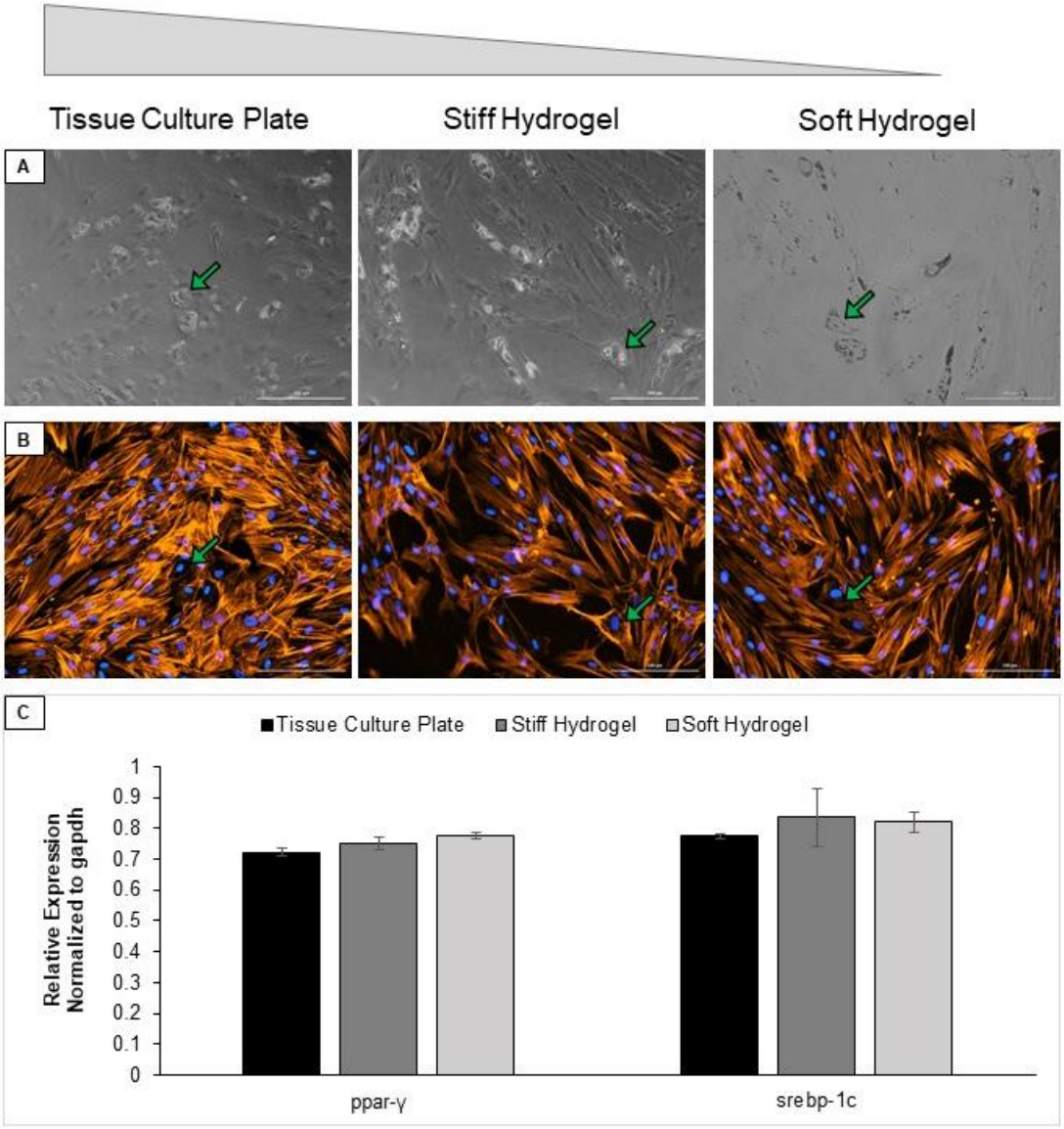

Figure 3-4: hMSCs retain the ability to differentiate toward adipogenic lineages on all surfaces. A) Phase contrast images of hMSCs at Day 7 of adipogenic differentiation. B) Morphology of hMSCs at Day 7 of adipogenic differentiaition, corresponding to the phase contrast images in Panel A. The cell nuclei are shown in blue, while the F-Actin filaments are shown in orange. Cells containing lipid vesicles demonstrated a rearrangement of F-Actin filaments, indicated by green arrows. C) Quantitative Reverse-Transcriptase PCR analysis of the adipogenic differentiation markers *ppar-γ* and *srebp1-c* in hMSCs at Day 7 of adipogenic differentiation. Results considered insignificant with $P > 0.05$. n=3. Scalebars: 200µm. *Reprinted with permission from Oxford Academic.*

3.5 Discussion

Previously, we demonstrated that PEGDMA hydrogels with elasticities within a physiologically relevant range (8-60 kPa) can be generated by varying the molecular weight of the polymer [48]. Here, we characterized hydrogels at the upper and lower ends of this range, specifically in terms of their swelling behavior and interactions with hMSCs. The swelling behavior of the hydrogels was used to determine the molecular weight between crosslinks (M_c), the pore sizes (ξ), and the equilibrium swelling ratio (Q). All three, as predicted were lower in the stiff hydrogels as compared to soft hydrogels. Variability in the swelling characteristics between the two samples was attributed to the higher percentage of PEGDMA Mw 20,000 within the soft hydrogels (**Table 3-1**). Next, we characterized hMSC interactions when cultured on the stiff and soft hydrogels. As the largest pores are nanometers in size and hMSCs have an approximate diameter range of 17.9 μm to 30.4 μm, there is no penetration of hMSCs into the hydrogel network. Thus, hMSCs are cultured two-dimensionally on the surface of these hydrogels.

When seeded on both soft and stiff hydrogels, hMSCs were shown to attach and remain viable (**Figure 3-1A**), further confirming the potential of this platform for use in cell culture and tissue generation. However, changes in morphology were observed in cells cultured on the different elasticities. Human MSCs cultured on the soft hydrogels maintained similar morphology to the tissue culture plate controls. In contrast, hMSCs cultured on stiff hydrogels displayed a more elongated morphology as compared to hMSCs cultured on tissue culture plates or soft hydrogels (**Figure 3-1B**). These differences in morphology could indicate a change in cell behavior, such as spontaneous

differentiation. Furthermore, there appeared to be consistently fewer hMSCs on the stiff hydrogels after 72 hours of culture. ImageJ quantification of the hMSCs shown in Figure 1B revealed significantly fewer cells on the stiff hydrogels (**Figure 3-1D**). The decrease in hMSCs could be the result of decreased attachment to the stiff hydrogels. However, attachment analysis 18 hours after seeding actually revealed an increased number of hMSCs attached to both hydrogel elasticities compared to tissue culture plate indicating that the difference is a result of changing cell behavior after attachment (**Figure 3-2A**).

AlamarBlue assays demonstrated that proliferation is significantly decreased in the cells cultured on either soft or stiff hydrogels. Human MSC proliferation on stiff hydrogels was shown to be significantly decreased 3-hours after the introduction of AlamarBlue. The differences in morphology and proliferation observed in hMSCs cultured on stiff hydrogels could be an indication of spontaneous differentiation. Quantitative RT-PCR analysis of the multipotency marker *sox2* revealed no significant differences in expression across the three elasticity conditions. However, further analysis of multipotency markers and markers of possible differentiation lineages could reveal that a subtle amount of spontaneous differentiation has taken place or longer time course studies may demonstrate more significant changes in multipotency. For the scope of this study, the differentiation potential of hMSCs on the three elasticity conditions was analyzed through chemically induced differentiation toward osteogenic and adipogenic lineages, rather than exploring the long-term effects of maintenance on each of these surfaces.

On all three elasticity conditions, hMSCs cultured in osteogenic differentiation media differentiated toward the osteogenic lineage, as evidenced by calcium deposition

and expression of bone specific markers. There was no significant difference in *runx2* expression, which is an essential transcription factor for osteoblastic differentiation (**Figure 3-3C**). However, there was a significant decrease in *alp* expression in hMSCs cultured on both hydrogel elasticities (**Figure 3-3C**). While lower levels of *alp* expression could indicate decreased osteogenesis, given the observation of calcium deposition and cell morphology, it is also possible that a decrease in *alp* expression is an indication of more rapid maturation of the resulting cells.

hMSCs cultured in adipogenic differentiation media also retained the ability to differentiate toward adipogenic lineages on all three elasticity conditions. hMSCs on all three elasticity conditions began forming lipid vesicles characteristic of adipogenic differentiation (**Figure 3-4A&B**). There was no significant difference in the expression of two key transcription factors involved in adipogenesis, *ppar-γ* and *srebp1-c*. Ultimately, no difference in hMSC differentiation toward adipogenic lineages was observed.

In summary, the data from this study gives insight into the properties and stem cell interactions of our previously established hydrogel platform, an inexpensive, highly tailorable platform that can be adapted to any number of cell-material interaction studies and applications. Changes in hMSC morphology and proliferation were observed in cells cultured on hydrogels, primarily those cultured on stiff hydrogels. These results demonstrate that the elastic tailorability of this hydrogel platform can produce changes in hMSC behavior and cell state, indicating a potential for these hydrogels to be used to generate a controlled environment for cell culture and tissue regeneration applications. Furthermore, based on the differentiation studies, the different hydrogel elasticities have

subtle effects on stem cell differentiation. This effect is observed primarily in osteogenic differentiation, which could indicate that cell lineages of higher elasticity are more susceptible to elasticity changes. The results of this study further suggest that the hydrogel platforms do affect stem cell behavior, opening the door to future investigations of the platform's potential for controlling stem cell fate. Better understanding of the biomaterial scaffolds utilized in regeneration, such as the studies shown here, is essential in optimizing their translational and clinical potential.

CHAPTER 4

POLY (ETHYLENE GLYCOL) HYDROGEL SCAFFOLDS WITH MULTISCALE POROSITY FOR CULTURE OF HUMAN ADIPOSE-DERIVED STEM CELLS

4.1 Permission for Publication

This chapter has been reproduced from the *Journal of Biomaterial Science, Polymer Edition* with permission from their publisher, Taylor and Francis.

4.2 Introduction

Parallel advances in biomimetic materials and stem cell technologies have the potential to enable the restoration and direct replacement of diseased cells and tissues.[125,178,179] Hydrogels are attractive material platforms for biomanufacturing because of their high biocompatibility,[120,180,181] hydrophilicity,[182,183] tissue-like architecture,[150,184] and innate biomimetic properties.[160] Hydrogel materials have become an important tool in developing better tissue engineering scaffolds because of their ability to provide structural support and high tissue density, while still closely resembling the *in vivo* environment.[125,132,185]

A significant portion of stem cell research has involved the use of immortalized or primary murine cell models for metabolic, pharmaceutical, and regenerative medical

studies. While murine and other rodent models are invaluable, they fail to accurately mimic human physiology and pathology at the cellular and molecular levels. Due to inter-species biological variability these stem cell sources will ultimately fail to achieve clinical translational milestones. Human adipose-derived stem cells (hASCs) are a promising, reliable cell source because they can be directly harvested from the patient's own adipose tissue making them patient-specific and clinically relevant. Human ASCs are an abundant source of adult multipotent stem cells.[41] This cell source can be easily and readily harvested from patients through minimally invasive lipoaspiration and are present in larger quantities when compared to bone marrow-derived mesenchymal stem cells (MSCs).[49,186] Like mesenchymal stem cells, adipose-derived stem cells are easily maintained in culture and have the potential to be directed towards osteogenic, chondrogenic, adipogenic, and myogenic lineages making them an ideal cell source for autologous tissue scaffolds.[49,187]

Cells are highly sensitive to their surroundings. The defined and specialized cell microenvironment, which is essential for tissue development and function, is the extracellular matrix (ECM).[53,54] The ECM can effect cell behavior by directly regulating cell functions through receptor-mediated signaling, and this network can control the mobilization of growth factors or differentiation factors.[53] This means that the ultimate decision for a stem cell to differentiate, proliferate, migrate, apoptose, or perform other functions, is a coordinated response to the molecular interactions with these ECM effectors.[55]

For an engineered biomaterial to be a successful tissue construct and support tissue growth and/or repair, it must support the formation of tissue-relevant mimics, as

well as promote cell attachment, cell migration, foster transport of nutrients and waste, and form new ECM.[57] Since the ECM is critical in cell proliferation and differentiation, tissue engineering approaches have widely explored exogenous three-dimensional ECM's to engineer new tissues from isolated cells.[58] Synthetic ECMs should facilitate the localization and delivery of cells to specific sites in the body, maintain a 3D space for the formation of new tissues, and guide the development of new tissues with appropriate functions.[53,58,59] Synthetic ECMs need a large surface-to-volume ratio to allow for a high density of cells. Since the ECM varies in different tissues and at different stages of development, choosing the appropriate mechanical and degradative properties are important.[54] Therefore, the chemical and physical properties of the biomaterial used in tissue engineering plays an important role as it can serve as a substrate for attachment, be used as a cell delivery vehicle, and activate specific cellular functions in localized regions.[60]

Hydrogels are three-dimensional crosslinked polymer networks widely studied for various biomedical applications including targeted drug delivery,[183] wound healing bioadhesives,[188] artificial skin,[189] articular cartilage,[190] biomanufacturing,[191] and tissue engineering.[125] A variety of natural and synthetic polymers have been used to synthesize hydrogels.[192] Of these, poly(ethylene glycol) (PEG) is FDA approved and widely used for commercial medical applications.[193] PEG hydrogels have been a popular choice of synthetic biomaterial for regenerative medicine applications for decades.[194] The innate PEG properties, such as hydrophilicity, biocompatibility, and non-ionic nature[194] allows for its use in medicine.[195] Most notable is the non-fouling, stealth properties of PEG which prevents proteins and cells in the body from interacting with the polymer,

eliminating immune reactions *in vivo.*[188,194] The non-degradability of pure PEG hydrogels creates a stable platform for examining material properties and cell-material interactions *in vitro.*[43,48] Photo-crosslinkable PEG derivatives such as poly(ethylene glycol) dimethacrylate (PEGDMA) have been utilized for the generation of a vast number of applications including coatings,[196] adhesives,[197] shape memory development,[198,199] and 3D bioprinting.[200,201] Dimethacrylate groups on PEGDMA allow for branched covalent crosslinking; this increases hydrogel network integrity[202] and surface functionalization potential providing application specific tailorability.[43,48]

The pore size of the hydrogel network is dependent on the starting polymer molecular weight, crosslinking density, and hydrophobic interactions incorporated during the synthesis process.[203] Altering the molecular weight or cross-linking density influences the bulk properties of the hydrogel network such as swelling, matrix elasticity, and cytotoxicity.[204] Previously, our group has reported that varying polymer percentage and PEG molecular weight will alter the mechanical properties of PEGDMA hydrogels.[48] This is advantageous for producing biomimetic scaffolds for cell seeding which mimics the elasticity of different natural tissues. The size of this innate porous network determines the rate of fluid exchange as well as the size of molecules that can diffuse into and out of the hydrogel.[120,205] Previously, PEGDMA hydrogels synthesized in our lab using UV polymerization demonstrated a sub-nano to nanoporous (~1-13 nm) network post-synthesis.[43] This nanostructure is suitable for the exchange of small molecules but is not optimal for the migration of cells which like hASCs in our experience had an approximate hydrodynamic radius of 15-16 microns will require pores on the micron scale.[206] The limitation of such scaffolds is that cells are cultured in a monolayer on the

surface of the hydrogel which only allows for 2D studies or cultures that require the cells to be encapsulated within the hydrogel network during the crosslinking process; which ultimately leads to potential exposure to free-radicals and/or ultra-violet (UV) exposure.[207–211] This exposure could potentially lead to irreversible alteration of the cells causing double-stranded DNA breaks affecting cell viability, proliferation, or gene expression. Such changes in cell behavior limits our ability to assess cell function in relation to material properties independent of chemical changes occurring during the synthesis process. To be able to investigate cell-material interactions in a 3D fashion, microporous scaffolds are a better option as they allow cells to integrate within the hydrogel network and provide more accurate examination of morphology and gene expression.[212]

Scaffolds that have porous networks are attractive for tissue engineering applications as they increase the surface area in which cells can attach and act as a temporary extracellular matrix for cells.[213,214] Kim et al. reports that porous polycaprolactone scaffolds created by a centrifugation method enhance hASC differentiation by altering the pore size of the material.[206] This group reports that pore sizes of approximately ~300-320 μm enhance osteogenesis and ~90-105 μm enhances myogenesis of hASCs.[206] This groups suggests that the varying ranges in pore sizes reported for enhancing differentiation of hASCs can be contributed to pore architecture formed during synthesis, varying materials, or the limited pore size ranges of scaffolds.[206]

Here we describe the synthesis of PEGDMA hydrogel scaffolds with multiscale porosity through mild post-processing, freeze-dry lyophilization. Freeze-dry lyophilization is a common drying method used to preserve material quality, architecture,

and physical and chemical properties. It is widely used in food preservation, stabilization of nutraceuticals[215] and solid protein pharmaceuticals to increase shelf life,[216–218] creation of porous materials for ion transport,[219] and tissue engineering.[220] Freeze-dry lyophilization has been explored for the generation of porous scaffolds using polymers such as chitosan, gelatin, alginate, hydroxyapatite/poly(hydroxybutyrate-co-valerate) (PHBV), silk fibroin, and hydroxyapatite-collagen blends.[221–227] These porous scaffolds of varying materials have been used to study the architecture created during freeze-dry lyophilization, the changes in material properties, and cell migration. There is some evidence to support the alterations of polymer material properties after freeze-dry lyophilization as seen in porous chitosan scaffolds.[182,228,229] Porous chitosan scaffolds of 1 - 250 μm pore sizes were obtained by varying the freezing conditions in the lyophilization step.

Despite the independent use of PEG based hydrogel scaffolds and use of freeze-dry lyophilization for a variety of applications, to the authors knowledge, the specific effect of freeze-dry lyophilization on PEG hydrogels has not been characterized. Materials that contain PEG in some capacity have been characterized by changes in swelling behavior, mechanical properties, and appearance using scanning electron microscopy (SEM).[230–232] While SEM provides information on hydrogel structure and morphology, these images are often obtained in a dry state after coating with a conductive material. Hydrogels synthesized for tissue engineering applications are utilized in a hydrated state, therefore it is vital to understand the innate hydrogel network in a swollen state to get a true understanding of the influence material properties have on stem cell fate. The inability to quantify hydrogels in their native swollen state has

hindered fully characterizing the effect of lyophilization on network pore size and structure of PEG based hydrogel biomaterials. In addition, to our knowledge PEG hydrogels have not been characterized using environmental scanning electron microscopy (ESEM).

Our group has demonstrated that varying the molecular weight of the polymer incorporated into the hydrogel network alters the bulk properties such as elasticity, swelling profile, and pore size creating hydrogel scaffolds to fit a variety of tissue engineering applications.[43,48] Here, co-blends (weight by weight, % wt.) of PEGDMA hydrogels molecular weight (MW) 20 kDa and 1 kDa; 0:20, 10:10, 15:5, and 17:3 were synthesized (**Figure 4-1**) in two thicknesses, 1 mm (thin) and 7 mm (thick). To determine how polymer MW, thickness, and drying method (air dried versus lyophilized), effect hydrogel properties (network pore size and formation of micropores) ESEM images were acquired along with traditional hydrogel swelling profiles to observe changes in pore morphology and swelling properties respectively. Using the synthesized lyophilized and non-lyophilized hydrogels, proliferation and morphology of hASCs on the scaffolds were evaluated using fluorescence imaging to evaluate cell-material compatibility.

4.3 Materials and Methods

4.3.1 Materials

Poly (ethylene glycol) dimethacrylate (PEGDMA) molecular weight (MW) 1 kDa and MW 20 kDa were purchased from Polysciences, PA, USA. The ultraviolet (UV) photoinitiator, 2-hydroxy-1-[4-(hydroxyethoxy) phenyl]-2-methyl-1 propanone (I2959), phosphate buffered saline (PBS) tablets were purchased from Sigma Aldrich, MO, USA.

Methacrylic acid (MAA) and heptane were purchased from Fisher Scientific, MA, USA. MAA was passed through a basic alumina column to remove inhibitor prior to use. 1-Ethyl-3-(3-dimethylaminopropyl) carbodiimide (EDC), sulfo- N-hydroxysulfosuccinimide (sulfo-NHS), 2-(N-morpholino) ethanesulfonic acid (MES) buffer, and 1X PBS solution were purchased from ThermoFisher Scientific, MA, USA.

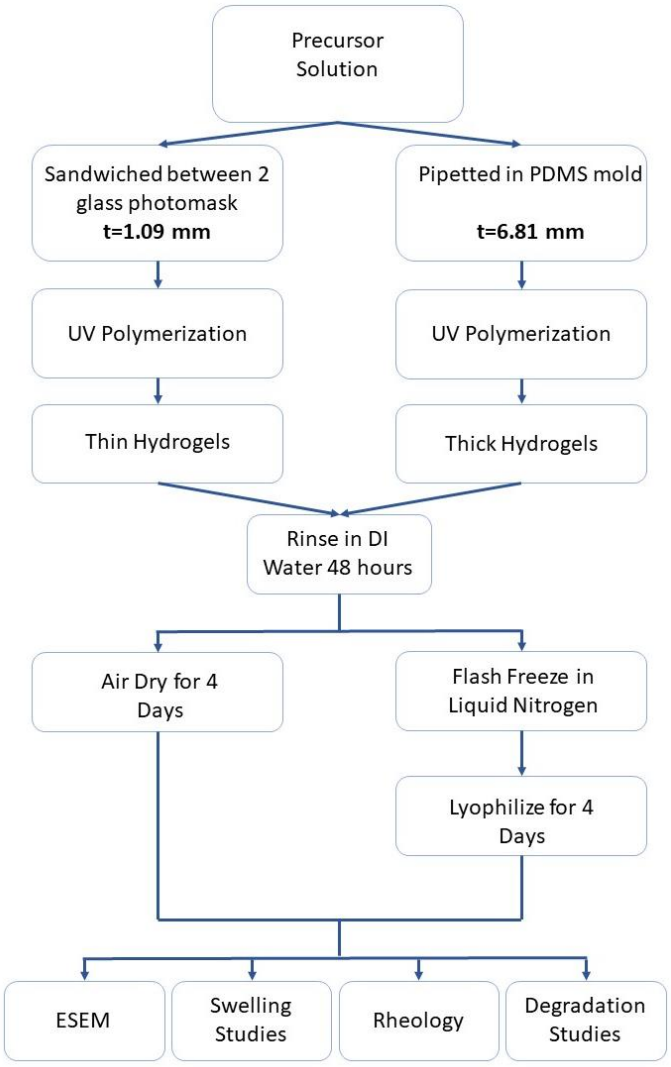

Figure 4-1: Experimental Process: Flowchart showing the factors varied for the synthesis of thin and thick hydrogels and step-wise post-synthesis treatments and subsequent analysis of hydrogels. *Reprinted with permission from Taylor & Francis.*

Human adipose-derived stem cells (hASCs) were purchased from LaCell, LLC. Minimum essential media (MEM) α, L-glutamine, penicillin streptomycin, alamarBlue™ reagent, Alexa Fluor 555 phalloidin, and diamidino-2-phenylindole, dihydrochloride (DAPI) were purchased from ThermoFisher Scientific, MA, USA. Methanol was

purchased from VWR. Bovine serum albumin (BSA) was purchased from Amresco. Fetal bovine serum (FBS) was purchased from Atlanta Biologicals. Formalin was purchased from Azer Scientific. Triton X-100 was purchased from Alfa Aesar. Unless otherwise stated, all materials were used as received.

4.3.2 Hydrogel Synthesis

Hydrogel precursor solutions containing a total of 20% wt. polymer were prepared with varying concentrations of MW 20 kDa and MW 1 kDa PEGDMA solutions as summarized in **Chapter 3**. Solutions: 0:20 (without PEGDMA MW 20 kDa and 20% (wt.) PEGDMA MW 1 kDa), 10:10 (10% wt. PEGDMA MW 20 kDa and 10% wt. PEGDMA MW 1 kDa), 15:5 (15% by wt. PEGDMA MW 20 kDa and 5% by wt. PEGDMA MW 1 kDa), and 17:3 (17% wt. PEGDMA MW 20 kDa and 3% wt. PEGDMA MW 1 kDa) were prepared with 0.1% wt. UV photoinitiator, I2959, 2% by wt. of PEGDMA MW 1 kDa of MAA and deionized water as previously reported by our group [43,48]. Precursor solution was sonicated for 20 minutes and then pipetted in between two glass photomasks separated by a 1 mm Teflon spacer and UV polymerized at 365 nm wavelengths at an intensity of ~37 mW/cm^2. Hydrogels of 2 thicknesses (t), 1 and 7 mm, were synthesized using Teflon spacers and poly (dimethyl siloxane) (PDMS) mold, respectively, between glass photomasks. Hydrogels of 1 mm thickness were called “thin” and 7 mm thickness were called “thick” hydrogels. The 0:20, 10:10, 15:5, and 17:3 hydrogel blends were UV polymerized for 5, 10, 15, and 20 minutes, respectively. Hydrogel samples were rinsed for 48 h in deionized (DI) water and dried using 2 methods, air-dried (AD) for 4 days, and freeze-dry lyophilized using liquid nitrogen (LYO) (**Figure 4-1**).

For cell culture studies, hydrogels were surface modified as previously described[43,48] to promote cell attachment. MAA was added to the hydrogel precursor solution to create carboxyl groups on the surface of the cured hydrogels. Using ESC chemistry these carboxyl groups can be activated to bond with amine groups. Briefly, hydrogels that had been stored in DI water, were incubated in 0.1 M MES buffer at pH 4.7 for 24 hours. EDC and Sulfo-NHS were added to the hydrogels at a 10-molar access (with respect to MAA concentration) and incubated for 30 minutes. Hydrogels were then incubated with a 0.2 μg concentration of Fibronectin for 4 hours. Hydrogels were then rinsed with 70% ethanol for 30 minutes followed by PBS for 24 hours and then placed in complete culture media for cell seeding.

4.3.3 Hydrogel Morphology

ESEM images were obtained post drying and 48 hours after rehydration with DI water using the FEI Quanta 3D FEG FIB/SEM system in ESEM mode at 20 kV. Dry state samples were imaged at 100 Pa using a secondary electron detector while the hydrated state samples were imaged using a gaseous secondary electron detector with a chamber pressure of 450 Pa. Hydrogel samples used in imaging were synthesized in the same batch, however separate samples were used for the dry and hydrated images.

4.3.4 Hydrogel Parameter Characterization

Immediately after UV polymerization, hydrogel discs of 19.5 mm were punched out from the thin hydrogel sheets and weighed in air and heptane (a solvent PEG hydrogels does not swell in) to obtain the relaxed state volume fraction, $v_{2,r}$ **Eq. 3-1** as described previously [43,175].

Hydrogel discs were then rinsed for 10 days in deionized (DI) water to remove any unreacted polymer with daily water changes. After rinsing, the hydrogel discs were dried in a vacuum oven at approximately 45°C for 5 days then weighed in air and heptane to obtain their dry state mass. The dried discs were swollen in phosphate buffered saline (PBS 1X) for 7 days to reach swollen equilibrium. Once at equilibrium the mass in air and heptane was recorded to obtain the volume fraction in the swollen state, $v_{2,s}$ **Eq. 3-2**.

$W_{a.d}$ is the hydrogel weight in dry state in air, $W_{n.d}$ is the hydrogel weight in dry state in heptane, $W_{a.s}$ is the hydrogel weight in swollen state in air, $W_{n.s}$ is the hydrogel weight in swollen state in heptane, $W_{a.r}$ is the hydrogel weight in the relaxed state in air, and $W_{n.r}$ is the hydrogel weight in the relaxed state in heptane. The equilibrium volume swelling ratio, Q, is the ratio of the equilibrium swollen volume with the polymer volume in the dry state.

The average molecular weight between crosslinks ($\bar{M}_c$) was calculated using the Peppas-Merrill equation **Eq. 3-3**. Where $\bar{M}_n$ is the number average molecular weight of the uncrosslinked polymer, *v* is the specific volume of the polymer, V_1 (18.016) is the molar volume of the water, and χ_1 is the polymer-solvent interaction parameter (0.426) [175]. For the hydrogel blends, the average weight percent combination of the two respective molecular weight polymers was computed to obtain $\bar{M}_n$. Pore size (ξ) was determined using **Eq. 3-4**.

The Flory polymer characteristic ratio (C_n), molecular weight of the monomer (M_r), and bond length along backbone chain (l) for PEG was reported to be 4, 44, and 1.47 Å, respectively.[175]

4.3.5 Equilibrium Hydrogel Swelling

Swelling percentage of hydrogels were studied in DI water at room temperature. The dry mass of the hydrogels was obtained and used in computing the percent swelling as a function of time over a period of 5 days. Swelling behavior of the hydrogels as a function of time was calculated as a percentage using **Eq. 3-5**, where w_f is the weight of the hydrogel at each time point and w_i is the initial dry weight of the hydrogel.

4.3.6 Rheology

Thin AD and LYO hydrogels were cut into 20 mm discs for rheology measurements. The shear elastic modulus (G') of each sample was measured using a Bohlin CVOR rheometer with a 20 mm parallel plate in oscillation mode. Amplitude sweeps at various oscillation frequencies, 0.1, 1, and 10 Hz, and a controlled strain range of 0.001 – 1 was used to determine the linear viscoelastic region (LVR). The G' was determined from a frequency sweep between 0.1 – 10 Hz at the stress and strain values obtained from the LVR for each sample. Gap height for each sample was obtained by measuring the thickness using Vernier calipers.

4.3.7 Degradation in Culture Conditions

For degradation studies thin hydrogels of each polymer blend were synthesized and dried as previously described in the synthesis section above and were treated in the same manner they were prior to cell seeding. After hydrogels were dried, they were placed into 0.1 M MES buffer for 24 hours. The next day the hydrogels were transferred into PBS and left to swell for 24 hours. After 24 hours the hydrogels were placed in CCM at 37 °C for 72 hours. These conditions were utilized to mimic the process of surface

modification the hydrogels require for cell seeding. Every 24 hours the mass of the hydrogels was recorded, and the swelling percentage was calculated using **Eq. 3-5**.

4.3.8 Stem Cell Maintenance

Human ASCs were cultured on 10 cm and/or 6 cm polystyrene tissue culture treated dishes. Cells were maintained in complete culture medium containing MEM α, 1% L-glutamine, 1 % penicillin streptomycin, and 16.5 % fetal bovine serum (FBS). Stem cells were incubated at 37 °C at 5 % CO_2.[43]

4.3.9 AlamarBlue™ Assay

Human ASCs were seeded on tissue culture plates, air-dried 10:10 hydrogels (1 mm thickness), and lyophilized 10:10 hydrogels (1 mm thickness). 10:10 hydrogels were selected for cell studies based off of previous data that demonstrated these air-dried blends have an elastic modulus of 50-60 kPa which is in a physiologically relevant range.[43,48] Cells were seeded on all surfaces at 2.0×10^3 cells/cm² and cultured in complete culture medium for 48 hours. At 48 hours, alamarBlue™ reagent was added to culture medium at 10 % of the sample volume. Blanks corresponding to tissue culture plates, air-dried hydrogels and lyophilized hydrogels were prepared by adding equivalent volumes of culture medium and alamarBlue™ reagent to corresponding wells without hASCs. Samples were incubated at 37 °C and protected from light. Fluorescence was measured using a BioTek Cytation 5 plate reader at excitation 560/emission 590. Readings were taken at 1, 2, 3, and 4 hours following introduction of alamarBlue™ reagent.

4.3.10 Phalloidin Staining

Human adipose-derived stem cells (hASCs) were cultured on tissue culture plates, thin 10:10 air-dried hydrogels, and thin 10:10 lyophilized hydrogel scaffolds. 10:10 hydrogels were selected for cell studies based off of previous data that demonstrated these air-dried blends have an elastic modulus of 50-60 kPa which is in a physiologically relevant range of bone [43,48]. Cells were seeded on all surfaces at $2.0x10^3$ cells/cm^2 and cultured in complete culture medium for 72 hours. After 72 hours phalloidin and DAPI stains were utilized to visualize cellular morphology of hASCs seeded on tissue culture plates, 10:10 thin AD samples, and 10:10 thin LYO samples. Human ASCs were fixed in 10 % formalin and permeabilized using 0.2 % TritonTM X-100. AlexaFluor® 555 phalloidin was prepared with methanol according to manufacturer's specifications. For staining of hASCs, a dilution of 1:40 methanolic stock to PBS with 1 % BSA was used. Staining was performed in an area protected from light and incubated for 15 minutes. DAPI was added at a final dilution of 1:2000 and incubated for an additional 5 minutes. Samples were then washed three times with PBS. Samples were imaged with 500 µL of PBS in each well.

4.3.11 Statistical Analysis

Swelling data is presented as mean ± standard error of the mean. Two-way ANOVA followed by Tukey's multiple comparison test, 3 factor ANOVA and factor interaction effect were determined using GraphPad Prism version 6.00 for Windows, GraphPad Software, La Jolla California USA. Effects were considered significant if the p value was less than 0.05. All data were collected in triplicate.

AlamarBlue™ and ESEM pore size data was analyzed using a one-way ANOVA followed by Tukey HSD post-hoc test from the online software available at astatsa.com. The data is presented as mean ± standard error of the mean. Significance was determined if the p value was less than 0.05 and each sample was measured in triplicate.

4.4 Results

4.4.1 Hydrogel Morphology

Environmental scanning electron microscopy (ESEM) was used to obtain cross-sectional images of the hydrogels in the dry (**Figure 4-2**) and hydrated state (**Figure 4-3**). Visual differences could be seen in morphology between air-dried (AD) and lyophilized (LYO) samples. For images with visible micropores, ImageJ was used to measure pore size (**Figure 4**). Specific values are available in **Appendix Table E-1**.

ESEM imaging in dry state: Samples imaged in the dry state (**Figure 4-2**) exhibited induced microporous structures visible in 17:3, 15:5, and 10:10 blends of the LYO samples. The 0:20 hydrogel swelling capability may have limited the water content within the hydrogel to a point that microporous structures were not formed. It is also possible that the pore size was within the network size or not visible with currently available technology. Within the thin LYO samples that were imaged in the dry state, the 15:5 hydrogels had a larger average pore size of 27. 53 ± 57.88 microns in comparison to the 17:3 which was 24.94 ± 11.44 microns but had less consistent pore diameter as evident from the higher standard deviation (**Appendix Table E-1**). Pores were not observed within any polymer blend for the AD hydrogel controls.

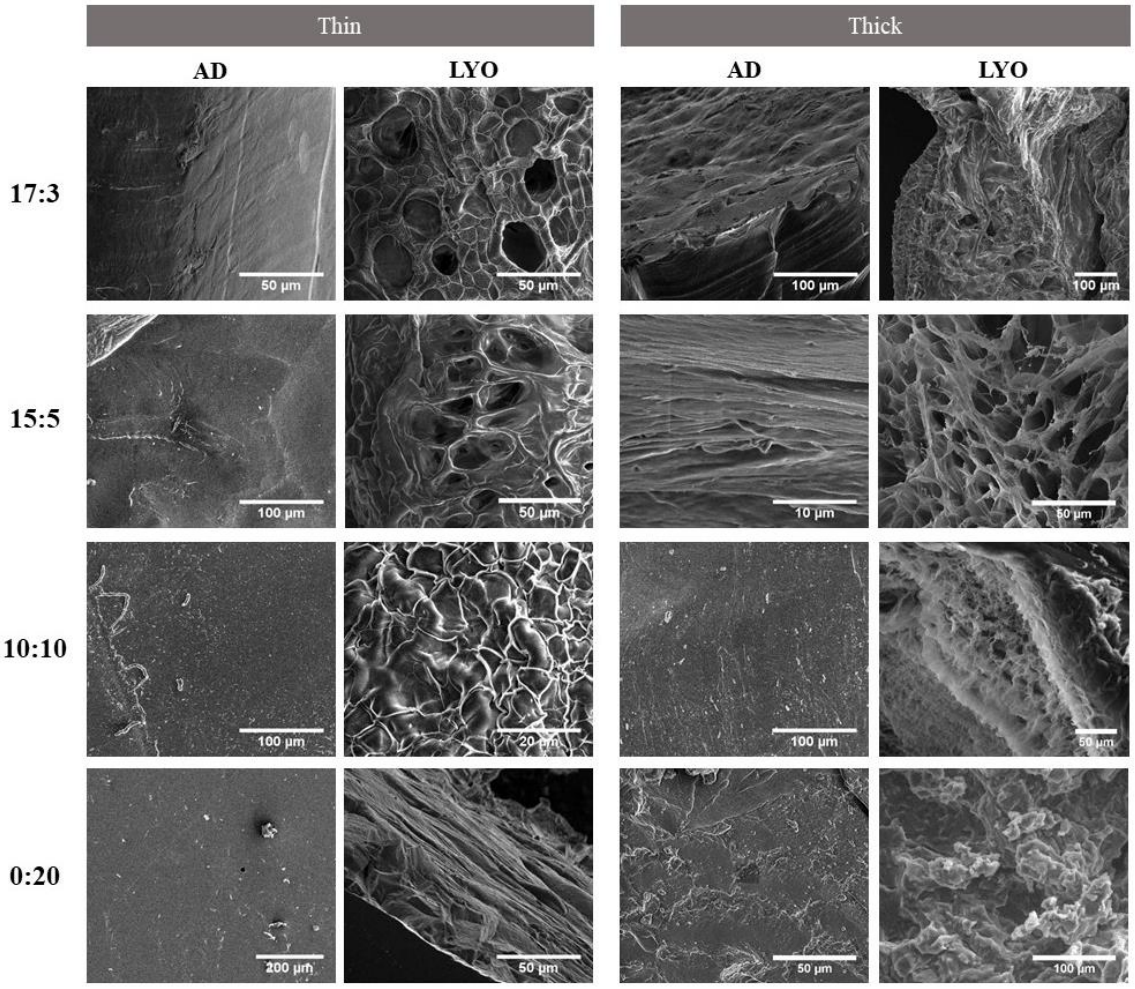

Figure 4-2: Dry state ESEM images of thick (7 mm) and thin (1 mm) air-dried (AD) and lyophilized (LYO) PEGDMA hydrogel blends (20 kDa : 1 kDa). *Reprinted with permission from Taylor & Francis.*

ESEM imaging in hydrated state: Hydrogel samples that were imaged in the rehydrated state using ESEM (**Figure 4-3**) demonstrated porous structures in all lyophilized hydrogel samples regardless of thickness. When imaged in the hydrated state, thickness appeared to affect pore size more than when the hydrogels were imaged in the dry state.

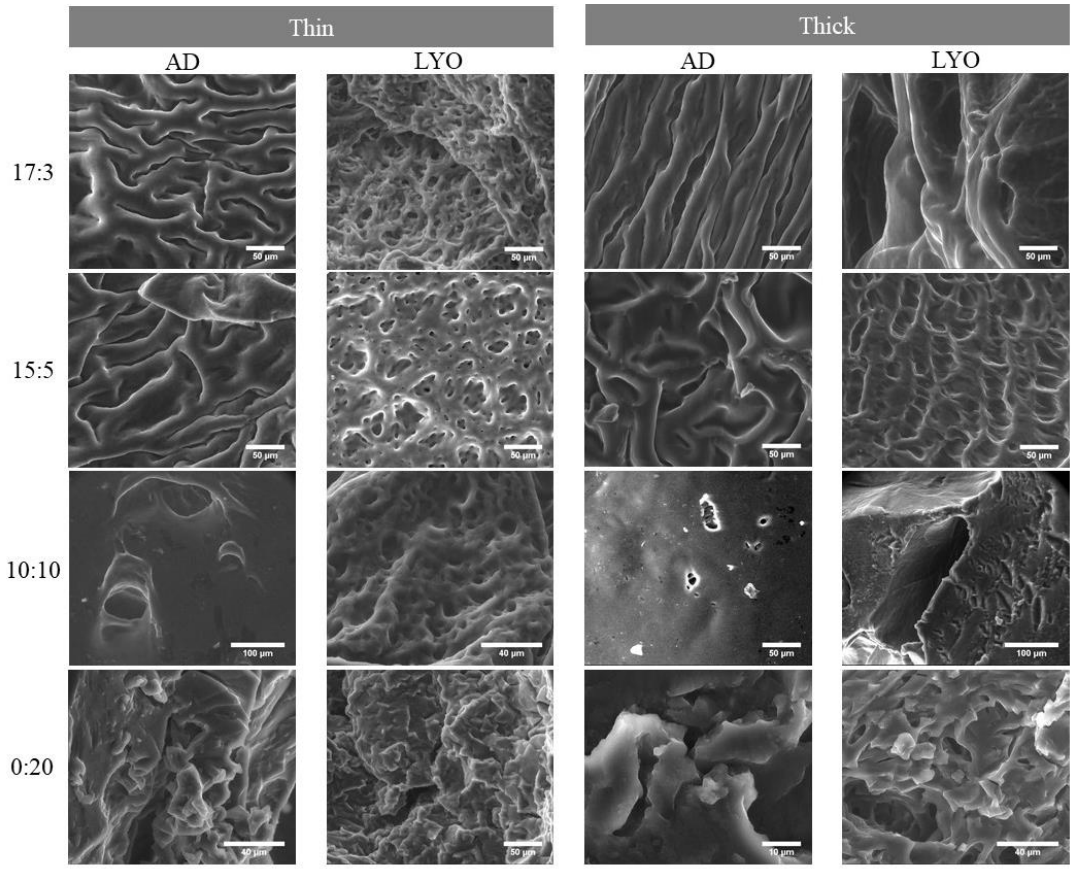

Figure 4-3: Hydrated state ESEM images of thick (7 mm) and thin (1 mm) air-dried (AD) and lyophilized (LYO) PEGDMA hydrogel blends (20 kDa : 1 kDa). *Reprinted with permission from Taylor & Francis.*

As seen in **Figure 4-4**, within the 17:3, 15:5, and 10:10 hydrogel blends, the thick hydrogels demonstrated larger pore sizes than their respective thin hydrogels. Hydrogel blends of 0:20 did not follow the same trends. This could be due to the incorporation of more, higher molecular weight polymer, demonstrating that polymer blend plays a crucial role in determining hydrogel properties.

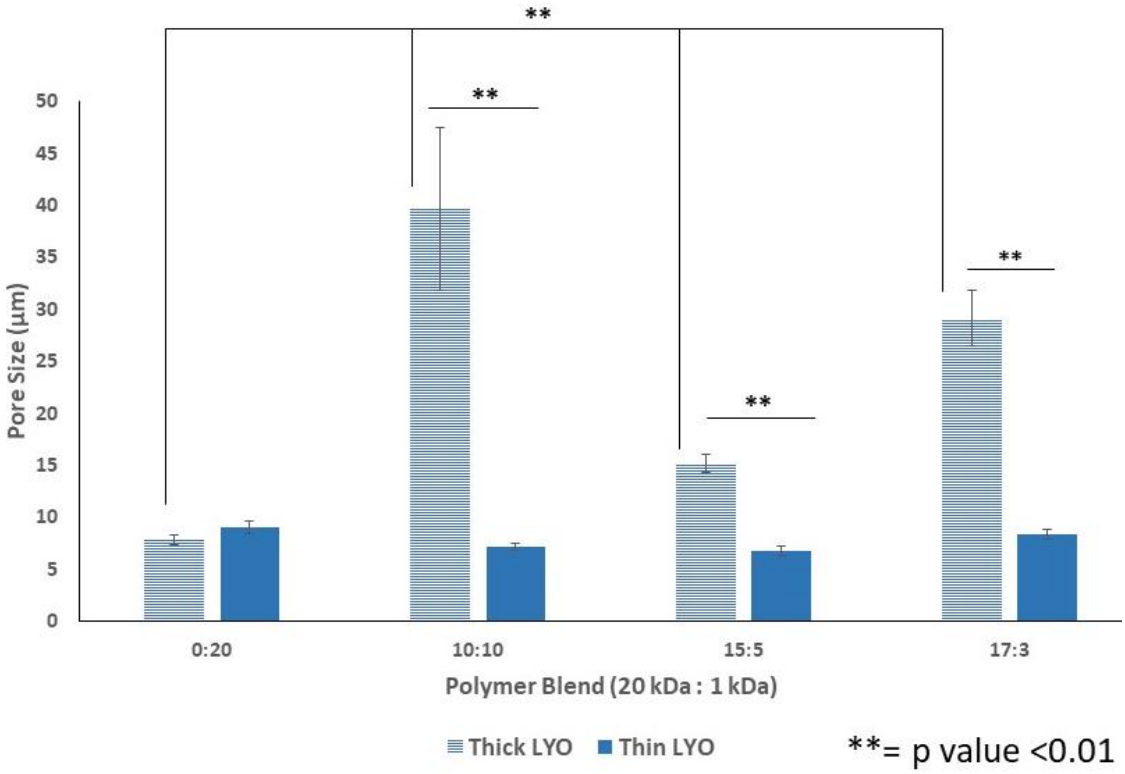

Figure 4-4: Average diameter of lyophilized samples as a function of polymer blend and sample thickness, calculated from ESEM images using ImageJ software. Average pore diameter of samples imaged in a rehydrated state. All samples are shown as the average ± standard error. Samples not shown did not have visible pores within ESEM images. There were no air-dried samples with measurable pore size diameters and were excluded from the graph. Each sample had 15-20 images analyzed when calculating pore diameter. *Reprinted with permission from Taylor & Francis.*

Thin LYO hydrogels appear to have a more uniform microporous structure when visually compared with their thick LYO counterparts as seen in **Figure 4-3**. Similar to ESEM images obtained in the dry state, there were no microporous structures visible in any AD hydrogel formulation when imaged in the hydrated state. The structures seen in **Figure 4-3** for AD samples do not resemble true pores and appear to be voids that could have been defects in the hydrogel or damage caused by cutting samples to obtain cross sectional images. The smooth surface of the hydrogel surface indicates that overall this is a uniform/flat, not a microporous network like those seen in the LYO samples.

Unexpectedly, the 10:10 thick LYO hydrogels demonstrated the largest pore size estimated through ESEM analysis.

4.4.2 Hydrogel Network Characterization

Bulk hydrogel parameters (**Table 4-1**), swollen volume fraction ($\nu_{2,s}$), equilibrium swelling ratio (Q), molecular weight between crosslinks ($\bar{M}_c$), and the pore size (ξ) were calculated as described above. The density (ρ) for each blend was also calculated during equilibrium swelling studies. The total percent polymer remained constant at 20% wt. for all polymer blends. The pore sizes described in **Table 4-1** represent the theoretical network pore sizes for thin, air-dried samples as they are air-dried for measurement purposes. Theoretical pore sizes were only calculated for thin samples.

Table 4-1 Bulk hydrogel network properties of AD PEGDMA hydrogel blends, MW 20 kDa: 1 kDa, n=3. *Reprinted with permission from Taylor & Francis.*

PEGDMA Hydrogel Blends 20 kDa : 1 kDa	**$\bar{M}_c$ (Da)**	**Q**	**ρ (g/cm^3)**	**$\nu_{2,s}$**	**ξ (nm)**
17:3	4691.12 ± 130.88	23.43 ± 0.91	1.00 ± 0.00	0.04 ± 0.00	12.28 ± 0.32
15:5	3321.29 ± 126.17	17.40 ± 0.57	1.02 ± 0.01	0.06 ± 0.02	9.59 ± 0.28
10:10	1379.11 ± 50.98	10.58 ± 0.26	1.02 ± 0.00	0.10 ± 0.02	5.11 ± 0.13
0:20	256.13 ± 8.32	5.56 ± 0.04	1.17 ± 0.00	0.18 ± 0.01	1.78 ± 0.03

The ratio of polymer percentage, PEGDMA MW 20 kDa to PEGDMA MW 1 kDa, was altered to determine how formulation will change bulk hydrogel properties. As expected, as the percentage of higher MW polymer was increased the calculated network pore size of the hydrogels increased as well. The molecular weight between crosslinks ($\overline{M}_c$) and swelling ratio (Q) also increase as the amount of PEGDMA MW 20 kDa is increased in the hydrogel blends. In calculating the hydrogel parameters, the MW of each hydrogel blend was based on a ratio of polymer MW. The trends observed through equilibrium swelling studies confirms hydrogel pore sizes of air-dried PEGDMA hydrogels increase as more of the higher MW polymer is incorporated. This allows for controlled tunability of hydrogel properties by only altering the polymer composition while the synthesis process remains constant.

4.4.3 Equilibrium Hydrogel Swelling as a Function of Post-Processing Drying Method

The hydrogel swelling profile was obtained as a function of time in deionized water over a period of 5 days. Three factors were evaluated: thickness, drying technique, and increasing percentage of PEGDMA MW 20 kDa polymer in hydrogel polymer composition. The factor combinations yielded 16 variations. Swelling profiles for all combinations of thickness and drying method were similar for polymer blends 0:20 and 10:10 of PEGDMA MW 20 kDa : 1 kDa (**Figure 4-5**).

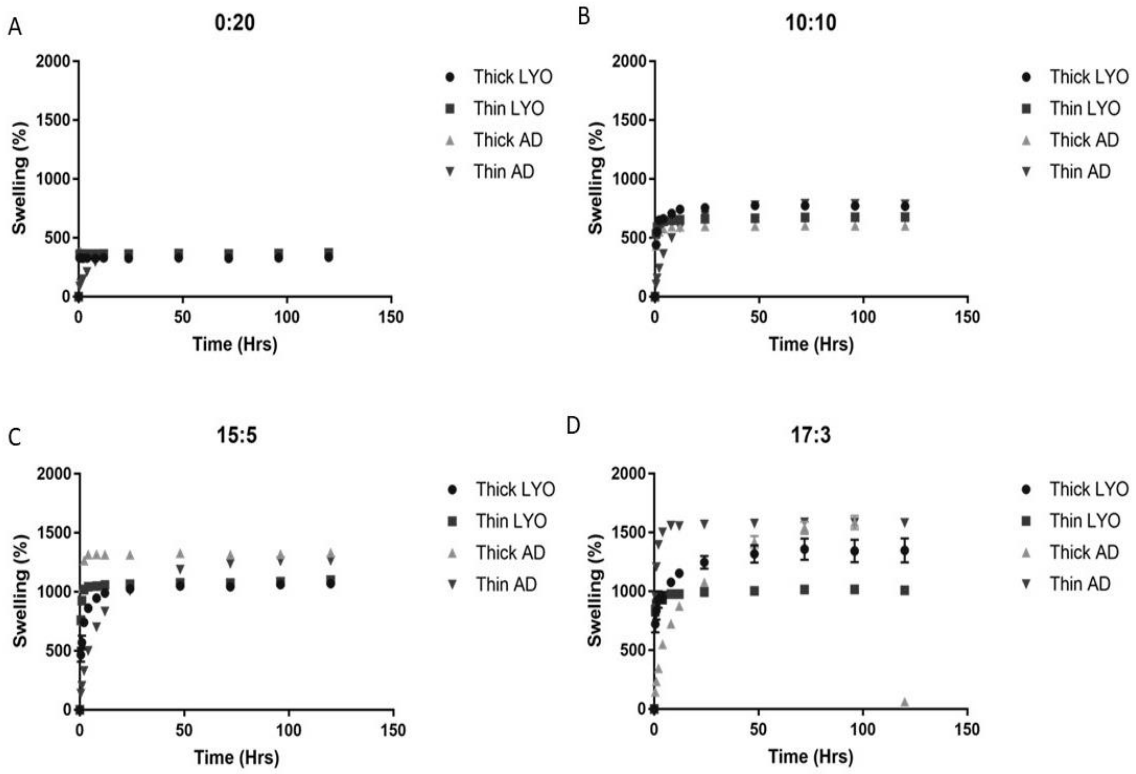

Figure 4-5: Swelling profile of PEGDMA blended hydrogels with increasing ratio of 20 kDa : 1 kDa molecular weight PEGDMA polymer as a function of polymer blends, n=3. *Reprinted with permission from Taylor & Francis.*

Thick LYO hydrogels achieved equilibrium in 3 days, thin LYO in 4 h, thin AD in 6 h, while the thick AD samples swelled slowly and did not achieve equilibrium within the 5 days studied (**Figure 4-6**).

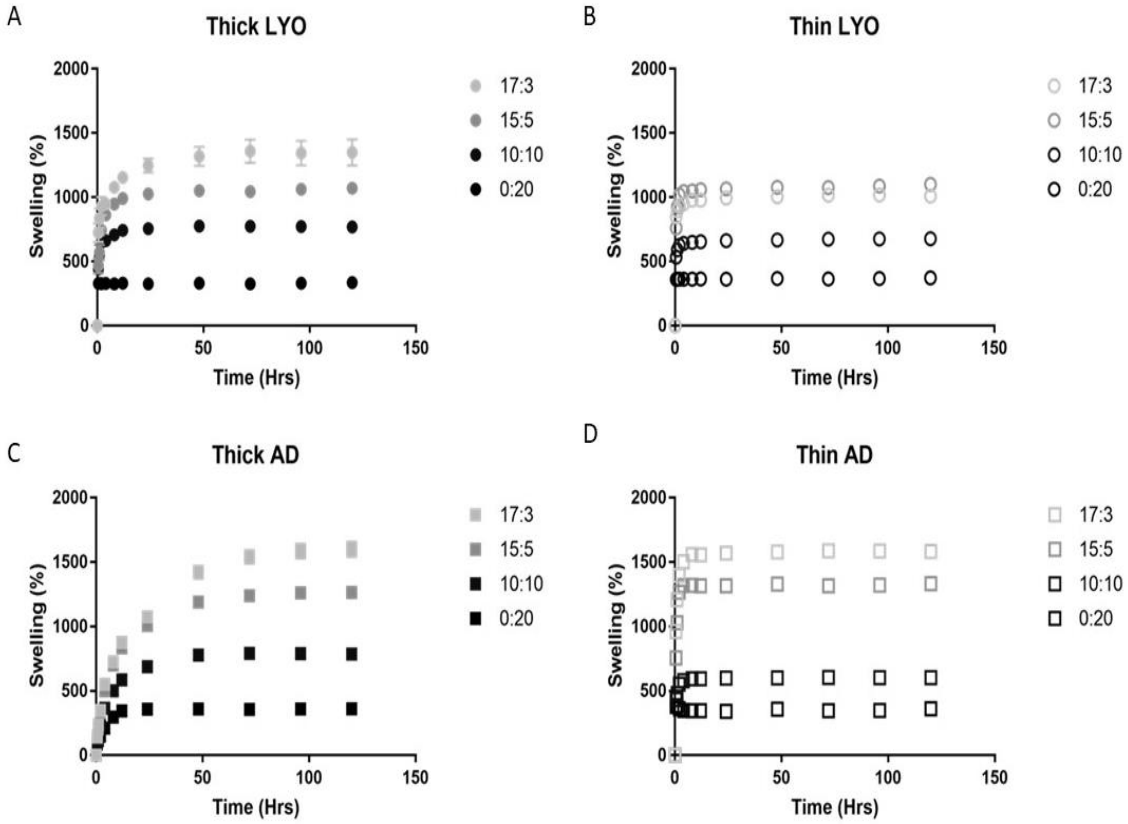

Figure 4-6: Swelling profile of PEGDMA blended hydrogels with increasing ratio of 20 kDa : 1 kDa molecular weight PEGDMA polymer as a function of polymer blends, post-drying process, and sample thickness; n=3. *Reprinted with permission from Taylor & Francis.*

No significant difference in swelling was observed after 8 h between the different combinations of thickness and drying methods for 0:20 combination of PEGDMA MW 20 kDa : 1 kDa (**Figure 4-5a**). For both 15:5 and 17:3 blends of PEGDMA MW 20 kDa : 1 kDa, there was no significant difference in the swelling profiles between the thick and thin lyophilized samples after 12 h (**Figure 4-5c & d**). No difference in swelling profile was observed between the thick and thin air-dried sample of 15:5 PEGDMA MW 20 kDa : 1 kDa after day 3.

4.4.4 Rheology

The shear elastic modulus of thin AD and LYO hydrogel blends was evaluated through rheology to have a better understanding of how drying method affects the physical properties of the hydrogels. As expected, the shear elastic modulus increased as the ratio of PEGDMA MW 1kDa increased regardless of drying method (**Table 4-2**). Flash freezing and drying via lyophilization reduced the shear elastic modulus of all hydrogel blends. This decrease in shear elastic modulus indicates that drying method not only influences hydrogel morphology, but actually alters the elastic modulus even if the polymer blend is held constant. The 0:20 hydrogel blends were too brittle to obtain measurements from as they would crack during flash freezing and we could not obtain a large enough sample to attempt rheological measurements.

4.4.5 Degradation in Culture Conditions

To confirm that these hydrogel blends would not degrade under cell culture conditions, they were subjected to a process that mimics the surface modification procedure required for cell seeding. Thin AD and LYO hydrogels of each polymer blend were swollen in MES buffer followed by PBS then kept in CCM for 72 hours. The hydrogels were only in CCM for 72 hours as that is the length of time cells were cultured on the chosen blend. All blends, regardless of drying method, demonstrated an ability to uptake fluid and keep a steady swelling percentage over time (**Figure 4-7**). The hydrogel blends that contained more of the higher MW polymer had the most swelling capacity, which was also seen in the equilibrium swelling studies performed in PBS. Degradation was only evaluated for thin AD and LYO samples as they were the hydrogels used for cell culture studies.

Table 4-2 Shear elastic modulus of thin AD and LYO hydrogel blends shown as the average ± standard error (kPa), n=3. *Reprinted with permission from Taylor & Francis.*

Drying Method	PEGDMA Hydrogel Blend 20 kDa : 1 kDa	Shear Elastic Modulus (kPa) ± Standard Error
AD	17:3	12.04 ± 0.606
AD	15:5	19.47 ± 1.010
AD	10:10	36.19 ± 2.030
AD	0:20	Too Brittle/Freeze Cracking
LYO	17:3	3.22 ± 1.45
LYO	15:5	3.65 ± 0.003
LYO	10:10	16.50 ± 7.44
LYO	0:20	Too Brittle/Freeze Cracking

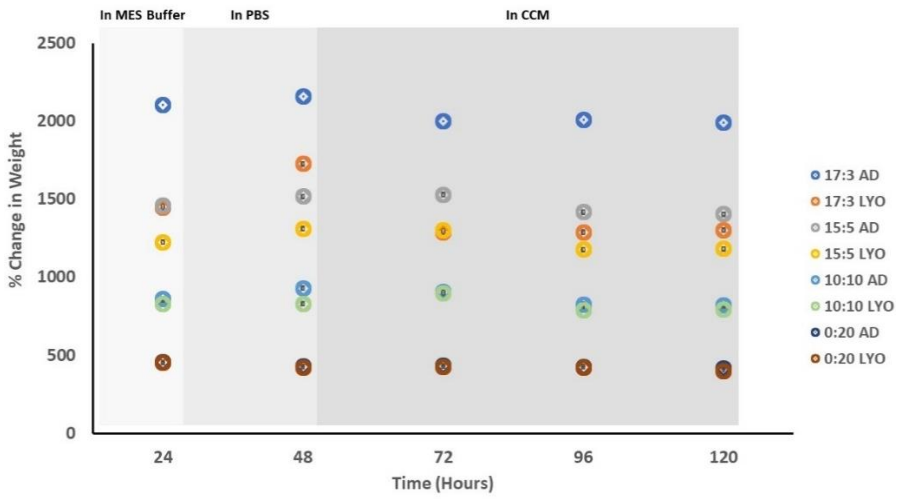

Figure 4-7: Degradation swelling performed utilizing a process that mimics surface modification required to seed cells on these hydrogel scaffolds. Thin AD and LYO samples were observed and their mass was recorded every 24 hours. The change in mass is presented as a function of percent change in weight ± standard deviation, n=3. *Reprinted with permission from Taylor & Francis.*

4.4.6 Human ASC Attachment and Proliferation on Hydrogel Scaffolds

Human ASCs were cultured on thin 10:10 AD hydrogels and thin 10:10 LYO hydrogels to observe if there were differences in cell attachment and viability between the two drying techniques. 10:10 hydrogels were selected for cell studies based off of previous data that demonstrated these air-dried blends have an elastic modulus and shear modulus in a physiologically relevant range.[43,48]

An alamarBlue™ assay was conducted with readings taken at 1, 2 3 and 4 hours post addition of alamarBlue™ (**Figure 4-8**). The alamarBlue™ assay was used to demonstrate the proliferation rates on the hydrogel surfaces in comparison to the tissue culture control. Analysis of hASCs on tissue culture plates, 10:10 thin AD hydrogels, and 10:10 thin LYO hydrogels suggest that there were no statistically significant differences between the surfaces at any timepoint during the 4-hour analysis.

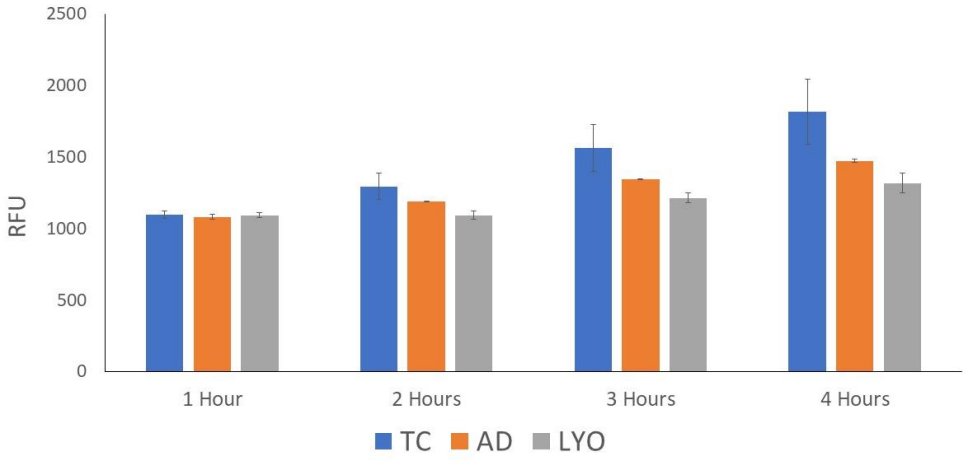

Figure 4-8: Fluorescent readings of hASCs cultured on tissue culture plates, 10:10 thin AD, and 10:10 thin LYO hydrogels 1, 2, 3, and 4 hours post addition of alamarBlue™, n=3. *Reprinted with permission from Taylor & Francis.*

Fluorescent images of hASCs cultured on the three surfaces 72 hours after seeding were taken to evaluate cell morphology (**Figure 4-9**). Phalloidin stains the f-actin filament of the cells highlighting the morphology of the cells on the three surfaces. A DAPI stain was done to visualize the cell nuclei. Overlay images were created to show both phalloidin and DAPI staining. Phase contrast images were also taken to help further characterize the morphology of the cells. Qualitative results show that the hASCs are attached to all three surfaces and remain viable. Morphologically, the cells remain in a spindle fiber like morphology typical of hASCs. Our scaffolds show cell behavior consistent with undifferentiated hASCs, including proliferation and normal cell morphology.

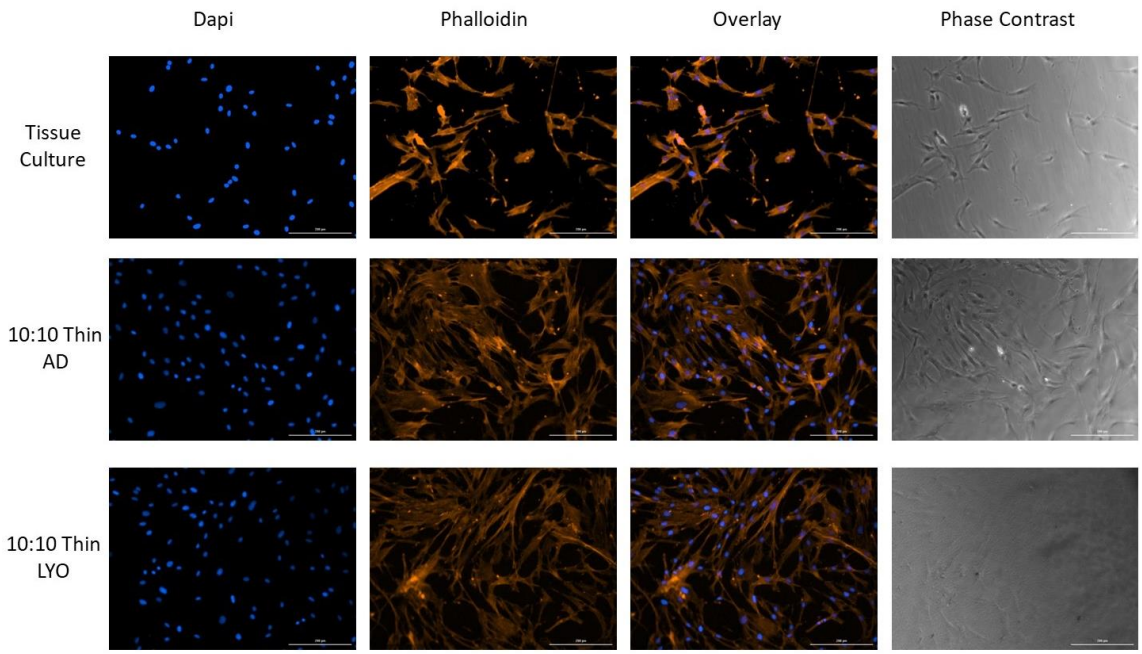

Figure 4-9: Phalloidin staining of hASCs. Fluorescent images show the morphology of hASCs cultured on the three surfaces 72 hours after seeding. Cell nuclei are shown in blue and f-actin filaments are shown in orange. Scalebars: 200 mm. *Reprinted with permission from Taylor & Francis*.

4.5 Discussion

In this work microporous PEGDMA hydrogel scaffolds were synthesized through freeze-dry lyophilization that could be used in the future to support systematic assessment of surface topography on human adipose-derived stem cell fate. The differences in hydrogel morphology between AD and LYO samples show that the drying method did alter the architecture of the hydrogel for blends that had the 20 kDa PEGDMA through the induction of micropores. When imaged in a dry state, thin and thick samples (**Figure 4-2**) of corresponding blends had similar morphologies, therefore it is not believed that thickness has a noticeable effect on hydrogel morphology when samples are dried.

To our knowledge this is the first time that PEG hydrogels have been imaged while in a hydrated state. This unique perspective allows for the visualization of the hydrogel blends in their native state in which they would be used for tissue engineering applications. Hydrated ESEM analysis indicated that polymer blend, thickness, and drying method all play a crucial role in determining the pore size and morphology of the hydrogel network and thereby influencing hydrogel behavior. The larger pore sizes seen within 10:10 thick LYO hydrogels when imaged in the hydrated state could be due to how the samples were prepared for imaging. As seen in **Figure 4-3**, some of the pore like structures seen in the images resemble large voids resembling cracks in the network rather than true pores. However, ESEM analysis of samples using ImageJ were all blinded and before analysis characteristics of a pore were determined to be 3D voids that penetrated multiple layers within the network for consistency. Theoretical network pore size calculations using the Peppas-Merrill equation derived from equilibrium

swelling studies presented nanoscale pore sizes for all AD control hydrogels (**Table 4-1**). These values explain why pores on AD hydrogels were not visible during ESEM imaging.

It was evident from the long-term swelling data collected as a function of post-processing drying methods that the interaction of sample thickness and drying method only affected the formulation with higher percentage of PEGDMA MW 20 kDa polymer within the composition. Thicker samples contained more polymer mass, thus had greater swelling prior to drying. The increase in higher molecular weight polymer led to an increased hydrogel swelling capacity. Thus, the presence of increased water content in PEGDMA blends with higher polymer percentage of MW 20 kDa. These results implied that the relaxation of the polymer chain was the more prominent driving factor in swelling rather than the drying method or sample thickness. The results also illuminate novel findings in this field with respect to sample thickness and drying method, both of which can be varied to alter the hydrogel architecture depending on the original hydrogel chemical composition. This opens a new factor to consider when synthesizing application specific hydrogels.

The rheology data provided insight into the physical properties of the hydrogel blends and how polymer blend and drying method can alter these properties. As expected, the shear elastic modulus decreased as the ratio of higher MW polymer increased in AD as well as LYO samples. In addition, drying method also caused a change in shear elastic modulus. All LYO samples that were investigated had a lower shear elasticity than that of their AD counterparts. The 17:3 LYO hydrogels had the lowest shear elastic modulus values while the 10:10 AD hydrogels had the highest shear

elastic modulus values. Previously, the Young's elastic modulus of the air dried then re-hydrated 10:10, 15:5, and 17:3 hydrogels blends[43,48] were within the physiologically relevant elasticity ranges for bone (50-60 kPa), cartilage (25-30 kPa) and muscle (8-10 kPa) [75,233]. In comparison the 10:10 AD hydrogel blend had a shear elastic modulus of ~36.19 kPa. Previous researchers have estimated the brain to have a shear modulus in this range through modeling based off of cadaver experiments.[234] Other groups such as Nordez and Hug have utilized supersonic shear imaging to estimate the elastic modulus of muscle. These researchers estimate that at rest muscle tissue has an elasticity of ~10-11 kPa and ~21-23 kPa to ~42-45 kPa at 3% and 7% of electromyographic activity.[235] As it is difficult to measure the elasticity of tissue in the body and there are some discrepancies in exact numbers, we chose to utilize the 10:10 hydrogel blend as it demonstrated a shear elastic modulus similar to estimates of physiologically relevant ranges. In addition, 10:10 thin LYO hydrogels had an average pore size closely resembling that of hASC diameter suggesting it as a potential scaffold for embedded cell culture and tissue engineering applications. Degradation analysis illustrates that all hydrogels, regardless of blend or drying method, retain their structural integrity and their swelling capabilities. Confirming that there is no hydrogel degradation indicates that we can reliably reproduce results when these scaffolds are utilized, which is especially important when they are used in conjunction with cells. The stability in cell culture conditions will allow us to further study them for use in tissue engineering applications.

Biocompatibility of AD and LYO hydrogels was observed utilizing tissue culture plates as a control since hASCs are commonly cultured on this surface. Over a 4-hour period incubated in alamarBlue™ reagent, hASCs cultured on 10:10 thin AD samples,

10:10 thin LYO samples, and tissue culture plates did not produce a statistically significant difference in fluorescence. These results demonstrate that overall the proliferation rates of hASCs are comparable between cells cultured on all three conditions. Phalloidin staining of the F-actin filaments of hASCs cultured on each scaffold qualitatively demonstrate that morphologically the cells hold a spindle-like morphology indicative of undifferentiated hASCs. The results of the alamarBlue™ assay and phalloidin staining demonstrates cell attachment and growth indicating cell-material biocompatibility. Future studies will investigate how altering the properties influence cell behavior on each hydrogel combination to create tuneable hydrogels to be utilized in tissue engineering applications such as repair, replacement, wound healing, and drug delivery.

CHAPTER 5

EVALUATING THE INFLUENCE OF BIOCHEMICAL CUES ON MYOGENIC DIFFERENTIATION OF HUMAN ADIPOSE-DERIVED STEM CELLS

5.1 Introduction

It was first documented in the 18th century that mature skeletal muscle possessed the ability to regenerate itself after chemical or physical injuries.[236] However, there are special cases where the injury to the skeletal muscle is too deleterious and the body cannot repair or replace the damaged area. Volumetric muscle loss (VML) is characterized by muscle injury that does not regenerate naturally and can occur due to combat injuries, traumatic injuries such as car wrecks, surgical procedures such as tumor removal, or abnormal muscle conditions such as muscular dystrophies.[237] Numerous studies have also shown that muscle degeneration, or atrophy, occurs as a consequence of exposure to microgravity during spaceflight, something experience by astronauts who spend significant periods of time on the International Space Station.[238–242] The most common treatments for VML including surgical procedures utilizing functional free muscle transfers is severely limited by donor tissue availability, is invasive, and contributes to an increase in scar tissue formation[237] and advanced bracing.[243,244] In 2015 it was reported that 4.5 million reconstructive surgeries characterized by volumetric

tissue damage due to combat or traumatic injuries were performed.[245] In 2016, a study evaluating acellular biological scaffolds, composed of extracellular matrix of porcine urinary bladder, for treating VML in a 13 patient clinical trial was published.[246] From this evaluation of 13 patients, 7 showed improvement, 3 had no change, and 3 had loss of function. While the muscle bulking was present post treatment, biopsies did not show evidence it was from muscle fiber formation.[247] Recovery outcomes for those suffering from VML are low and can likely lead to a lifetime of disability. It is estimated that the disability cost per patient, including lost wages ranges between $340,000-$440,000.[248] There is a growing need to find a solution to this debilitating and costly condition that affects so many individuals. Producing 3D tissue scaffolds by combining biomaterials, a cell source, and biochemical or physiochemical cues to direct skeletal muscle differentiation has the potential to revolutionize the way in which VML is treated. Fully developed myogenic tissue scaffolds will eliminate the need for donor tissue and potentially restore function to the affected muscle. Despite this need, the challenge in producing these dynamic scaffolds still lies in creating an environment that mimics the natural extracellular matrix found in skeletal muscle tissue and allows the reliable differentiation of stem cell populations towards a myogenic lineage.

Here we aim to understand how biochemical cues from media components and EMC proteins influence myogenic differentiation of hASCs. Adipose-derived stem cells are an abundant and reliable source of adult multipotent stem cells[41] that are easily and readily harvested from patients through minimally invasive lipoaspirates and are present in larger quantities in contrast to bone marrow-derived mesenchymal stem cells (MSCs).[49,186] Like MSCs, adipose-derived stem cells can differentiate towards the

osteogenic, chondrogenic, adipogenic, and myogenic lineages while being easy to maintain in culture making them an ideal cell source for autologous tissue scaffolds.[49,187] Adipose stem cells are also immunoprivileged and are genetically stable in long-term culture.[186] The ease with which these multipotent stem cells can be harvested and maintained, along with their differentiation potential makes them an attractive, clinically relevant cell source for tissue engineering applications. Finally, the fact that hASCs can be used in an autologous manner makes them a top candidate in tissue engineering applications for the treatment of tissue damage and degeneration.

While several groups have shown that hASCs have the potential to differentiate towards a myogenic lineage,[49–51] there is no universal myogenic differentiation media that yields greater than 15% myogenic differentiation.[52] Previously, Huri et al.[249] reported on a myogenic media B (Myo B) for directing myogenic differentiation in hASCs. In the study, hASCs were seeded onto culture plates coated with type I collagen and exposed to myogenic induction media (MIM) for 24 hours. Huri et al. looked at how providing a biophysical stimulant would influence stem cell differentiation towards the myogenic lineage in combination with the MIM. Groups were either "static" meaning exposed to MIM but not experiencing uniaxial strain, or "dynamic" which were cells exposed to MIM and uniaxial strain for one hour each day. Static cells did not begin to show myotube formation until day 14 and even at day 21 there were significantly fewer myotubes compared to the dynamic group. Cells cultured under dynamic conditions began forming myotubes as early as day 7 and had 5-fold more myotubes than static conditions by day 21. Immunohistochemistry of the late stage marker, myosin heavy chain (MHC) was also observed between the two groups. Static cultures never expressed

MHC while dynamic samples began expressing MHC by day 21. This study shows that while MIM alone can induce myotube formation, this media is insufficient in demonstrating cells that are terminally differentiating towards a myogenic lineage as observed by the absence of MHC expression.

Additionally, Zuk et al.[49] previously reported on myogenic media C (Myo C) for differentiation of lipoaspirate (PLA) cells towards a myogenic lineage. In this study, Zuk et al. seeded processed lipoaspirate cells, also known as adipose-derived stem cells in myogenic media (MM) for 1, 3 and 6 weeks. Differentiation towards a myogenic lineage was determined utilizing reverse transcriptase polymerase chain reaction (RT-PCR) and evaluating expression level of cells cultured in MM compared to those cultured in control media. Cells cultured in MIM expressed six common skeletal muscle markers (myoD, myf5, myf6, MHC, myogenin, and desmin). These were the only results on myogenesis published in this article, however it was a continuation of Mizuno et al.'s publication on myogenic differentiation[51] where it was determined that only 15% of PLA cells could be differentiated towards the myogenic lineage. While this media does induce hASCs towards a myogenic lineage, the efficiency is low and leaves room for improvement.

Additional research is required to determine the optimal conditions for hASC myogenic differentiation to find a more efficient and reliable protocol for successful myogenic differentiation. Here we aim to optimize myogenic differentiation conditions of hASCs to advance the likelihood of utilizing this abundant cell source for treating muscle tissue damage and degeneration. To accomplish this, we evaluated the influence of the two different media (Myo B and Myo C) individually and in combination with

altered surface chemistry by coating tissue culture dishes with extracellular matrix proteins (**Figure 5-1**).

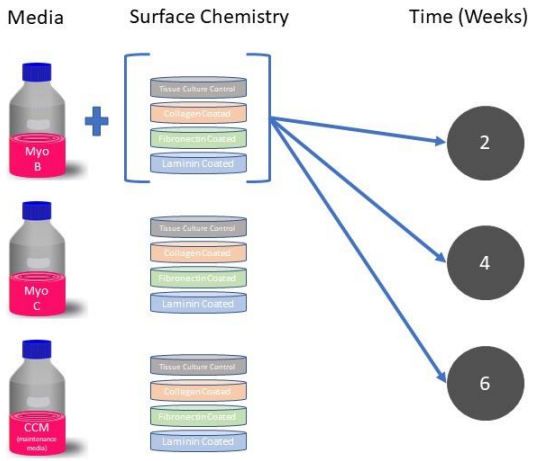

Figure 5-1: Schematic illustrating the combination of media, extracellular matrix protein, and time point to be evaluated. Each media (Myo B, Myo C, and CCM) will be cultured on plates coated with collagen type I, fibronectin, laminin, and tissue culture controls for 2, 4, and 6 weeks.

Since the biochemical stimulation of the media alone do not efficiently induce myogenic differentiation, we paired collagen type I, fibronectin, and laminin with the media to evaluate how altering the surface chemistry cells on which cells are cultured influences myogenic differentiation potential. Collagen type I is one of the earliest extracellular matrix proteins that is associated with the myogenesis process,[236] and collagen is also the most abundant structural protein found in skeletal muscle.[250] Fibronectin is a critical cellular protein for cell-cell and cell-surface interactions, and some studies have also shown the presence of fibronectin during proliferation of muscle precursor cells.[236] Finally, laminin is utilized as it is the most abundant glycoprotein in the basal membrane of the ECM and has been shown to elongate muscle precursor

cells.[236] The important role of these three proteins in myogenesis extracellular matrix formation is why they were chosen for inclusion in these studies.

To evaluate the role environmental chemistry has on hASCs, human ASC's were cultured in Myo B, Myo C, or complete culture media (CCM) in combination with either collagen, fibronectin, or laminin for 6 weeks. Reverse-transcriptase polymerase chain reaction (RT-PCR) of six common skeletal muscle markers was used to determine gene expression and immunofluorescence was utilized to qualitatively evaluate myogenic protein expression. Human skeletal myoblasts (HSkMs) were cultured and used as a positive control. These cells were also used to optimize myogenic primers for RT-PCR and MYOD immunofluorescence.

Moving forward the media plus protein combination that initially yielded the most promising results were utilized. To further promote myogenesis 5-azacytidine, a DNA methylation inhibitor,[251] was added to Myo B and Myo C medias for 24 hours, after which timethey were returned to normal Myo B and Myo C medias for 6 weeks. Under these conditions, myogenesis was confirmed through RT-PCR of early, mid and late muscle markers as well as immunofluorescence of myosin and MYOD. This combination of biochemical stimulation lays groundwork for proceeding with creating a scaffold that will effectively and efficiently mimic that of the natural ECM of skeletal muscle for potential regenerative therapies.

5.2 Materials and Methods

5.2.1 Materials

Human skeletal myoblasts were purchased from Invitrogen and cultured according to manufacturer protocol. Human adipose-derived stem cells (hASCs) were purchased from LaCell, LLC. Minimum essential media (MEM) α, low glucose Dulbecco's modified eagles medium (DMEM) L-glutamine, penicillin streptomycin, Alexa Fluor 555 phalloidin, and diamidino-2-phenylindole, dihydrochloride (DAPI), MYOD monoclonal antibody were purchased from ThermoFisher Scientific, MA, USA. Methanol was purchased from VWR. Monoclonal myosin antibody, hydrocortisone, and 5-azacytidine were purchased from Sigma Aldrich, MO, USA. Bovine serum albumin (BSA) was purchased from Amresco. Fetal bovine serum (FBS) was purchased from Atlanta Biologicals. Formalin was purchased from Azer Scientific. Triton X-100 was purchased from Alfa Aesar. Unless otherwise stated, all materials were used as received.

5.2.2 Human Skeletal Myoblast Culture

Human SkMs were thawed into media composed of low glucose DMEM and 2 % horse serum. Cells were then centrifuged at 180 x g for 5 minutes. The media was aspirated leaving a cell pellet. This was then resuspended in low glucose DMEM and 2 % horse serum and seeded onto a 6 well polystyrene tissue culture plate. Cells were cultured for 48 hours before collecting RNA or performing immunofluorescence.

5.2.3 Stem Cell Maintenance

Human Adipose-Derived Stem Cells (hASC) were cultured on 10 cm tissue culture treated polystyrene dishes in complete culture medium (CCM) containing α MEM

1x, 16.5% Fetal Bovine Serum (FBS), 1% L-glutamine 200mM (100x), and 1% Penicillin Streptomycin. Cells were incubated at 37 °C at 5% CO_2 and media was changed every other day to ensure the cells were receiving proper nutrients.

5.2.4 Differentiation Medias

Human ASCs in 24 well plates were cultured in low glucose myogenic "B" media (Myo B) and low glucose myogenic "C" media (Myo C) for 2, 4, and 6 weeks. Myo B media contained low glucose Dulbecco's Modified Eagle Media, 5 % Horse Serum, 1 % Penicillin Streptomycin, and 1 % L-glutamine.[249] Myo C media contained low glucose Dulbecco's Modified Eagle Media, 10% Fetal Bovine Serum, 5% horse serum, 50µM hydrocortisone resuspended in ethanol, and 1% Penicillin Streptomycin.[49] Cells were passaged, seeded for experiments, and cultured in CCM for 24 hours. At this point 5-azacytidine was added at a10 µM concentration in Myo C media (referred to as AZA Myo C) and cells were cultured for 24 hours. Cells were then switched to Myo C for their respective studies. Cells cultured in Myo B were switched to differentiation media 24 hours after passaging and exposure to CCM. Myogenic media was changed every 48 hours (**Figure 5-2**).

Myogenic Media "B"	Myogenic Media "C"	Complete Culture Media
• Dulbecco's Modified Eagle Media • 5 % Horse Serum • 1 % Penicillin-Streptomycin • 1 % L-glutamine	• Dulbecco's Modified Eagle Media • 10 % Fetal Bovine Serum • 5 % Horse Serum • 50 µM Hydrocortisone • 1 % Penicillin-Streptomycin	• Alpha MEM • 16.5 % Fetal Bovine Serum • 1 % L-glutamine • 1% Penicillin-Streptomycin

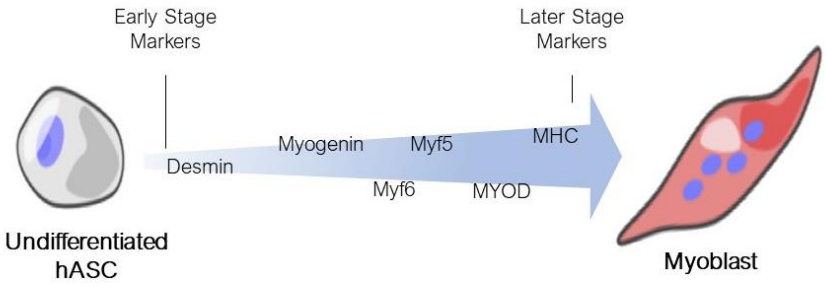

Figure 5-2: Media components utilized and expectation of gene expression timeline during myogenesis**.** Each media has different biomolecules to stimulate cell growth or differentiation. The genes *myf5* and *myod* are considered the master regulators of myogenesis.

5.2.5 Surface Modification

To assess the influence of extracellular matrix proteins on cellular differentiation, 24 well non-treated tissue culture plates were coated with different extracellular matrix proteins. These proteins included: 0.02 µg/µL concentration of collagen type 1, laminin, or fibronectin diluted in PBS. Protein solutions were added at 250 µL per well and rocked at 4 °C for 24 hours. Plates were then blocked with 1% BSA for 1 hour before cells were passaged and seeded onto the surfaces.

5.2.6 Reverse Transcriptase-Polymerase Chain Reaction (RT-PCR)

RT-PCR and was utilized to determine if common myogenic markers, *desmin, myf5, myf6, myogenin, mhc, and myod* were expressed in hASCs after 2, 4, and 6 weeks in culture with the various surface modifications and different medias. RNA was collected from cells cultured in each combination of conditions and extracted from each

experimental group using TRIzol reagent following the manufacturer's protocol. The RNA was quantified using a Take3 plate on a BioTek plate reader. cDNA was synthesized following the protocol provided by Quanta Biosciences for their cDNA SuperMix kit. Samples were denatured at 60 °C and underwent 35 cycles of PCR.

5.2.7 Immunofluorescence and Phalloidin Staining

Immunofluorescence staining of MYOD and Myosin antibody were used to visualize transcription proteins used in muscle differentiation. Human ASCs were fixed in 10% formalin and permeabilized using 0.2% Triton™ X-100. Immunofluorescence was performed using MYOD specific antibody at a dilution of 1:200 and a myosin specific antibody at a dilution of 1:150. Both were diluted in a 1 % BSA solution and fix cells were incubated for 24 hours at 4 °C. AlexaFluor® 488 and AlexaFluor® 555 secondary antibodies were used at a 1:1000 dilution and incubated for 50 minutes at 4 °C. After AlexaFluor® 555 phalloidin was prepared with methanol according to manufacturer's specifications. A dilution of 1:40 to PBS with 1% BSA was used for phalloidin staining and incubated for 20 minutes at 4 °C. DAPI was added at a final dilution of 1:2000 and incubated for 10 minutes at room temperature. Samples were then washed three times with PBS and imaged with 500 µL of PBS in each well. Immunofluorescence and staining were performed in an area protected from light.

5.2.8 Hydrogel Synthesis

Hydrogel precursor solutions containing a total of 20% wt. polymer (17 % MW 20,000 and 3 % MW 1000) were prepared as summarized in **Chapter 3**. Prior to cell culture, hydrogels were functionalized via EDC/Sulfo-NHS chemistry as previously described[48] using collagen type I in place of fibronectin.

5.3 Results

5.3.1 Human Skeletal Myoblast Controls

Before beginning experiments utilizing hASCs, human skeletal myoblasts (HSkMs) were cultured to optimize primers and the MYOD antibody. Human SkMs were utilized as a positive control for RT-PCR analysis. Primers for *desmin, myogenin, mf5, myf5, mhc, and myod* were designed for these experiments. MYOD, myogenin, myf5 and myf6 are transcription factors belonging to the myogenic regulatory factor (MRF) family.[252] This family of basic helix-loop-helix transcription factors are only expressed in skeletal muscle and so are considered master regulators of skeletal myogenesis.[253] The housekeeping gene *gapdh* was used as a control for the integrity of the cDNA from samples. The cDNA synthesized from HSkM RNA expressed each of these genes as identified by the bands depicted in (**Figure 5-3**). The single bands for each gene corresponded to the appropriate product size indicating these primers were sufficient to identify expression of these genes.

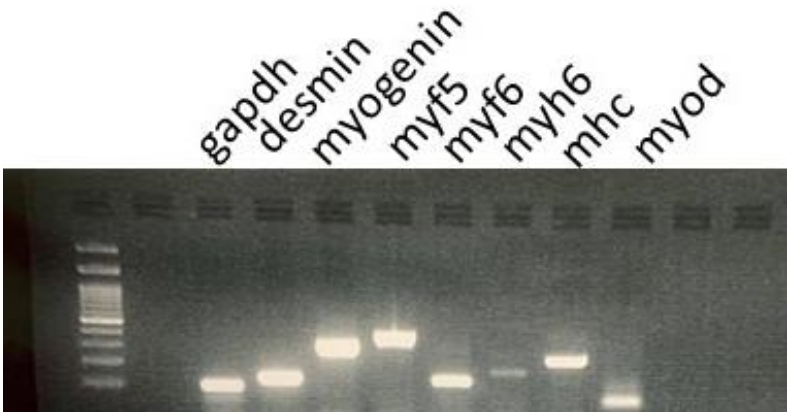

Figure 5-3: RT-PCR of HSkMs expressing myogenic markers. Human skeletal myoblasts show expression of the myogenic genes *desmin, myogenin, myf5, myf6, myh6, myh,* and *myod*. Primers were optimized at 60 °C for 35 cycles.

Human SkMS were also utilized to optimize antibody dilutions of the MYOD antibody. The dilutions tested were 1:100, 1:200, 1:400, 1:500, and 1:1000 as seen in **(Figure 5-4**). Exposure corrections had to be applied to visualize the antibody at the 1:500 and 1:1000 dilutions. The 1:400 dilution did not need exposure corrections; however, the images are much darker compared to the lower dilutions. Due to this, the dilution of 1:200 was chosen as the optimal dilution. Phalloidin stain was also utilized to visualize the morphology of the cytoskeleton. The HSkMs exhibit analigned, multinucleated morphology. This morphology is the ideal goal sought in hASC myogenic differentiation. In addition, DAPI was used to visualize cell nuclei. From the overlay images, we can see MYOD is localized to the cell nuclei og fully differentiated cells.

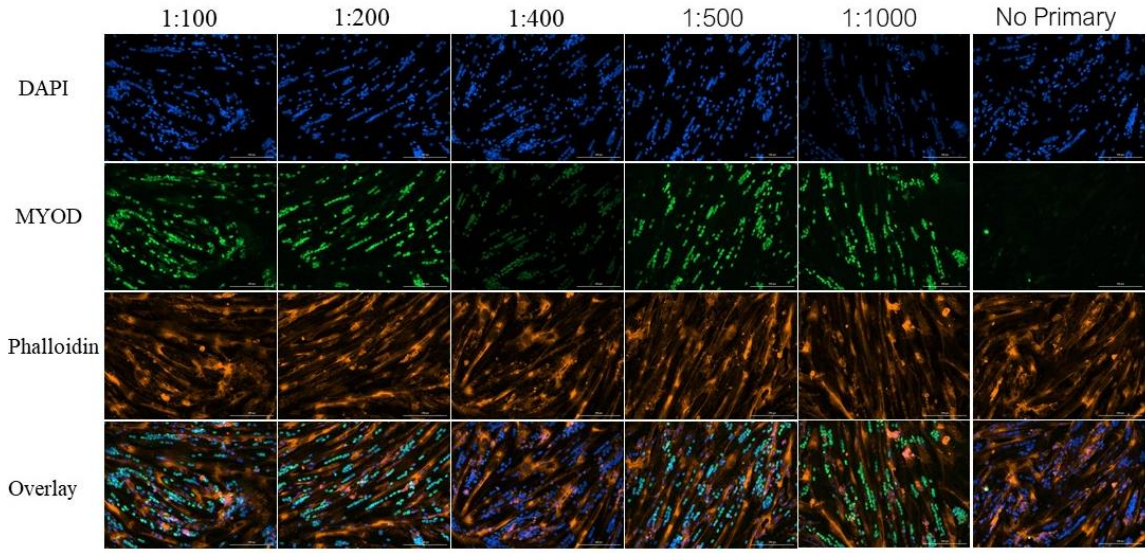

Figure 5-4: Immunofluorescence of HSkMs using the antibody anti-MYOD and phalloidin. The immunofluorescence shows MYOD localized in the cell nuclei (green) of all cells. The phalloidin staining the f-actin filaments shows a highly aligned morphology. From these images a 1:200 dilution of MYOD was chosen.

5.3.2 Culture of hASCs in Differentiation Media Alone

Human ASC's were initially cultured in Myo B, Myo C, and CCM (used as a negative control) for 2, 4, and 6 weeks on standard tissue culture treated polystyrene 24 well plates. However, after initial analysis, it was found 2 and 4 weeks were not sufficient time points for detecting the expression of multiple myogenic markers and therefore is not shown. At 6 weeks RNA was collected from all samples and cDNA was synthesized. After gel electrophoresis it was determined that hASCs cultured in Myo B and Myo C expressed the genes *desmin*, *myogenin*, *myf6*, and *mhc*. However, the negative control showed expression of these genes as well. The absence of *myf 5* and *myod* expression indicate there is not mature skeletal muscle differentiation taking place as the expression of one or the other is required for skeletal muscle differentiation.[253]

Immunofluorescence using antibodies against Myod and Myosin were utilized to qualitatively evaluate protein expression in the samples. The hASCs that were only exposed to biochemical factors via media did not express any Myod indicating no definitive myogenic differentiation. Cells cultured in the different medias did exhibit myosin expression. You can see in **(Figure 5-5)** that hASCs cultured in Myo C media show an aligned morphology with thick bands of myosin expression. While cells cultured in Myo B express myosin, you can see the morphology is circular which is not indicative of myoblast morphology. The results from RT-PCR and immunofluorescence of those cells cultured in different medias do not show definitive myogenic differentiation and therefore we hypothesized would require the introduction of additional biomolecules to attempt to drive differentiation towards a myogenic lineage.

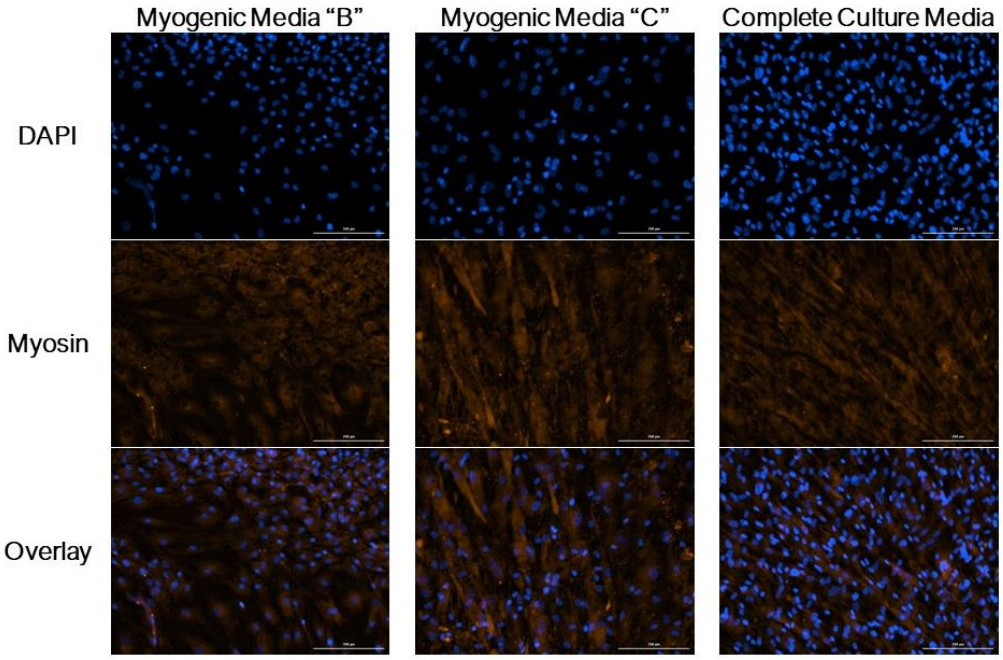

Figure 5-5: Immunofluorescence of hASCs using anti-myosin (skeletal fast) antibody. Myosin expression (orange) shows an aligned morphology in cells cultured in Myo C media.

5.3.3 Culture of hASCs in Differentiation Media on Protein Coated Plates

Non-treated polystyrene tissue culture plates were coated with collagen type I, fibronectin, and laminin at a concentration of 0.02 µg/µL for all proteins. Each protein was diluted in PBS to coat each well and plates were kept at 4 °C for 24 hours before blocking each well with BSA to prevent nonspecific binding. Human ASCs were then seeded on plates coated with collagen type I, fibronectin, laminin, and tissue culture treated wells as a control. Cells were cultured in either Myo B, Myo C, or CCM for 6 weeks. This gave 12 different sample combinations to analyze. It was determined that the best course of action was to collect RNA at 6 weeks and evaluate expression of myogenic genes through RT-PCR to determine which combination of media and ECM protein is the most effective for promoting myogenic differentiation.

Through RT-PCR analysis we determined that Myo C was a more efficient differentiation media compared to Myo B. This is due to the brighter band expression in Myo C samples and the consistency between samples. While all media and protein combinations expressed *desmin*, *myogenin*, *myf6,* and *mhc*, there was still no expression of *myf5* or *myod* (**Figure 5-6**).

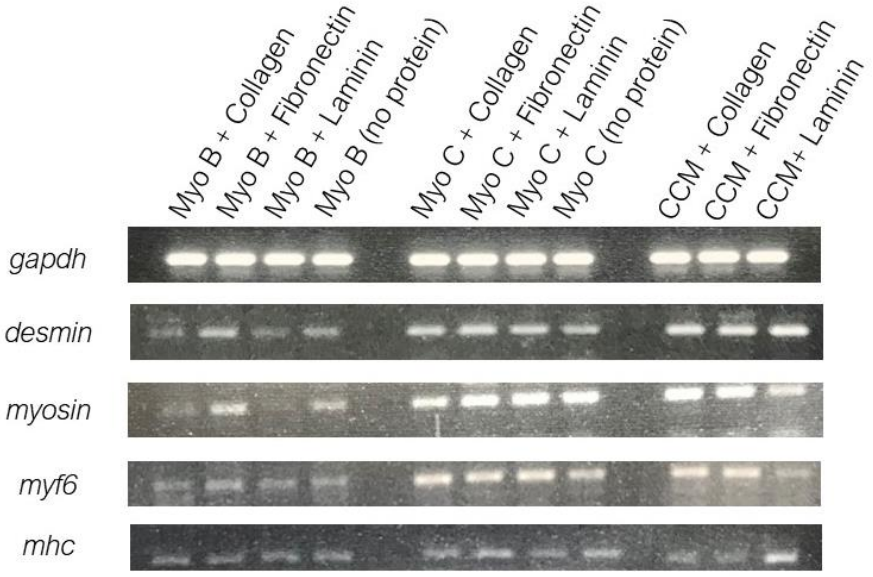

Figure 5-6: RT-PCR of hASCs cultured in different media and protein combinations. End point PCR shows expression of early myogenic markers in all samples. However, Myo B samples appear to have the lowest expression levels. No samples express *myf5* or *myod*.

Based on the immunofluorescence images from hASCs cultured in only media along with RT-PCR results, i Myo C was determined to be the more effective media for inducing myogenic differentiation of hASCs with no noticeable differences observed in the expression profile of cells cultured in Myo C on the three different protein coated surfaces. Therefore, for ease and affordability collagen type I was selected for further studies.

5.3.4 Introduction of 5'-azacytidine to Myo C Media

The combination of Myo C media and collagen type I did not yield expression of *myod* or *myf5*. In attempt to enhance myogenic differentiation and observe expression of all four MRF transcription factors, 5-azacytidine, a DNA methylation inhibitor, was added at a 10 µM concentration for 24 hours[249] in Myo C media (referred to as Aza C). Cells were also cultured on collagen type I coated plates. The combination of 5-

azacytidine in Myo C for 24 hours followed by 6 weeks of culture in Myo C on collage type I coated plates led to the expression of all four MRFs in hASCs as seen in (**Figure 5-7**). The expression of *myf5* is consistent across all Aza C samples while *myod* is only expressed slightly in one sample. This could be due to where the cells where in the cell cycle, as this has been shown to affect which gene(s) are expressed during myogenesis.[254]

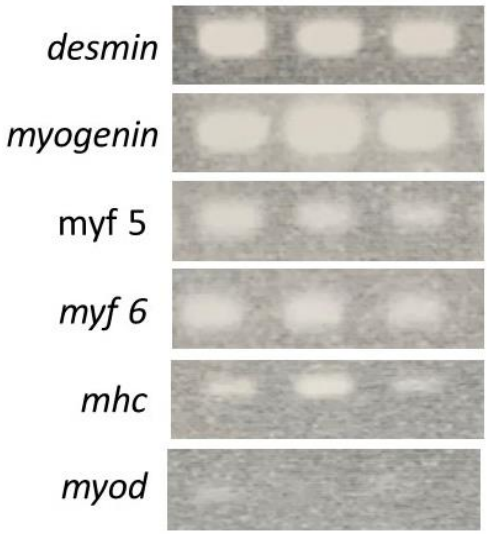

Figure 5-7: RT-PCR of hASCs cultured in 5-azacytidine**.** Human ASCs that were exposed to 5-azacytidine for 24 hours on collagen coated plates with Myo C media for a total time of 6 weeks express the master regulator myf5 consistently in triplicate.

In addition, hASCs cultured in Aza C on collagen type I coated plates were the first to show expression of MYOD through immunofluorescence (**Figure 5-8**). The expression is not isolated to the nuclei that was seen in human skeletal myoblast controls however, they are expressing MYOD which is one of the master regulators of myogenesis. This shows that myogenic differentiation is taking place in hASCs when they are cultured on collagen type I coated plates in Aza C media.

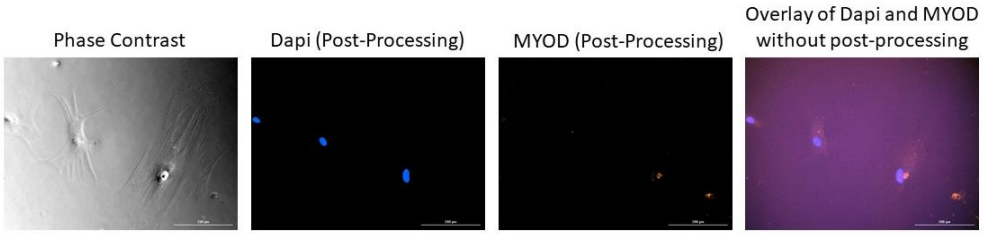

Figure 5-8: MYOD immunofluorescence of hASCs exposed to 5-azacytidine**.** After 24-hour exposure to 5-azacytidine followed by 6 weeks in Myo C media on collagen coated plates, MYOD (orange) and Dapi (blue) stain were used to determine if MYOD protein was expressed. The overlay image shows MYOD expression localizing around the cell nuclei. This was the first set of samples that demonstrated any MYOD expression, indicating it is the more efficient differentiation protocol.

5.3.5 Myogenic Differentiation of hASCs cultured on 17:3 PEGDMA hydrogels

The 17:3 PEGDMA hydrogels that have an elastic modulus of 8-10 kPa were surface modified and coated with collagen type I. Human ASCs were seeded on the surface of 17:3 hydrogels and cultured for a total time of 2 weeks. Cells were initially seeded in CCM, but at the 24-hour timepoint CCM was replaced with Myo C media that contained 5-azacytidine. Cells were cultured in Myo C + 5-azacytidine for 24 hours and then switched to regular Myo C media for the remainder of the 2 weeks. At two weeks, cells began to peel off of the hydrogel surface due to over-confluences, so RNA was collected and cells were fixed for immunofluorescence.

Gene expression was analyzed in duplicates using RT-PCR. There was no expression of early myogenic markers in samples cultured on 17:3 collagen coated hydrogels. There was expression of later myogenic markers including *myf6, mhc,* and the master regulator *myod* (**Figure 5-9**). The expression of *myod* in samples cultured

on hydrogels is greater compared to those on tissue culture plates that underwent the same surface modification and were exposed to the same media components.

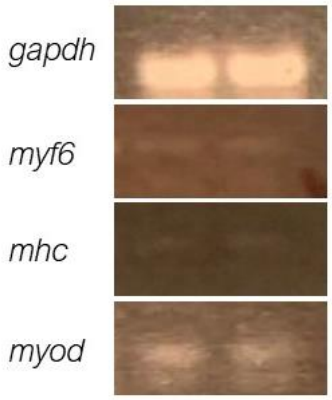

Figure 5-9: RT-PCR of myogenic markers that are expressed when hASCs are cultured on 17:3 PEGDMA hydrogels. These hydrogels were surface modified and coated with collagen type I. Cells were exposed to 5-azacytidine for 24 hours then cultured in Myo C media for 2 weeks. The hASCs only expressed late myogenic markers.

Immunofluorescence was also utilized to visualize the expression of the myogenic proteins myosin and myod. The hASCs exhibited myosin expression and showed an aligned myosin morphology in the immunofluorescence images (**Figure 5-10**).

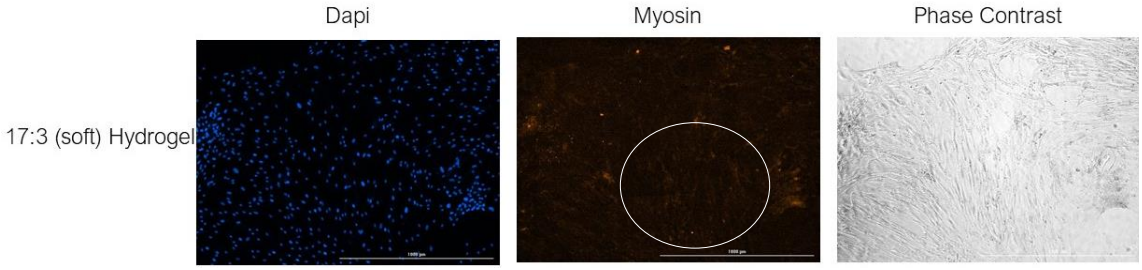

Figure 5-10: Immunofluorescence images of the myosin protein. The white circle highlights an area with an increase in the aligned morphology of myosin that is associated with myogenic differentiation. Scalebars: 1000 µm.

Most notable of the immunofluorescence that was performed is the expression of MYOD in hASCs cultured on the collagen coated hydrogels. When hASCs were cultured on tissue culture plates for 6 weeks after exposure to 5-azacytidine there is very little MYOD expressed in the immunofluorescence images (**Figure 5-8**). Here, after only 2 weeks after exposure to 5-azacytidine there is a much more MYOD protein being expressed (**Figure 5-11**). Also, of note is the localization of MYOD in cell nuclei that is beginning to take place, which is indicative of myoblast formation. This is seen in the overlay image by the appearance of purple coloring. The purple color is created due to the blue from the Dapi stain and the orange from the MYOD antibody.

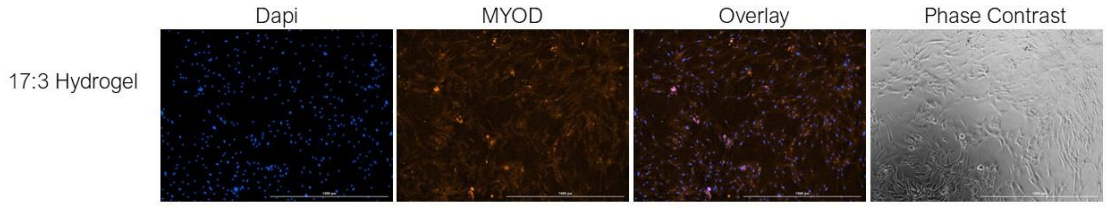

Figure 5-11: Immunofluorescence using the anti-MYOD antibody to qualitatively evaluate protein expression. You can see much higher levels of MYOD expression compared to cells cultured on tissue culture. In addition, the overlay image of Dapi and MYOD shows MYOD localizing in cell nuclei which is indicative of myoblast formation. Scalebars: 1000 µm.

Finally, hASCs that were cultured on the 17:3 collagen coated hydrogels were stained with phalloidin and Dapi. This allows for the visualization of the cytoskeleton of cells and their morphology. From the phalloidin stain (**Figure 5-12**) we can see a highly aligned morphology with the cytoskeletons beginning to compact and create a fibrous morphology. This is not a morphology typical of undifferentiated hASCs. It is very similar to the morphology of human skeletal myoblasts as shown in **Figure 5-4**. The

overlay image shows multinucleation taking place as well, which is typical of human skeletal myoblasts.

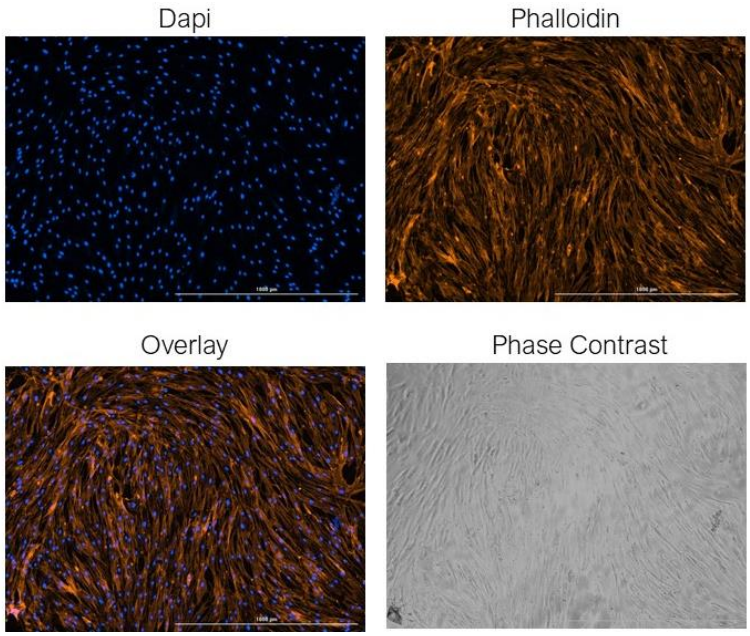

Figure 5-12: Phalloidin staining of the f-actin filaments shows the cytoskeleton morphology to be compact and highly aligned. The overlay image depicts multinucleation of cells beginning to take place. Scalebars: 1000 µm.

5.4 Discussion

This work focused on optimizing myogenic differentiation conditions utilizing different combination of biomolecules. We utilized two media recipes previously reported in literature to promote myogenic differentiation in combination with three ECM proteins in an attempt to enhance differentiation efficiency. Human ASCs did not express *myf5* or *myod* when cultured in myogenic media alone or when combined with one of the three selected ECM proteins. Once 5-azacytidine was introduced to Myo C media,

however, cells that were cultured on collagen type I coated plates began expressing these master regulators of myogenesis.

When hASCs were cultured on collagen coated 17:3 hydrogels an increase in expression of MYOD, one of the master regulators of myogenesis, demonstrated using RT-PCR was observed. In addition, there was no expression of early myogenic markers, only late markers were expressed. In addition, we see an increase in MYOD protein expression as seen through immunofluorescence images. The MYOD is also beginning to show localization in the cell nuclei, which is typical of fully differentiated human skeletal myoblasts. Phalloidin and Dapi staining also shows a cell morphology and multinucleation similar to that seen in human myoblast samples. It appears that when cultured on 17:3 PEGDMA hydrogels, hASCs show an increase in myogenic differentiation potential. The cells were exposed to the same surface ECM protein, collagen type I, and the same concentration of 5-azacytidine, yet when cultured on PEGDMA hydrogels at only 2 weeks we see greater expression of master regulators and morphologies typically of myoblasts.

There is still more to be done in order to further enhance myogenic differentiation of hASCs through the use of chemical and physical cues. We show that biochemical stimulation alone may not be enough to fully differentiate hASCs towards a myogenic lineage. However, when the only factor that was changed was surface elasticity (comparing the hydrogel to tissue culture plates) we see a dramatic difference in differentiation potential. This indicates that physical factors such as surface elasticity has a synergistic effect with biochemical stimulation in terms of myogenic differentiation potential. Future work will begin to incorporate other extracellular with Aza C media in

order to determine if combining biomolecules with other external factors will enhance differentiation further than what we show in these experiments. Optimizing myogenic conditions is the first step in being able to create functional tissue patches to treat muscle loss and damage.

CHAPTER 6

CONCLUSIONS AND FUTURE DIRECTIONS

6.1 Research Summary

There are numerous factors that can influence stem cell fate. The environmental stimulus, chromatin modifiers, signal transduction molecules, and transcription factors all impact the ultimate decision the cell makes. Modification to even one of these factors will change the genes expressed and the decision to continue self-renewal or differentiate. My Ph.D. project has specifically focused on investigating how changes in environmental stimuli influences cell fate by utilizing a tailorable PEGDMA hydrogel platform. Through the tailorability of the PEGDMA hydrogel platform, I have been able to evaluate environmental stimuli such as: surface elasticity, surface topography, and the incorporation of biochemical factors and their effect on stem cell fate.

In **Chapter 3** PEGDMA hydrogel elasticity was altered by changing the ratio of high molecular weight polymer (MW 20,000) to low molecular weight polymer (MW 1000) while keeping the total percent polymer constant at 20 % w/w. A "soft" hydrogel with elasticity of 8-10 kPa and a "stiff" hydrogel with elasticity of 50-60 kPa were utilized as a scaffold for hMSCs and compared to a standard polystyrene tissue culture plate used as the control. Human MSCs attached to the hydrogels and remained viable

after seeding, demonstrating biocompatibility. However, after 72 hours, cell density on stiff hydrogels was much lower when compared to tissue culture controls, indicating a decrease in proliferation rates, confirmed by an alamarBlue™ assay. When cultured in maintenance media (CCM) hMSCs cultured on all three surfaces maintained their multipotent potential as depicted through qRT-PCR. Osteogenic and adipogenic differentiation of cells cultured on soft and stiff hydrogels was also analyzed. There was a significant difference in expression of early osteogenic markers when cells were cultured on stiff hydrogels. This could be an indication of less efficient differentiation potential, or that cells were further along in differentiation than those on tissue culture or soft hydrogels. These studies demonstrate that the elasticity adult stem cells are cultured on influences their behavior and cell state, indicating the potential for using this hydrogel platform to create a controlled environment for tissue engineering applications.

Chapter 4 focused on the development of PEGDMA hydrogel platforms with multiscale porosity through flash freezing and lyophilization. Hydrogels of varying thickness, polymer blend, and drying method were evaluated in this work. Environmental scanning electron microscopy (ESEM) imaging of hydrogels in a hydrated state demonstrated that freeze-dry lyophilization altered the hydrogel architecture when compared to air-dried controls. This change in architecture created pores of varying sizes leading to polymers with multiscale porosity. Freeze-dry lyophilization also caused a change in shear elastic modulus when compared to their air-dried counterparts. While hydrogel topography and elastic moduli were altered by drying method, lyophilized samples exhibited the same absence of degradation in media as air-dried samples. Human ASCs were cultured on lyophilized and air-dried hydrogels of the same PEGDMA blend

and both demonstrated biocompatibility regardless of drying method. By altering the porosity and therefore topography of the PEGDMA hydrogels through drying method, this gives more flexibility and tailorability for potential use for tissue engineering scaffolds.

Lastly, the work in **Chapter 5** evaluated the efficiency of myogenic differentiation of hASCs through extracellular exposure to different biomolecules. By altering the components of culture medias and by surface coating the plates they were cultured on with different extracellular proteins, we observed differences in differentiation potential. Exposure to culture media alone led to differences in myosin expression in hASCs. Those cultured in Myo C demonstrated an aligned morphology, like what would be seen in human skeletal myoblast cells. When hASCs were cultured in differentiation medias combined with different surface proteins, expression of several early myogenic markers was expressed. However, the master regulators *myf5* and *myod* were still not expressed. The methylation inhibitor 5-azacytidine was added into Myo C media for 24 hours before being switched to normal Myo C media. The incorporation of this methylation inhibitor led to the expression of *myf5* and *myod* in hASCs after 6 weeks, indicating myogenic differentiation. When biochemical factors were combined with PEGDMA hydrogels that have an elasticity similar to muscle tissue,[48] we saw a dramatic increase in MYOD expression in a much shorter time frame. This demonstrates that all environmental stimuli influence cell fate and combinations of various extracellular cues should be investigated further.

6.2 Future Directions

The ultimate goal of this work was to gain a better understanding of cell fate as a function of cell environment. From this work a tailorable PEGDMA hydrogel platform that allows for more in-depth cell-material studies has been created. By altering the properties of the hydrogel such as elasticity, surface topography, and different biomolecules that can be attached to the surface, I was able to create the ideal environment to study how to best control cell fate. In addition, utilizing different biomolecules we were able to differentiate hASCs towards a myogenic lineage, opening up more areas of possible research in the future. In **Chapter 3** it is shown that hydrogel elasticity influences cell proliferation and osteogenic differentiation potential. This preliminary work has led to a possible future project where the lab could further explore why stiffer hydrogel have a significant influence on stem cell differentiation. Quantitative RT-PCR of middle and late differentiation markers would distinguish if the decrease was due to cells being further differentiated or if the change is a decrease in differentiation efficiency.

The multiscale porosity PEGDMA hydrogels discussed in **Chapter 4** demonstrated hASC biocompatibility and retain their innate hydrogel properties. This offers an additional way to tailor PEGDMA hydrogels and explore stem cell multipotency, proliferation rates, and differentiation potential on. Since the work in **Chapter 3** demonstrated that elasticity influences cell behavior, studies should be conducted on how this change in network architecture affects cell state. We know that drying method alters the shear elastic modulus, thus it is likely cells would behave

differently on lyophilized and air-dried scaffolds. In addition, it has been previously been shown by other groups that pore size and matrix architecture influence cell proliferation and differentiation ability.[255–259] Therefore, the change in architecture seen through different drying methods will likely initiate a change in cell behavior. Since osteogenesis and adipogenesis in adult stem cells is highly characterized, these routes of differentiation potential should be explored on the multiscale PEGDMA scaffolds.

Myogenesis of hASCs discussed in **Chapter 5** only utilizes biomolecules through media and surface coating standard non-treated tissue culture plates. Culturing the cells exposed to different biomolecules on the PEGDMA hydrogels of varying elasticity would be the next step. Since the "soft" (17:3) hydrogels have an elasticity of 8-10 kPa it is hypothesized that this would enhance myogenic differentiation. This is due to skeletal muscle tissue having an elastic modulus of ~10-11 kPa.[235] There are no universal myogenic differentiation medias so utilizing the extracellular environment would be an ideal option to further explore the differentiation potential of hASCs. This work has shown that utilizing different biomolecules can stimulate hASC differentiation towards a myogenic lineage. This opens up another area of research that can be explored in terms of cell-material interactions.

6.3 Conclusions

Despite the abundance of research in this field, the interactions between stem cells and the external environment created using biomaterial substrates are not well understood. This research is helping to bridge this knowledge gap utilizing PEGDMA hydrogels with adult stem cells. The PEGDMA hydrogels that our lab utilizes can be

produced in large quantities, and they are an affordable scaffolding option. In addition, they can easily be tailored as demonstrated throughout this research. This work has demonstrated that substrate elasticity alone can influence stem cell behavior with altering attachment, proliferation, and differentiation potential. Utilizing freeze-dry lyophilization as a post-processing drying method, PEGDMA hydrogels of multiscale porosity were created. Through ESEM imaging it was shown that this changes the hydrogel architecture and surface morphology. This provides a novel PEDGMA platform that can be used to investigate how surface topography influences cell fate. In addition, to our knowledge, this was the first time that PEGDMA hydrogels were imaged in the hydrated state using ESEM. Finally, we show that hASCs myogenic differentiation potential is influenced by various biomolecules. While there are a few myogenic differentiation medias reported in literature, when used alone, we could not confirm hASC differentiation. By combing these medias with different extracellular matrix proteins and the methylation inhibitor 5-azacytidine, we were able to confirm myogenic differentiation through RT-PCR.

The long-term goal of this work is to create affordable, clinically relevant scaffolds that can reliably control stem cell fate via external stimuli. This research supports this goal in providing an understanding of how elasticity and biomolecules influence adult stem cell differentiation potential. In addition, the creation of hydrogels with multiscale porosity yields another way in which this platform can be tailored to create an environment to direct stem cell fate. This project has opened several new opportunities for research that can move the field of tissue engineering forward through the pursuit of creating a biomaterial scaffold that can control stem cell fate.

APPENDIX A

NATURAL AND HYBRID HYDROGELS IN-DEPTH DISCUSSION

A.1 Natural Hydrogels:

Hydrogels synthesized from natural polymers are frequently used because they are components of, or have macromolecular properties that are similar to the extracellular matrix.[31,260] Collagen, fibrin, hyaluronate, alginate, and chitosan are synthetic polymers that have been used to create hydrogels in hopes to revolutionize the tissue engineering field.[139] Collagen is one of the main component of the extracellular matrix of mammalian tissues such as skin, bone, cartilage, tendon and ligaments.[261] Collagen has been used for several tissue engineering application including for endothelial tissue scaffolds and the formation of porous, spongy scaffolds.[31,261] One issue with utilizing collagen is the potential antigenicity.[261] Fibrin is another natural polymer used in tissue engineering. Fibrin is advantageous in that scaffolds can be created using the patient's own blood eliminating the chance of immune response to the scaffold.[262] It has been studied to be a scaffold for adipose tissue, muscle, skin, articular cartilage, ocular tissue, and cardiovascular purposes.[261,262] The main concern with fibrin for tissue engineering purposes is that it undergoes enzymatic degradation and it has poor mechanical strength.[261,262] Another commonly used natural polymer in tissue engineering is hyaluronic acid (HA). Hyaluronic acid is a polysaccharide found naturally in the extracellular matrix which is one reason it is a popular material in tissue engineering.[31,261,263] However, hyaluronic acid can be degraded by hyaluronidase, naturally found in tissues, and suffers from low mechanical strength.[261,264,265] Alginate has been studied in regenerative medicine for applications such as cell encapsulation, drug stabilization, transplantation of chondrocytes, hepatocytes, and islets of Langerhans

to treat diabetes.[139,266] Unfortunately it is hard to control swelling behavior and they tend to rapidly degrade due to ion loss.[139,267] The final natural polymer of note is chitosan. Chitosan has a high molecular weight and is the second most abundant biopolymer found in crustacean shells and fungi cell walls.[268] It is structurally similar to glycosaminoglycans and has been studied for bone regeneration, articular cartilage repair, and most notably for wound dressings.[261,268,269] This information is summarized in **Table A-1**. The main concern with natural polymers is the source. Some of these materials are harvested from other species and there is concern for an immune response using materials from a different origin.[132,139]

A.2 Hybrid Hydrogels:

Synthetic/natural hybrid polymers or semi-synthetic polymers, incorporates desirable features from both types of polymers. Synthetic hydrogels are typically passive scaffolds and biologically inert while natural polymers typically aid in the regulation of cell responses having critical biologic functions.[145] Thus, combining the two yields a bioactive hydrogel scaffold. These hybrid hydrogels create bioactive hydrogels without a complicated synthesis for bioconjugation. The natural extracellular matrix can be thought of as a hybrid material with the rigid structural components interacting and support soft biomolecules like cells, signaling factors, and enzymes.[270] The goal of any tissue scaffold is to mimic the natural cell environment as closely as possible making hybrid polymer scaffolds an attractive approach. Combining the properties from the synthetic and natural polymers has the potential to increase mechanical stability, provide a better architecture, and more favorable chemical compositions.[270]

Table A-1. An overview of natural polymers used in making hydrogel biomaterials.

Polymer	**Uses**	**Disadvantages**	**Advantages**
alginate	Cell encapsulation, drug stabilization, transplantation of chondrocytes, hepatocytes, and islets of Langerhans	Degrades uncontrollably and unpredictably through loss of divalent ions into surrounding medium	Successful encapsulation and immunoprotection of transplanted cells
chitosan	Rigid tissue replacements	Degraded by lysozyme	High molecular weight, second most abundant natural biopolymer
collagen	Fiber and space filling	Degraded by metalloproteases	Excellent biocompatibility and biodegradability
Hyaluronan	Wound healing	Degraded by hyaluronidase	Only non-sulfated GAG and major constituent of ECM
fibrin	Engineer tissues with skeletal muscle cells, smooth muscle cells and chondrocytes	Limited in mechanical strength	Harvested from patient's blood removing chance of immune response/rejection

APPENDIX B

HYDROGELS IN BIOMANUFACTURING

There is a growing list of tissues that have the potential to be successfully engineered in the near future. This is largely due to the recent advancements in stem cell biology and the recognition of the unique biological properties of stem cells.[271] For tissue regeneration to become a clinical reality these materials need to be producible on a large scale. This drive for the need of large-scale production leads us to the field of advanced biomanufacturing. The field of advanced biomanufacturing relies on the reproducible and efficient generation of biocompatible materials for the study of cellular properties and directed differentiation as well as the creation of clinically-relevant tissues for therapeutic applications.[48] Previously, tissues such as the skin, cornea, mucosal membrane (epithelial surfaces), and skeletal tissues have been successfully engineered using stem cell strategies. Studies are being conducted using stem cells in engineering tissues such as the heart muscle, pancreas, liver, cartilage, and bone among others.[271] There are numerous techniques in biomanufacturing to achieve the goal of tissue replacement and regeneration. These techniques include electrospinning, freeze-drying, melt molding, membrane lamination, gas foaming, and 3-D printing.[48,272] These processes can be too complex or expensive for large-scale productions, so there is a need to develop more accessible ways to manufacture the materials.[48]

There are two fundamental approaches that can be used for biomanufacturing to improve tissue function: the bottom-up approach and top-down approach.[273] The bottom-up approach relies on self-assembly or directed-assembly of a scaffold from smaller components. A common characteristic of this approach is micro- or even nanoscale structures assembling into macroscopic objects.[272] The ability of the cell aggregates to

fuse is based on the concept of tissue fluidity. The drawback to this approach is that not all cell types are able to produce sufficient extracellular matrix, form cell-cell junctions, or migrate.[273] The top-down approach is the most common strategy for tissue engineering, and the one this review will focus on. The top-down approach is a scaffold-based approach.[273] In this approach cells are seeded on a scaffold that is not only biocompatible, but biodegradable as well. The cells are expected to proliferate in the scaffold and create their own extracellular matrix.[272] The success of this method is dependent on the materials and the manufacturing processes.[273] Hydrogel scaffolds tailored for stem cell differentiation is of particular interest in biomanufacturing for tissue replacement and regeneration.

Stem cells have the ability to self-renew and maintain at least one differentiated tissue type throughout the lifespan of the organism.[274] Stem cell development is a very complex process. There has to be a precise balance among many events of the cell including self-renewal, differentiation, apoptosis, and migration.[77] Mesenchymal stem cells are undifferentiated multipotent cells that have the ability to differentiate into multiple tissues of mesenchymal origin in response to the appropriate signals.[275] The unique properties of self-renewal and differentiation make stem cells ideal for the use of large scale production for tissue engineering.[48]

Hydrogels constructed from synthetic polymers seeded with stem cells offers a possible solution to the need for large scale biomanufacturing in tissue engineering. The tailorable nature of hydrogel scaffolds can provide stem cells with the appropriate cues and cellular microenvironment for differentiation and proliferation.[276] Hydrogels provide a three-dimensional environment for stem cells. 3-D environments have been shown to

enhance osteogenic, hematopoietic, neural, and chondrogenic differentiation. By altering the substrate properties, surface interactions, scaffold degradation rate, or the microenvironment of the hydrogel can directly influence the behavior of stem cells.[277] For example, the elasticity of hydrogels can be widely varied. This means the strain environment within the hydrogels can provide the appropriate mechanical stimuli for stem cell differentiation towards a particular lineage.[278] The optimum elastic modulus depends on the stem cell type and the lineage in which it is being directed.[279] This is just one modification that can influence the differentiation of stem cells. Other modifications in the hydrogel environment have the potential to affect stem cell lineage as well. Hydrogels seeded with stem cells undoubtedly provides a platform of great promise of large-scale manufacturing for tissue engineering.

The large-scale biomanufacturing of hydrogels can be accomplished by stereolithographic and inkjet printing processes.[273] Stereolithography is one of the most developed and most accurate forms of rapid prototyping.[280] The conventional stereolithography apparatus uses ultraviolet light to solidify photosensitive polymers.[281] The three-dimensional structures can be precisely fabricated in a layer-by-layer approach. It is principally based on the spatially controlled solidification of a liquid photo-polymerisable resin upon illumination.[280] Stereolithography allows for the creation of three-dimensional hydrogel structures with feature sizes ranging from micrometers to centimeters, with the option of incorporating matrices with varied properties and structure.[282] Poly(ethylene glycol) (PEG) hydrogels produced by stereolithography has been discussed in multiple studies.[273,280,283] PEG hydrogels (and others similar to PEG) undergo UV polymerization at low light intensities for short periods of time with low

organic solvent levels so the stereolithographic process can be carried out in the presence of cells, such as stem cells seeded in the polymer matrix.[273]b

Inkjet printing is a noncontact printing technology that uses tiny ink drops to reproduce digital patterns, and is highly biocompatible with biological systems.[284] Inkjet printing allows for rapid and inexpensive printing of cells, materials and other protein molecules.[285] For manufacturing of hydrogels using inkjet printing, the material jetting processes emit a stream of hydrogel microparticles to an exact co-ordinate. The process of hydrogel formation is based on the deposition of bio-ink particles in well-defined topological patterns into bio-paper sheets of biocompatible gels. The construct is then transferred to a bioreactor to fuse the bio-ink particles.[273] PEG and PEG-peptide hydrogels have been synthesized using this process and shown promising results with stem cell differentiation.[284]

Large-scale biomanufacturing in tissue engineering poses challenges that need to be overcome for the clinical availability of tissue repair and regeneration. The customizability of hydrogels combined with the unique self-renewal and differentiation properties of stem cells shows promise as a solution for the challenges facing tissue engineering. Large-scale biomanufacturing of these hydrogels seeded with stem cells could be made possible in the near future with advancements in rapid prototyping processes such as stereolithography and inkjet bioprinting. Through the combined efforts of cell biologists, engineers, material scientists, mathematicians, geneticists, and clinicians, the successful large-scale biomanufacturing of hydrogels is on the horizon.[191]

APPENDIX C

SUPPLEMENTAL INFORMATION FOR CHAPTER 3

C.1 RNA Concentrations

Table C-2. Concentration of RNA used for qRT-PCR analysis of multipotency, osteogenic, and adipogenic markers. *Reprinted with permission from Oxford Academic.*

Cell Type	RNA Concentration
Undifferentiated MSCs	0.150 μg
MSC-Derived Adipocytes	0.150 μg
MSC-Derived Osteocytes	0.050 μg

C.2 Primer Sequences

Table C-3. Primer sequences utilized in qRT-PCR. *Reprinted with permission from Taylor & Francis.*

	Specificity	**Primer sequence (5' – 3')**
gapdh	Housekeeping gene	F: AGGGCTGCTTTTAACTCTGGT R: CCCCACTTGATTTTGGAGGGA
sox2	Undifferentiated hMSCs marker	F: GGCAGCTACAGCATGATGCAGAGC R: CTGGTCATGGAGTTGTACTGCAGG
runx2	Osteogenic marker	F: CTCACTACCACACCTACCTG R: TCAATATGGTCGCCAAACAGATTC
alp	Osteogenic marker	F: CTAACTCCTTAGTGCCAGAG R: CATGATGACATTCTTAGCCAC
ppar- γ	Adipogenic marker	F: GCTGTTATGGGTGAAACTCTG R: ATAAGGTGGAGATGCAGGTTC
srebp-1c	Adipogenic marker	F: CTCTTGAAGCCTTCCTGAG R: GCACTGACTCTTCCTTGAT

APPENDIX D

SUPPLEMENTAL INFORMATION FOR CHAPTER 4

D.1 Pore Size Estimation Using ImageJ Software

Average diameter of induced micropores as a function of polymer blend, drying method, and sample condition, calculated from ESEM images using ImageJ software. Samples without a reported average induced micropore size were samples that did not have visible pores. The average induced pore size was generated from the average measured pore size from ~15-20 images from 1 sample of each sample set.

Table D-4. Average pore size as a function of polymer blend, drying method, hydrogel state, and thickness. *Reprinted with permission from Taylor & Francis.*

PEGDMA Hydrogel Blends 20 kDa : 1 kDa	Drying Method	Hydrogel State	Thickness (mm)	Average Induced Micropore Size (μm)
17:3	AD	dry	1	-
17:3	LYO	dry	1	24.94 ± 11.44
17:3	AD	dry	7	-
17:3	LYO	dry	7	38.65 ± 27.92
17:3	AD	hydrated	1	-
17:3	LYO	hydrated	1	8.43 ± 8.74
17:3	AD	hydrated	7	-
17:3	LYO	hydrated	7	29.17 ± 20.50
15:5	AD	dry	1	-
15:5	LYO	dry	1	27. 53 ± 57.88
15:5	AD	dry	7	-
15:5	LYO	dry	7	20.74 ± 15.56
15:5	AD	hydrated	1	-
15:5	LYO	hydrated	1	6.82 ± 7.88
15:5	AD	hydrated	7	-
15:5	LYO	hydrated	7	15.21 ± 12.22
10:10	AD	dry	1	-
10:10	LYO	dry	1	14.86 ± 7.41
10:10	AD	dry	7	-
10:10	LYO	dry	7	-
10:10	AD	hydrated	1	-
10:10	LYO	hydrated	1	7.26 ± 5.47
10:10	AD	hydrated	7	-
10:10	LYO	hydrated	7	39.70 ± 63.26
0:20	AD	dry	1	-
0:20	LYO	dry	1	-
0:20	AD	dry	7	-
0:20	LYO	dry	7	-
0:20	AD	hydrated	1	-
0:20	LYO	hydrated	1	9.08 ± 7.01
0:20	AD	hydrated	7	-
0:20	LYO	hydrated	7	7.89 ± 9.04

BIBLIOGRAPHY

1. Nerem, R. M. Regenerative medicine: the emergence of an industry. doi:10.1098/rsif.2010.0348.focus

2. Chen, C., Dubin, R., Meen, & & Kim, C. Emerging trends and new developments in regenerative medicine: a scientometric update. *Expert Opin. Biol. Ther.* **14**, 1295–1317 (2014).

3. Mano, J. F. *et al.* Natural origin biodegradable systems in tissue engineering and regenerative medicine: present status and some moving trends. *J. R. Soc. Interface* **4**, 999–1030 (2007).

4. Mason, C. & Dunnill, P. A brief definition of regenerative medicine. *Regenerative Medicine* **3**, 1–5 (2008).

5. Ingber, D. E. & Levin, M. What lies at the interface of regenerative medicine and development? in *Development* **134**, 2541–2547 (2007).

6. Heidary Rouchi, A. & Mahdavi-Mazdeh, M. Regenerative medicine in organ and tissue transplantation: Shortly and practically achievable? *International Journal of Organ Transplantation Medicine* **6**, 93–98 (2015).

7. Gurtner, G. C. & Chapman, M. A. Regenerative medicine: Charting a new course in wound healing. *Adv. Wound Care* **5**, 314–328 (2016).

8. Donnenberg, V. S., Zimmerlin, L., Rubin, J. P. & Donnenberg, A. D. Regenerative therapy after cancer: What are the risks? *Tissue Eng. - Part B Rev.* **16**, 567–575 (2010).

9. Badylak, S. F. & Nerem, R. M. Progress in tissue engineering and regenerative medicine. *Proceedings of the National Academy of Sciences of the United States of America* **107**, 3285–3286 (2010).

10. Slaughter, B. V., Khurshid, S. S., Fisher, O. Z., Khademhosseini, A. & Peppas, N. A. Hydrogels in regenerative medicine. *Advanced Materials* **21**, 3307–3329 (2009).

11. Tissue Engineering and Regenerative Medicine. Available at:

https://www.nibib.nih.gov/science-education/science-topics/tissue-engineering-and-regenerative-medicine. (Accessed: 11th December 2019)

12. O'Brien, F. J. Biomaterials & scaffolds for tissue engineering. *Materials Today* **14**, 88–95 (2011).

13. Biedermann, T., Bö Ttcher-Haberzeth, S. & Reichmann, E. Tissue engineering of skin. Burns Tissue engineering of skin. (2009). doi:10.1016/j.burns.2009.08.016

14. MacNeil, S. Biomaterials for tissue engineering of skin. *Materials Today* **11**, 26–35 (2008).

15. Petit-Zeman, S. Regenerative medicine: The regeneration of tissues and organs offers a radical new approach to the treatment of injury and disease. It's a new medicine for a new millennium, but does the reality match the hype? *Nature Biotechnology* **19**, 201–206 (2001).

16. Transplant trends - UNOS. Available at: https://unos.org/data/transplant-trends/. (Accessed: 11th December 2019)

17. Organ Donation Statistics | Organ Donor. Available at: https://www.organdonor.gov/statistics-stories/statistics.html#waiting-list. (Accessed: 10th January 2020)

18. Marx, V. *ORGANS FROM THE LAB*. (2015).
19. Engineering Implantable, Laboratory-Grown Organs To Cure Disease. Available at: https://www.forbes.com/sites/robinseatonjefferson/2018/06/13/engineering-implantable-laboratory-grown-organs-to-cure-disease/#2e3a25f77bcb. (Accessed: 7th March 2020)

20. Yoo, J. J., Meng, J., Oberpenning, F. & Atala, A. *BLADDER AUGMENTATION USING ALLOGENIC BLADDER SUBMUCOSA SEEDED WITH CELLS*.

21. Ott, H. C. *et al.* Regeneration and orthotopic transplantation of a bioartificial lung. (2010). doi:10.1038/nm.2193

22. Mann, B. K. & West, J. L. Tissue engineering in the cardiovascular system: Progress toward a tissue engineered heart. *Anat. Rec.* **263**, 367–371 (2001).

23. Dhandayuthapani, B. *et al.* Polymeric Scaffolds in Tissue Engineering Application: A Review. *Int. J. Polym. Sci.* **2011**, 1–19 (2011).

24. *Development of biodegradable calcium phosphate cement for bone tissue engineering*.

25. Burg, K. J. L., Porter, S. & Kellam, J. F. Biomaterial developments for bone tissue

engineering.

26. Yoshikawa, H. & Myoui, A. Bone tissue engineering with porous hydroxyapatite ceramics. *Journal of Artificial Organs* **8**, 131–136 (2005).

27. Yoshikawa, H., Tamai, N., Murase, T. & Myoui, A. Interconnected porous hydroxyapatite ceramics for bone tissue engineering. doi:10.1098/rsif.2008.0425.focus

28. Bretcanu, O. *et al.* Electrospun nanofibrous biodegradable polyester coatings on Bioglass®-based glass-ceramics for tissue engineering. *Mater. Chem. Phys.* **118**, 420–426 (2009).

29. Stevens, M. M. Biomaterials for bone tissue engineering. *Materials Today* **11**, 18–25 (2008).

30. Seitz, H., Rieder, W., Irsen, S., Leukers, B. & Tille, C. Three-dimensional printing of porous ceramic scaffolds for bone tissue engineering. *J. Biomed. Mater. Res. Part B Appl. Biomater.* **74B**, 782–788 (2005).

31. Khan, O. F. & Sefton, M. V. Endothelialized biomaterials for tissue engineering applications in vivo. *Trends in Biotechnology* **29**, 379–387 (2011).

32. Ma, P. X. Biomimetic materials for tissue engineering. *Advanced Drug Delivery Reviews* **60**, 184–198 (2008).

33. Agrawal, C. M. & Ray, R. B. Biodegradable polymeric scaffolds for musculoskeletal tissue engineering. *J. Biomed. Mater. Res.* **55**, 141–150 (2001).

34. Gunatillake, P. & Adhikari, R. Biodegradable Synthetic Polymers for Tissue Engineering. 1–16 (2003). doi:10.22203/eCM.v005a01

35. Liu, X. & Ma, P. X. *Polymeric Scaffolds for Bone Tissue Engineering*. *Annals of Biomedical Engineering* **32**, (2004).

36. Malafaya ∗, P. B., Silva, G. A. & Reis, R. L. Natural-origin polymers as carriers and scaffolds for biomolecules and cell delivery in tissue engineering applications ☆. (2007). doi:10.1016/j.addr.2007.03.012

37. Swetha, M. *et al.* Biocomposites containing natural polymers and hydroxyapatite for bone tissue engineering. *International Journal of Biological Macromolecules* **47**, 1–4 (2010).

38. Metcalfe, A. D. & Ferguson, M. W. J. Tissue engineering of replacement skin: The crossroads of biomaterials, wound healing, embryonic development, stem cells and regeneration. *Journal of the Royal Society Interface* **4**, 413–417 (2007).

39. Griffith, L. G. & Naughton, G. Tissue engineering - Current challenges and expanding opportunities. *Science* **295**, (2002).

40. POLAK, J. M. & BISHOP, A. E. Stem Cells and Tissue Engineering: Past, Present, and Future. *Ann. N. Y. Acad. Sci.* **1068**, 352–366 (2006).

41. Gimble, J. M., Katz, A. J. & Bunnell, B. A. Adipose-derived stem cells for regenerative medicine. *Circ. Res.* **100**, 1249–60 (2007).

42. Das, R. K. & Zouani, O. F. A review of the effects of the cell environment physicochemical nanoarchitecture on stem cell commitment. *Biomaterials* **35**, 5278–5293 (2014).

43. Whitehead, A. K., Barnett, H. H., Caldorera-Moore, M. E. & Newman, J. J. Poly (ethylene glycol) hydrogel elasticity influences human mesenchymal stem cell behavior. *Regen. Biomater.* (2018). doi:10.1093/rb/rby008

44. Heimbuck, A. M. *et al.* Development of Responsive Chitosan–Genipin Hydrogels for the Treatment of Wounds. *ACS Appl. Bio Mater.* **2**, 2879–2888 (2019).

45. Ma, Z., Kotaki, M., Inai, R. & Ramakrishna, S. Potential of Nanofiber Matrix as Tissue-Engineering Scaffolds. *Tissue Eng.* **11**, 101–109 (2005).

46. Van Vlierberghe, S., Dubruel, P. & Schacht, E. Biopolymer-Based Hydrogels As Scaffolds for Tissue Engineering Applications: A Review. *Biomacromolecules* **12**, 1387–1408 (2011).

47. Engineering the cell–material interface for controlling stem cell adhesion, migration, and differentiation. *Biomaterials* **32**, 3700–3711 (2011).

48. Patel, N. R., Whitehead, A. K., Newman, J. J. & Caldorera-Moore, M. E. Poly(ethylene glycol) Hydrogels with Tailorable Surface and Mechanical Properties for Tissue Engineering Applications. *ACS Biomater. Sci. Eng.* **3**, 1494–1498 (2017).

49. Zuk, P. A. *et al.* Human adipose tissue is a source of multipotent stem cells. *Mol. Biol. Cell* **13**, 4279–95 (2002).

50. Gimble, J. M., Grayson, W., Guilak, F., Lopez, M. J. & Vunjak-Novakovic, G. Adipose tissue as a stem cell source for musculoskeletal regeneration. *Front. Biosci. (Schol. Ed).* **3**, 69–81 (2011).

51. Mizuno, H. *et al.* Myogenic differentiation by human processed lipoaspirate cells. *Plast. Reconstr. Surg.* **109**, 199–209; discussion 210-1 (2002).

52. Forcales, S.-V. Potential of adipose-derived stem cells in muscular regenerative therapies. *Front. Aging Neurosci.* **7**, 123 (2015).

53. Rosso, F., Giordano, A., Barbarisi, M. & Barbarisi, A. From Cell-ECM interactions to tissue engineering. *J. Cell. Physiol.* **199**, 174–180 (2004).

54. Stevens, M. M. & George, J. H. Exploring and Engineering the Cell Surface Interface. *Science (80-.).* **310**, (2005).

55. Lutolf, M. P. & Hubbell, J. A. Synthetic biomaterials as instructive extracellular microenvironments for morphogenesis in tissue engineering. *Nat. Biotechnol.* **23**, 47–55 (2005).

56. The composition of extracellular matrix-Biobool News | biobool.com. *biobool* (2017). Available at: https://www.biobool.com/news/61.html. (Accessed: 21st January 2018)

57. Kim, U.-J., Park, J., Joo Kim, H., Wada, M. & Kaplan, D. L. Three-dimensional aqueous-derived biomaterial scaffolds from silk fibroin. *Biomaterials* **26**, 2775–2785 (2005).

58. Kim, B.-S. & Mooney, D. J. Development of biocompatible synthetic extracellular matrices for tissue engineering. *Trends Biotechnol.* **16**, 224–230 (1998).

59. Khademhosseini, A., Langer, R., Borenstein, J. & Vacanti, J. P. Microscale technologies for tissue engineering and biology. *Proc. Natl. Acad. Sci. U. S. A.* **103**, 2480–7 (2006).

60. Shin, H., Jo, S. & Mikos, A. G. Biomimetic materials for tissue engineering. *Biomaterials* **24**, 4353–4364 (2003).

61. Anderson, D. G., Putnam, D., Lavik, E. B., Mahmood, T. A. & Langer, R. Biomaterial microarrays: rapid, microscale screening of polymer–cell interaction. *Biomaterials* **26**, 4892–4897 (2005).

62. Boyan, B. D., Hummert, T. W., Dean, D. D. & Schwartz, Z. Role of material surfaces in regulating bone and cartilage cell response. *Biomaterials* **17**, 137–146 (1996).

63. Choi, C.-H. *et al.* Cell interaction with three-dimensional sharp-tip nanotopography. *Biomaterials* **28**, 1672–1679 (2007).

64. Zelzer, M. *et al.* Investigation of cell–surface interactions using chemical gradients formed from plasma polymers. *Biomaterials* **29**, 172–184 (2008).

65. Recum, A. F. Von *et al.* Surface Roughness, Porosity, and Texture as Modifiers of

Cellular Adhesion. *Tissue Eng.* **2**, 241–253 (1996).

66. Lange, R. *et al.* Cell-extracellular matrix interaction and physico-chemical characteristics of titanium surfaces depend on the roughness of the material. *Biomol. Eng.* **19**, 255–261 (2002).

67. Tsai, R. Y. L. & McKay, R. D. G. Cell contact regulates fate choice by cortical stem cells. *J. Neurosci.* **20**, 3725–3735 (2000).

68. Javazon, E. H., Colter, D. C., Schwarz, E. J. & Prockop, D. J. Rat Marrow Stromal Cells are More Sensitive to Plating Density and Expand More Rapidly from Single-Cell-Derived Colonies than Human Marrow Stromal Cells. *Stem Cells* **19**, 219–225 (2001).

69. Kiger, A. A., White-Cooper, H. & Fuller, M. T. Somatic support cells restrict germline stem cell self-renewal and promote differentiation. *Nature* **407**, 750–754 (2000).

70. Purpura, K. A. Sustained In Vitro Expansion of Bone Progenitors Is Cell Density Dependent. *Stem Cells* **22**, 39–50 (2004).

71. Zandstra, P. W., Le, H.-V., Daley, G. Q., Griffith, L. G. & Lauffenburger, D. A. Leukemia inhibitory factor (LIF) concentration modulates embryonic stem cell self-renewal and differentiation independently of proliferation. *Biotechnol. Bioeng.* **69**, 607–617 (2000).

72. Yamashita, Y. M. & Fuller, M. T. Asymmetric centrosome behavior and the mechanisms of stem cell division. *Journal of Cell Biology* **180**, 261–266 (2008).

73. Yamashita, Y. M. & Fuller, M. T. Asymmetric stem cell division and function of the niche in the Drosophila male germ line. *International Journal of Hematology* **82**, 377–380 (2005).

74. Rehfeldt, F., Engler, A. J., Eckhardt, A., Ahmed, F. & Discher, D. E. Cell responses to the mechanochemical microenvironment-Implications for regenerative medicine and drug delivery. *Advanced Drug Delivery Reviews* **59**, 1329–1339 (2007).

75. Engler, A. J., Sen, S., Sweeney, H. L. & Discher, D. E. Matrix Elasticity Directs Stem Cell Lineage Specification. *Cell* **126**, 677–689 (2006).

76. Butcher, D. T., Alliston, T. & Weaver, V. M. A tense situation: Forcing tumour progression. *Nature Reviews Cancer* **9**, 108–122 (2009).

77. Pavlovic, M. & Balint, B. Short History of Stem Cells Transplantation with Emphasis on Hematological Disorders. in 1–5 (Springer New York, 2013).

doi:10.1007/978-1-4614-5505-9_1

78. Chen, Q.-Z., Harding, S. E., Ali, N. N., Lyon, A. R. & Boccaccini, A. R. Biomaterials in cardiac tissue engineering: Ten years of research survey. *Mater. Sci. Eng. R Reports* **59**, 1–37 (2008).

79. Burgess, R. *Stem cells : a short course*.

80. Hayes, M., Curley, G., Ansari, B. & Laffey, J. G. Clinical review: Stem cell therapies for acute lung injury/acute respiratory distress syndrome - hope or hype? *Critical Care* **16**, (2012).

81. Mitalipov, S. & Wolf, D. Totipotency, pluripotency and nuclear reprogramming. *Adv. Biochem. Eng. Biotechnol.* **114**, 185–199 (2009).

82. Seydoux, G. & Braun, R. E. Pathway to Totipotency: Lessons from Germ Cells. *Cell* **127**, 891–904 (2006).

83. Wu, J., Yamauchi, T., Carlos, J. & Belmonte, I. An overview of mammalian pluripotency. (2016). doi:10.1242/dev.132928

84. De, A. *et al.* Hallmarks of pluripotency. doi:10.1038/nature15515

85. Niwa, H. How is pluripotency determined and maintained? doi:10.1242/dev.02787

86. Pera, M., Reubinoff, B. & Trounson, A. Human embryonic stem cells. 5–10 (2000).

87. Evans, M. J. & Kaufman, M. H. Establishment in culture of pluripotential cells from mouse embryos. *Nature* **292**, 154–156 (1981).

88. Martin, G. R. *Isolation of a pluripotent cell line from early mouse embryos cultured in medium conditioned by teratocarcinoma stem cells (embryonic stem cells/inner cell masses/differentiation in vsitro/embryonal carcinoma cells/growth factors)*. *Developmental Biology* **78**, (1981).

89. Yu, J. *et al.* Induced Pluripotent Stem Cell Lines Derived from Human Somatic Cells. *Science (80-.).* **318**, (2007).

90. Badylak, S. F., Taylor, D. & Uygun, K. Whole-Organ Tissue Engineering: Decellularization and Recellularization of Three-Dimensional Matrix Scaffolds. *Annu. Rev. Biomed. Eng.* **13**, 27–53 (2011).

91. De Wert, G. & Mummery, C. OPINION Human embryonic stem cells: research, ethics and policy. doi:10.1093/humrep/DEG143

92. Hentze, H. *et al.* Teratoma formation by human embryonic stem cells: Evaluation of essential parameters for future safety studies. *Stem Cell Res.* **2**, 198–210 (2009).

93. Grinnemo, K.-H. *et al. Human embryonic stem cells are immunogenic in allogeneic and xenogeneic settings*. *Reproductive BioMedicine Online* **13**,

94. Takahashi, K. & Yamanaka, S. Induction of Pluripotent Stem Cells from Mouse Embryonic and Adult Fibroblast Cultures by Defined Factors. *Cell* **126**, 663–676 (2006).

95. Takahashi, K. *et al.* Induction of Pluripotent Stem Cells from Adult Human Fibroblasts by Defined Factors. *Cell* **131**, 861–872 (2007).

96. Yu, J. & Thomson, J. A. Pluripotent stem cell lines. (2008). doi:10.1101/gad.1689808

97. Li, Y. *et al.* Engineering-derived approaches for iPSC preparation, expansion, differentiation and applications. *Biofabrication* **9**, (2017).

98. Schwartzentruber, J. *et al.* Molecular and functional variation in iPSC-derived sensory neurons. *Nat. Genet.* **50**, 54–61 (2018).

99. Malik, N. & Rao, M. S. A review of the methods for human iPSC derivation. in *Methods in Molecular Biology* **997**, 23–33 (2013).

100. Kim, K. *et al.* Epigenetic memory in induced pluripotent stem cells. *Nature* **467**, 285–290 (2010).

101. Bunnell, B. A., Flaat, M., Gagliardi, C., Patel, B. & Ripoll, C. Adipose-derived stem cells: Isolation, expansion and differentiation. *Methods* **45**, 115–120 (2008).

102. Pittenger, M. F. *et al.* Multilineage Potential of Adult Human Mesenchymal Stem Cells. *Science (80-.).* **284**, (1999).

103. Gage, F. H. Mammalian neural stem cells. *Science* **287**, 1433–1438 (2000).

104. Blanpain, C., Lowry, W. E., Geoghegan, A., Polak, L. & Fuchs, E. Self-renewal, multipotency, and the existence of two cell populations within an epithelial stem cell niche. *Cell* **118**, 635–648 (2004).

105. Wang, A. & Farmer, D. Placenta-derived multipotent stem cells. (2018).

106. Miki, T. & Strom, S. Amnion-derived pluripotent/multipotent stem cells. *Stem Cell Rev.* **2**, 133–141 (2006).

107. Minguell, J., Erices, A. & Conget, P. Mini-Review: Mesenchymal Cells. *Stem Cell*

Technol. 1–5 (2015). doi:10.1177/153537020122600603

108. Strem, B. M. *et al.* Multipotential differentiation of adipose tissue-derived stem cells. *Keio Journal of Medicine* **54**, 132–141 (2005).

109. Chen, F. H., Rousche, K. T. & Tuan, R. S. Technology Insight: adult stem cells in cartilage regeneration and tissue engineering. *Nat. Clin. Pract. Rheumatol.* **2**, 373–382 (2006).

110. Tuan, R. S. *et al.* Adult mesenchymal stem cells and cell-based tissue engineering. *Arthritis Res. Ther.* **5**, 32 (2003).

111. Jorgensen, C., Gordeladze, J. & Noel, D. Tissue engineering through autologous mesenchymal stem cells. *Curr. Opin. Biotechnol.* **15**, 406–410 (2004).

112. Li, W.-J. *et al.* A three-dimensional nanofibrous scaffold for cartilage tissue engineering using human mesenchymal stem cells. *Biomaterials* **26**, 599–609 (2005).

113. Kern, S., Eichler, H., Stoeve, J., Klüter, H. & Bieback, K. Comparative Analysis of Mesenchymal Stem Cells from Bone Marrow, Umbilical Cord Blood, or Adipose Tissue. *Stem Cells* **24**, 1294–1301 (2006).

114. Caplan, A. I. Adult mesenchymal stem cells for tissue engineering versus regenerative medicine. *J. Cell. Physiol.* **213**, 341–347 (2007).

115. Gimble, J. M. & Guilak, F. Adipose-derived adult stem cells: Isolation, characterization, and differentiation potential. *Cytotherapy* **5**, 362–369 (2003).

116. Prockop, D. J. Marrow stromal cells as stem cells for nonhematopoietic tissues. *Science* **276**, 71–74 (1997).

117. Kolios, G. & Moodley, Y. Introduction to Stem Cells and Regenerative Medicine. *Respiration* **85**, 3–10 (2013).

118. Oligopotent stem cells are distributed throughout ...: Full Text Finder Results. Available at: http://resolver.ebscohost.com/openurl?sid=google&auinit=F&aulast=Majo&atitle=Oligopotent+stem+cells+are+distributed+throughout+the+mammalian+ocular+surface&id=doi%3A10.1038%2Fnature07406&title=Nature&volume=456&issue=7219&date=2008&spage=250&site=ftf-live. (Accessed: 16th December 2019)

119. Landers, R., Hübner, U., Schmelzeisen, R. & Mülhaupt, R. Rapid prototyping of scaffolds derived from thermoreversible hydrogels and tailored for applications in tissue engineering. *Biomaterials* **23**, 4437–4447 (2002).

120. Hoffman, A. S. Hydrogels for biomedical applications. *Adv. Drug Deliv. Rev.* **64**, 18–23 (2012).

121. Bjugstad, K. B. *et al.* Biocompatibility of PEG-Based Hydrogels in Primate Brain. *Cell Transplant.* **17**, 409–415 (2008).

122. Kharkar, P. M., Kiick, K. L. & Kloxin, A. M. Designing degradable hydrogels for orthogonal control of cell microenvironments. *Chem. Soc. Rev.* **42**, 7335–7372 (2013).

123. Sant, S., Hancock, M. J., Donnelly, J. P., Iyer, D. & Khademhosseini, A. Biomimetic gradient hydrogels for tissue engineering. *Can. J. Chem. Eng.* **88**, 899–911 (2010).

124. Ratner, B. D. (Buddy D. . *Biomaterials science : an introduction to materials in medicine*. (Academic Press, 2013).

125. Lee, K. Y. & Mooney, D. J. Hydrogels for tissue engineering. *Chem. Rev.* **101**, 1869–79 (2001).

126. Singhal, R. & Gupta, K. A Review: Tailor-made Hydrogel Structures (Classifications and Synthesis Parameters). *Polym. - Plast. Technol. Eng.* **55**, 54–70 (2016).

127. Mohite, P. & Adhav, S. A hydrogels: Methods of Preparation and Applications. *Int. J. Adv. Pharmeceutics* **6**, 79–85 (2017).

128. Qiu, Y. & Park, K. Environment-sensitive hydrogels for drug delivery. *Advanced Drug Delivery Reviews* **53**, 321–339 (2001).

129. Bahram, M., Mohseni, N. & Moghtader, M. An Introduction to Hydrogels and Some Recent Applications. in *Emerging Concepts in Analysis and Applications of Hydrogels* (InTech, 2016). doi:10.5772/64301

130. Peppas, N. A., Keys, K. B., Torres-Lugo, M. & Lowman, A. M. Poly(ethylene glycol)-containing hydrogels in drug delivery. *J. Control. Release* **62**, 81–87 (1999).

131. Ahmed, E. M. Hydrogel: Preparation, characterization, and applications: A review. *Journal of Advanced Research* **6**, 105–121 (2015).

132. Drury, J. L. & Mooney, D. J. Hydrogels for tissue engineering: scaffold design variables and applications. *Biomaterials* **24**, 4337–4351 (2003).

133. Fejerskov, B., Jensen, B. E. B., Jensen, N. B. S., Chong, S.-F. & Zelikin, A. N. Engineering Surface Adhered Poly(vinyl alcohol) Physical Hydrogels as

Enzymatic Microreactors. *ACS Appl. Mater. Interfaces* **4**, 4981–4990 (2012).

134. Kamoun, E. A., Kenawy, E. R. S. & Chen, X. A review on polymeric hydrogel membranes for wound dressing applications: PVA-based hydrogel dressings. *Journal of Advanced Research* **8**, 217–233 (2017).

135. Dhanaji Patil, S. *et al.* PEG-A versatile conjugating ligand for drugs and drug delivery systems. *Artic. J. Control. Release* (2014). doi:10.1016/j.jconrel.2014.06.046

136. Nuttelman, C. R., Henry, S. M. & Anseth, K. S. Synthesis and characterization of photocrosslinkable, degradable poly(vinyl alcohol)-based tissue engineering scaffolds. *Biomaterials* **23**, 3617–3626 (2002).

137. Suggs, L. J. *et al.* In vitro andin vivo degradation of poly(propylene fumarate-co-ethylene glycol) hydrogels. *J. Biomed. Mater. Res.* **42**, 312–320 (1998).

138. Tran, R. T., Gyawali, D. & Yang, J. Biodegradable Injectable Systems for Bone Tissue Engineering. in (2013). doi:10.1039/9781849733458-00419

139. and, K. Y. L. & Mooney*, D. J. Hydrogels for Tissue Engineering. (2001). doi:10.1021/CR000108X

140. da Silva, R. M. P., Mano, J. F. & Reis, R. L. Smart thermoresponsive coatings and surfaces for tissue engineering: switching cell-material boundaries. *Trends Biotechnol.* **25**, 577–583 (2007).

141. Kim, D. J. *et al.* Formation of Thermoresponsive Gold Nanoparticle/PNIPAAm Hybrids by Surface-Initiated, Atom Transfer Radical Polymerization in Aqueous Media. *Macromol. Chem. Phys.* **206**, 1941–1946 (2005).

142. Sundelacruz, S. & Kaplan, D. L. Stem cell- and scaffold-based tissue engineering approaches to osteochondral regenerative medicine. *Seminars in Cell and Developmental Biology* **20**, 646–655 (2009).

143. Tan, H. & Marra, K. Injectable, Biodegradable Hydrogels for Tissue Engineering Applications. *Materials (Basel).* 1746–1767 (2010). doi:doi:10.3390/ma3031746

144. Yu, L. & Ding, J. Injectable hydrogels as unique biomedical materials. (2008). doi:10.1039/b713009k

145. Zhu, J. & Marchant, R. E. Design properties of hydrogel tissue-engineering scaffolds. *Expert Rev. Med. Devices* **8**, 607–26 (2011).

146. Barnett, H. H. *et al.* Poly (Ethylene Glycol) Hydrogel Scaffolds with Multiscale Porosity for Culture of Human Adipose- Derived Stem Cells. *J. Biomater. Sci.*

Polym. Ed. 1–19 (2019). doi:10.1080/09205063.2019.1612725

147. Zhang, W., Ma, C. & Ciszkowska, M. Mass Transport in Thermoresponsive Poly(N-isopropylacrylamide-co-acrylic acid) Hydrogels Studied by Electroanalytical Techniques: Swollen Gels. *J. Phys. Chem. B* **105**, 3435–3440 (2001).

148. Cuchiara, M. P., Allen, A. C. B., Chen, T. M., Miller, J. S. & West, J. L. Multilayer microuidic PEGDA hydrogels. (2010). doi:10.1016/j.biomaterials.2010.03.031

149. Amsden, B. Solute Diffusion within Hydrogels. Mechanisms and Models. (1998). doi:10.1021/MA980765F

150. Khademhosseini, A. & Langer, R. Microengineered hydrogels for tissue engineering. *Biomaterials* **28**, 5087–5092 (2007).

151. Bártolo, P. J., Chua, C. K., Almeida, H. A., Chou, S. M. & Lim, A. S. C. Biomanufacturing for tissue engineering: Present and future trends. *Virtual Phys. Prototyp.* **4**, 203–216 (2009).

152. Discher, D. E. Tissue Cells Feel and Respon to the Stiffness of Their Substrate. *Science (80-.).* **310**, 1139–1143 (2005).

153. Banerjee, A. *et al.* The influence of hydrogel modulus on the proliferation and differentiation of encapsulated neural stem cells. *Biomaterials* **30**, 4695–4699 (2009).

154. Holst, J. *et al.* letters Substrate elasticity provides mechanical signals for the expansion of hemopoietic stem and progenitor cells. *Nat. Biotechnol.* **28**, 1123–1128 (2011).

155. Gilbert, P. M. *et al.* Substrate Elasticity Regulates Skeletal Muscle Stem Cell Self-Renewal in Culture. *Science (80-.).* **1902**, 1078–1081 (2010).

156. Engler, A. J., Rehfeldt, F., Sen, S. & Discher, D. E. Microtissue elasticity: measurements by atomic force microscopy and its influence on cell differentiation. *Methods Cell Biol.* **83**, 521–545 (2007).

157. Saha, K. *et al.* Substrate modulus directs neural stem cell behavior. *Biophys. J.* **95**, 4426–4438 (2008).

158. Yang, C. *et al.* Spatially patterned matrix elasticity directs stem cell fate. *Proc. Natl. Acad. Sci.* **113**, E4439–E4445 (2016).

159. Wen, J. H. *et al.* Interplay of matrix stiffness and protein tethering in stem cell differentiation. *Nat. Mater.* **13**, 979–987 (2014).

160. Annabi, N. *et al.* 25th anniversary article: Rational design and applications of hydrogels in regenerative medicine. *Advanced Materials* **26**, 85–124 (2014).

161. Karmaker, A. C., Dibenedetto, A. & and Goldberg, A. J. Extent of conversion and its effect on the mechanical performance of Bis-GMA/PEGDMA-based resins and their composites with continuous glass fibres. *J. Mater. Sci. Mater. Med.* **8**, 333–401 (1997).

162. Elisseeff, J. *et al.* Transdermal photopolymerization for minimally invasive implantation. *Proc. Natl. Acad. Sci. U. S. A.* **96**, 3104–3107 (1999).

163. Bryant, S. J. & Anseth, K. S. Controlling the spatial distribution of ECM components in degradable PEG hydrogels for tissue engineering cartilage. *J. Biomed. Mater. Res. A* **64**, 70–79 (2003).

164. Zhu, J. Bioactive modification of poly(ethylene glycol) hydrogels for tissue engineering. *Biomaterials* **31**, 4639–56 (2010).

165. Asakura, a, Komaki, M. & Rudnicki, M. Muscle satellite cells are multipotential stem cells that exhibit myogenic, osteogenic, and adipogenic differentiation. *Differentiation.* **68**, 245–253 (2001).

166. Lee, O. K. *et al.* Isolation of multipotent mesenchymal stem cells from umbilical cord blood. *Blood* **103**, 1669–1675 (2004).

167. Bieback, K., Kern, S., Klüter, H. & Eichler, H. Critical parameters for the isolation of mesenchymal stem cells from umbilical cord blood. *Stem Cells* **22**, 625–634 (2004).

168. Mackay, A. M. *et al.* Chondrogenic differentiation of cultured human mesenchymal stem cells from marrow. *Tissue Eng.* **4**, 415–428 (1998).

169. NIH. 645 Studies found for: Mesenchymal stem cells.

170. Yousefi, A. M. *et al.* Prospect of stem cells in bone tissue engineering: A review. *Stem Cells Int.* (2016). doi:10.1155/2016/6180487

171. Patrick, C. W. Tissue engineering strategies for adipose tissue repair. *Anat. Rec.* **263**, 361–366 (2001).

172. Fan, H., Liu, H., Toh, S. L. & Goh, J. C. H. Enhanced differentiation of mesenchymal stem cells co-cultured with ligament fibroblasts on gelatin/silk fibroin hybrid scaffold. *Biomaterials* **29**, 1017–1027 (2008).

173. Dezawa, M. *et al.* Bone marrow stromal cells generate muscle cells and repair

muscle degeneration. *Science* **309**, 314–7 (2005).

174. Ponticiello, M. S., Schinagl, R. M., Kadiyala, S. & Barry, F. P. Gelatin-based resorbable sponge as a carrier matrix for human mesenchymal stem cells in cartilage regeneration therapy. *J. Biomed. Mater. Res.* **52**, 246–255 (2000).

175. Caldorera-Moore, M. *et al.* Swelling behavior of nanoscale, shape- and size-specific, hydrogel particles fabricated using imprint lithography. *Soft Matter* **7**, 2879 (2011).

176. Bryant, S. J., Nuttelman, C. R. & Anseth, K. S. Cytocompatibility of UV and visible light photoinitiating systems on cultured NIH/3T3 fibroblasts in vitro. *J. Biomater. Sci. Polym. Ed.* **11**, 439–457 (2000).

177. Bryant, S. J., Bender, R. J., Durand, K. L. & Anseth, K. S. Encapsulating chondrocytes in degrading PEG hydrogels with high modulus: Engineering gel structural changes to facilitate cartilaginous tissue production. *Biotechnol. Bioeng.* **86**, 747–755 (2004).

178. Kim, T. G., Shin, H. & Lim, D. W. Biomimetic Scaffolds for Tissue Engineering. *Adv. Funct. Mater.* **22**, 2446–2468 (2012).

179. Ha, T. L. B. Biomimetic scaffolds for stem cell-based tissue engineering. in *Biomimetic Biomaterials* (ed. Ruys, A. J.) 181–206 (Woodhead Publishing, 2013). doi:10.1533/9780857098887.2.181

180. Nguyen, K. T. & West, J. L. Photopolymerizable hydrogels for tissue engineering applications. *undefined* (2002).

181. Raic, A., Rödling, L., Kalbacher, H. & Lee-Thedieck, C. Biomimetic macroporous PEG hydrogels as 3D scaffolds for the multiplication of human hematopoietic stem and progenitor cells. *Biomaterials* **35**, 929–940 (2014).

182. Wu, X., Black, L., Santacana-Laffitte, G. & Patrick, C. W. Preparation and assessment of glutaraldehyde-crosslinked collagen–chitosan hydrogels for adipose tissue engineering. *J. Biomed. Mater. Res. Part A* **81A**, 59–65 (2007).

183. Peppas, N. A., Bures, P., Leobandung, W. & Ichikawa, H. Hydrogels in pharmaceutical formulations. *Eur. J. Pharaceutics Biopharm.* 27–46 (2000).

184. Liu Tsang, V. & Bhatia, S. N. Three-dimensional tissue fabrication. *Adv. Drug Deliv. Rev.* **56**, 1635–1647 (2004).

185. Bryant, S. J., Bender, R. J., Durand, K. L. & Anseth, K. S. Encapsulating chondrocytes in degrading PEG hydrogels with high modulus: Engineering gel structural changes to facilitate cartilaginous tissue production. *Biotechnol. Bioeng.*

86, 747–755 (2004).

186. Lindroos, B., Suuronen, R. & Miettinen, S. The Potential of Adipose Stem Cells in Regenerative Medicine. *Stem Cell Rev. Reports* **7**, 269–291 (2011).

187. Sun, N. *et al.* Feeder-free derivation of induced pluripotent stem cells from adult human adipose stem cells. *Proc. Natl. Acad. Sci. U. S. A.* **106**, 15720–5 (2009).

188. Lih, E., Lee, J. S., Park, K. M. & Park, K. D. Rapidly curable chitosan–PEG hydrogels as tissue adhesives for hemostasis and wound healing. *Acta Biomater.* **8**, 3261–3269 (2012).

189. Mao, J. *et al.* Study of novel chitosan-gelatin artificial skin in vitro. *J. Biomed. Mater. Res.* **64A**, 301–308 (2003).

190. Ma, R., Xiong, D., Miao, F., Zhang, J. & Peng, Y. Novel PVP/PVA hydrogels for articular cartilage replacement. *Mater. Sci. Eng. C* **29**, 1979–1983 (2009).

191. Bártolo, P. J., Chua, C. K., Almeida, H. A., Chou, S. M. & Lim, A. S. C. Biomanufacturing for tissue engineering: Present and future trends. *Virtual Phys. Prototyp.* **4**, 203–216 (2009).

192. Lin, C.-C. & Metters, A. T. Hydrogels in controlled release formulations: Network design and mathematical modeling. *Adv. Drug Deliv. Rev.* 1379–1408 (2006).

193. Harris, J. M. & Chess, R. B. Effect of pegylation on pharmaceuticals. *Nat. Rev. Drug Discov.* **2**, 214–221 (2003).

194. Lin, C.-C. & Anseth, K. S. PEG Hydrogels for the Controlled Release of Biomolecules in Regenerative Medicine. *Pharm. Res.* **26**, 631–643 (2009).

195. Zhang, L. *et al.* Nanoparticles in medicine: Therapeutic applications and developments. *Clinical Pharmacology and Therapeutics* **83**, 761–769 (2008).

196. Boodagh, P., Guo, D.-J., Nagiah, N. & Tan, W. Evaluation of electrospun PLLA/PEGDMA polymer coatings for vascular stent material. *J. Biomater. Sci. Polym. Ed.* **27**, 1086–1099 (2016).

197. Zeng, Z. *et al.* An in situ forming tissue adhesive based on poly(ethylene glycol)-dimethacrylate and thiolated chitosan through the Michael reaction. *J. Mater. Chem. B* **4**, 5585–5592 (2016).

198. Antony, G. J. M., Jarali, C. S., Aruna, S. T. & Raja, S. Tailored poly(ethylene) glycol dimethacrylate based shape memory polymer for orthopedic applications. *J. Mech. Behav. Biomed. Mater.* **65**, 857–865 (2017).

199. Feng, Y. *et al.* Synthesis and characterization of biodegradable, amorphous, soft IPNs with shape-memory effect. *Polym. Adv. Technol.* **23**, 382–388 (2012).
200. Cui, X., Breitenkamp, K., Finn, M. G., Lotz, M. & D'Lima, D. D. Direct human cartilage repair using three-dimensional bioprinting technology. *Tissue Eng. Part A* **18**, 1304–12 (2012).

201. Gao, G. *et al.* Bioactive nanoparticles stimulate bone tissue formation in bioprinted three-dimensional scaffold and human mesenchymal stem cells. *Biotechnol. J.* **9**, 1304–1311 (2014).

202. Bäckström, S. *et al.* Tailoring Properties of Biocompatible PEG-DMA Hydrogels with UV Light. *Mater. Sci. Appl.* **03**, 425–431 (2012).

203. Hule, R. A. *et al.* Correlations between structure, material properties and bioproperties in self-assembled beta-hairpin peptide hydrogels. *Faraday Discuss.* **139**, 251–64; discussion 309-25, 419–20 (2008).

204. Peppas, N. A., Hilt, J. Z., Khademhosseini, A. & Langer, R. Hydrogels in Biology and Medicine: From Molecular Principles to Bionanotechnology. *Adv. Mater.* **18**, 1345–1360 (2006).

205. Weber, L. M., Lopez, C. G. & Anseth, K. S. Effects of PEG hydrogel crosslinking density on protein diffusion and encapsulated islet survival and function. *J. Biomed. Mater. Res. A* **90**, 720–9 (2009).

206. Kim, T. H., Oh, S. H., Kwon, E. B., Lee, J. Y. & Lee, J. H. In vitro evaluation of osteogenesis and myogenesis from adipose-derived stem cells in a pore size gradient scaffold. *Macromol. Res.* **21**, 878–885 (2013).

207. Huh, D., Hamilton, G. A. & Ingber, D. E. From 3D cell culture to organs-on-chips. *Trends Cell Biol.* **21**, 745–54 (2011).

208. Fedorovich, N. E. *et al.* The effect of photopolymerization on stem cells embedded in hydrogels. *Biomaterials* **30**, 344–353 (2009).

209. Tibbitt, M. W. & Anseth, K. S. Hydrogels as extracellular matrix mimics for 3D cell culture. *Biotechnol. Bioeng.* **103**, 655–663 (2009).

210. Underhill, G. H., Chen, A. A., Albrecht, D. R. & Bhatia, S. N. Assessment of hepatocellular function within PEG hydrogels. *Biomaterials* **28**, 256–270 (2007).

211. Benton, J. A., DeForest, C. A., Vivekanandan, V. & Anseth, K. S. Photocrosslinking of gelatin macromers to synthesize porous hydrogels that promote valvular interstitial cell function. *Tissue Eng. Part A* **15**, 3221–30 (2009).

212. El-Sherbiny, I. M. & Yacoub, M. H. Hydrogel scaffolds for tissue engineering: Progress and challenges. *Glob. Cardiol. Sci. Pract.* **2013**, 316–42 (2013).

213. Ho, M.-H. *et al.* Preparation of porous scaffolds by using freeze-extraction and freeze-gelation methods. *Biomaterials* **25**, 129–138 (2004).

214. Pan, Z. & Ding, J. Poly(lactide-co-glycolide) porous scaffolds for tissue engineering and regenerative medicine. *Interface Focus* **2**, 366–77 (2012).

215. Murugeshu, A., Astete, C., Leonardi, C., Morgan, T. & Sabliov, C. M. Chitosan/PLGA particles for controlled release of α-tocopherol in the GI tract via oral administration. *Nanomedicine* **6**, 1513–1528 (2011).

216. Wang, W. Lyophilization and development of solid protein pharmaceuticals. *Int. J. Pharm.* **203**, 1–60 (2000).

217. Toniazzo, T., Peres, M. S., Ramos, A. P. & Pinho, S. C. Encapsulation of quercetin in liposomes by ethanol injection and physicochemical characterization of dispersions and lyophilized vesicles. *Food Biosci.* **19**, 17–25 (2017).

218. Nikolaeva, L. L. *et al.* Lyophilization as a Method for Stabilizing Pharmaceuticals. *Pharm. Chem. J.* **51**, 307–311 (2017).

219. Lee, G., Lee, C., Yoon, C.-M., Kim, M. & Jang, J. High-Performance Three-Dimensional Mesoporous Graphene Electrode for Supercapacitors using Lyophilization and Plasma Reduction. *ACS Appl. Mater. Interfaces* **9**, 5222–5230 (2017).

220. Shapiro, L. & Cohen, S. Novel alginate sponges for cell culture and transplantation. *Biomaterials* **18**, 583–590 (1997).

221. Zmora, S., Glicklis, R. & Cohen, S. Tailoring the pore architecture in 3-D alginate scaffolds by controlling the freezing regime during fabrication. *Biomaterials* **23**, 4087–4094 (2002).

222. Yunoki, S. *et al.* Control of pore structure and mechanical property in hydroxyapatite/collagen composite using unidirectional ice growth. *Mater. Lett.* **60**, 999–1002 (2006).

223. Mandal, B. B. & Kundu, S. C. Cell proliferation and migration in silk fibroin 3D scaffolds. *Biomaterials* **30**, 2956–2965 (2009).

224. Sultana, N. & Wang, M. Fabrication of HA/PHBV composite scaffolds through the emulsion freezing/freeze-drying process and characterisation of the scaffolds. *J. Mater. Sci. Mater. Med.* 2555–2561 (2007).

225. Sandra Van Vlierberghe, † *et al.* Porous Gelatin Hydrogels: 1. Cryogenic Formation and Structure Analysis. (2007). doi:10.1021/BM060684O

226. Nettles, D. L., Elder, S. H. & Gilbert, J. A. Potential Use of Chitosan as a Cell Scaffold Material for Cartilage Tissue Engineering. *Tissue Eng.* **8**, 1009–1016 (2002).

227. Mucha, M., Michalak, I., Balcerzak, J. & Tylman, M. Chitosan Scaffolds, films and microgranules for medical application preparation and drug release studies. *Polimery* **57**, 714–721 (2012).

228. Madihally, S. V. & Matthew, H. W. T. Porous chitosan scaffolds for tissue engineering. *Biomaterials* **20**, 1133–1142 (1999).

229. Heimbuck, A. M., Priddy-Arrington, T. R., Sawyer, B. J. & Caldorera-Moore, M. E. Effects of post-processing methods on chitosan-genipin hydrogel properties. *Mater. Sci. Eng. C* **98**, 612–618 (2019).

230. Arcaute, K., Mann, B. K. & Wicker, R. B. Fabrication of Off-the-Shelf Multilumen Poly(Ethylene Glycol) Nerve Guidance Conduits Using Stereolithography. *Tissue Eng. Part C. Methods* **17**, 27–38 (2011).

231. Temenoff, J. S., Steinbis, E. S. & Mikos, A. G. Effect of drying history on swelling properties and cell attachment to oligo(poly(ethylene glycol) fumarate) hydrogels for guided tissue regeneration applications. *J. Biomater. Sci. Polym. Ed.* **14**, 989–1004 (2003).

232. Luong, P. T., Browning, M. B., Bixler, R. S. & Cosgriff-Hernandez, E. Drying and storage effects on poly(ethylene glycol) hydrogel mechanical properties and bioactivity. *J. Biomed. Mater. Res. A* **102**, 3066–76 (2014).

233. Cox, T. R. & Erler, J. T. Remodeling and homeostasis of the extracellular matrix: implications for fibrotic diseases and cancer. *Dis. Model. Mech.* **4**, 165–178 (2011).

234. Mukherjee, S., Chawla, N. A. & Karthikeyan Non-Member, M. B. *Review of Mechanical Properties of Human Body Soft Tissues in the Head, neck and spine*.

235. Nordez, A. & Hug, F. Muscle shear elastic modulus measured using supersonic shear imaging is highly related to muscle activity level. *J. Appl. Physiol.* **108**, 1389–1394 (2010).

236. Grounds, M. D. Towards Understanding Skeletal Muscle Regeneration. *Pathol. Res. Pract.* **187**, 1–22 (1992).

237. Fuoco, C., Petrilli, L. L., Cannata, S. & Gargioli, C. Matrix scaffolding for stem

cell guidance toward skeletal muscle tissue engineering. *J. Orthop. Surg. Res.* **11**, 86 (2016).

238. Demontis, G. C. *et al.* Human Pathophysiological Adaptations to the Space Environment. *Front. Physiol.* **8**, 547 (2017).

239. Fitts, R. H., Riley, D. R. & Widrick, J. J. Physiology of a Microgravity Environment Invited Review: Microgravity and skeletal muscle. *J. Appl. Physiol.* **89**, 823–839 (2000).

240. Lai, D. *et al.* Human endometrial mesenchymal stem cells restore ovarian function through improving the renewal of germline stem cells in a mouse model of premature ovarian failure. *J. Transl. Med.* **13**, 155 (2015).

241. Blaber, E., Sato, K. & Almeida, E. A. C. Stem cell health and tissue regeneration in microgravity. *Stem Cells Dev.* **23 Suppl 1**, 73–8 (2014).

242. Shen, H. *et al.* Effects of spaceflight on the muscles of the murine shoulder. *FASEB J.* **31**, 5466–5477 (2017).

243. Grogan, B. F. & HSU, M. J. R. Volumetric Muscle Loss. *J. Am. Acad. Orthop. Surg.* **19**, S35–S37 (2011).

244. Nuutila, K. *et al.* Gene expression profiling of skeletal muscle after volumetric muscle loss. *Wound Repair Regen.* **25**, 408–413 (2017).

245. Grasman, J. M., Zayas, M. J., Page, R. L. & Pins, G. D. Biomimetic scaffolds for regeneration of volumetric muscle loss in skeletal muscle injuries. *Acta Biomater.* **25**, 2–15 (2015).

246. Dziki, J. *et al.* An acellular biologic scaffold treatment for volumetric muscle loss: results of a 13-patient cohort study. *npj Regen. Med.* **1**, (2016).

247. Greising, S. M. *et al.* Unwavering Pathobiology of Volumetric Muscle Loss Injury. *Sci. Rep.* **7**, (2017).

248. Consortium, M. T. E. Volumetric Muscle Loss (VML) Repair Following Extremity Trauma. Available at: https://mtec-sc.org/volumetric-muscle-loss-vml-repair-following-extremity-trauma/.

249. Yilgor Huri, P. *et al.* Biophysical cues enhance myogenesis of human adipose derived stem/stromal cells. *Biochem. Biophys. Res. Commun.* **438**, 180–185 (2013).

250. Gillies, A. R. & Lieber, R. L. Structure and function of the skeletal muscle extracellular matrix. *Muscle Nerve* **44**, 318–31 (2011).

251. Christman, J. K. 5-Azacytidine and 5-aza-2'-deoxycytidine as inhibitors of DNA methylation: mechanistic studies and their implications for cancer therapy. *Oncogene* **21**, 5483–95 (2002).

252. Meregalli, F. & Torrente, Y. Mesenchymal Stem Cells as Muscle Reservoir. *J. Stem Cell Res. Ther.* **1**, (2011).

253. Rudnicki, M. *et al.* MyoD or Myf-5 Is Required for the Formation of Skeletal Muscle. *Cell* **75**, 1351–1359 (1993).

254. Kitzmann, M. *et al.* The muscle regulatory factors MyoD and Myf-5 undergo distinct cell cycle-specific expression in muscle cells. *J. Cell Biol.* **142**, 1447–1459 (1998).

255. Matsiko, A., Gleeson, J. P. & O'Brien, F. J. Scaffold mean pore size influences mesenchymal stem cell chondrogenic differentiation and matrix deposition. *Tissue Eng. - Part A* **21**, 486–497 (2015).

256. Zhang, Y. *et al.* The effects of pore architecture in silk fibroin scaffolds on the growth and differentiation of mesenchymal stem cells expressing BMP7. *Acta Biomater.* **6**, 3021–3028 (2010).

257. Kasten, P. *et al.* Porosity and pore size of β-tricalcium phosphate scaffold can influence protein production and osteogenic differentiation of human mesenchymal stem cells: An in vitro and in vivo study. *Acta Biomater.* **4**, 1904–1915 (2008).

258. Ma, T., Li, Y., Yang, S. & Kniss, D. A. Effects of pore size in 3-D fibrous matrix on human trophoblast tissue development. *Biotechnol. Bioeng.* **70**, 606–618 (2000).

259. Di Luca, A. *et al.* Gradients in pore size enhance the osteogenic differentiation of human mesenchymal stromal cells in three-dimensional scaffolds. *Sci. Rep.* **6**, 1–13 (2016).

260. Dang, J. & Leong, K. Natural Polymers for Gene Delivery and Tissue Engineering. *Adv. Drug Deliv. Rev.* 487–499 (2006).

261. Zhao, W., Jin, W., Cong, Y., Liu, Y. & Fu, J. Degradable natural polymer hydrogels for articular cartilage tissue engineering. *J. Chem. Technol. Biotechnol.* **88**, (2013).

262. Ahmed, T. A. E., Dare, E. V & Hincke, M. Fibrin: A Versatile Scaffold for Tissue Engineering Applications. doi:10.1089/ten.teb.2007.0435

263. Zheng Shu, X., Liu, Y., Palumbo, F. S., Luo, Y. & Prestwich, G. D. In situ crosslinkable hyaluronan hydrogels for tissue engineering. *Biomaterials* **25**, 1339–1348 (2004).

264. Payan, E., Jouzeau, J. Y., Lapicque, F., Muller, N. & Netter, P. Hyaluronidase degradation of hyaluronic acid from different sources: Influence of the hydrolysis conditions on the production and the relative proportions of tetra- and hexasaccharide produced. *Int. J. Biochem.* **25**, 325–329 (1993).

265. Burdick, J. A. & Prestwich, G. D. Hyaluronic acid hydrogels for biomedical applications. *Adv. Mater.* **23**, (2011).

266. Wong, M. Alginates in Tissue Engineering. in *Biopolymer Methods in Tissue Engineering* 77–86 (Humana Press). doi:10.1385/1-59259-428-X:77

267. Lee, C. *et al.* Bioinspired, calcium-free alginate hydrogels with tunable physical and mechanical properties and improved biocompatibility. *Biomacromolecules* **14**, 2004–2013 (2013).

268. Di Martino, A., Sittinger, M. & Risbud, M. V. Chitosan: A versatile biopolymer for orthopaedic tissue-engineering. *Biomaterials* **26**, 5983–5990 (2005).

269. Croisier, F. & Jérôme, C. Chitosan-based biomaterials for tissue engineering. *European Polymer Journal* **49**, 780–792 (2013).

270. Jia, X. & Kiick, K. L. Hybrid multicomponent hydrogels for tissue engineering. *Macromolecular Bioscience* **9**, 140–156 (2009).

271. Bianco, P. & Robey, P. G. Stem cells in tissue engineering. *Nature* **414**, 118–121 (2001).

272. Lu, T., Li, Y. & Chen, T. Techniques for fabrication and construction of three-dimensional scaffolds for tissue engineering. *Int. J. Nanomedicine* **8**, 337–50 (2013).

273. Pereira, R. F., Almeida, H. A. & Bártolo, P. J. Biofabrication of Hydrogel Constructs. in 225–254 (Springer Netherlands, 2013). doi:10.1007/978-94-007-6010-3_8

274. Collins, C. A. *et al.* Stem Cell Function, Self-Renewal, and Behavioral Heterogeneity of Cells from the Adult Muscle Satellite Cell Niche. *Cell* **122**, 289–301 (2005).

275. Pountos, I., Corscadden, D., Emery, P. & Giannoudis, P. V. Mesenchymal stem cell tissue engineering: Techniques for isolation, expansion and application. *Injury* **38**, S23–S33 (2007).

276. Burdick, J. A. & Vunjak-Novakovic, G. Engineered Microenvironments for Controlled Stem Cell Differentiation. *Tissue Eng. Part A* **15**, 205–219 (2009).

277. Dawson, E., Mapili, G., Erickson, K., Taqvi, S. & Roy, K. Biomaterials for stem cell differentiation. *Adv. Drug Deliv. Rev.* **60**, 215–228 (2008).

278. Schmedlen, R. H., Masters, K. S. & West, J. L. Photocrosslinkable polyvinyl alcohol hydrogels that can be modified with cell adhesion peptides for use in tissue engineering. *Biomaterials* **23**, 4325–4332 (2002).

279. Banerjee, A. *et al.* The influence of hydrogel modulus on the proliferation and differentiation of encapsulated neural stem cells. *Biomaterials* **30**, 4695–4699 (2009).

280. Seck, T. M., Melchels, F. P. W., Feijen, J. & Grijpma, D. W. Designed biodegradable hydrogel structures prepared by stereolithography using poly(ethylene glycol)/poly(d,l-lactide)-based resins. *J. Control. Release* **148**, 34–41 (2010).

281. Chan, V. *et al.* Three-dimensional photopatterning of hydrogels using stereolithography for long-term cell encapsulation. *Lab Chip* **10**, 2062 (2010).

282. Zorlutuna, P., Jeong, J. H., Kong, H. & Bashir, R. Stereolithography-Based Hydrogel Microenvironments to Examine Cellular Interactions. *Adv. Funct. Mater.* **21**, 3642–3651 (2011).

283. Dhariwala, B., Hunt, E. & Boland, T. Rapid Prototyping of Tissue-Engineering Constructs, Using Photopolymerizable Hydrogels and Stereolithography. *Tissue Eng.* **10**, 1316–1322 (2004).

284. Gao, G., Yonezawa, T., Hubbell, K., Dai, G. & Cui, X. Inkjet-bioprinted acrylated peptides and PEG hydrogel with human mesenchymal stem cells promote robust bone and cartilage formation with minimal printhead clogging. *Biotechnol. J.* **10**, 1568–1577 (2015).

285. Ilkhanizadeh, S., Teixeira, A. I. & Hermanson, O. Inkjet printing of macromolecules on hydrogels to steer neural stem cell differentiation. *Biomaterials* **28**, 3936–3943 (2007).